ปฏิกิริยาออกซิเดชันของอนิลินและไนโตรเบนซิน ในกระบวนการฟลูอิดไดซ์เบดเฟนตัน

นางสาวลดาพร ขุณิกากรณ์

วิทยานิพนธ์นี้เป็นส่วนหนึ่งของการศึกษาตามหลักสูตรปริญญาวิทยาศาสตรมหาบัณฑิต
สาขาวิชาการจัดการสิ่งแวดล้อม (สหสาขาวิชา)
บัณฑิตวิทยาลัย จุฬาลงกรณ์มหาวิทยาลัย
ปีการศึกษา 2548

ISBN 974-53-2786-7

OXIDATION OF ANILINE AND NITROBENZENE IN FLUIDIZED-BED FENTON PROCESS

Miss Ladaporn Khunikakorn

A Thesis Submitted in Partial Fulfillment of the Requirements
for the Degree of Master of Science Program in Environmental Management
(Inter-Department)
Graduate School
Chulalongkorn University
Academic Year 2005

ISBN 974-53-2786-7

Thesis Title	Oxidation of aniline and nitrobenzene in fluidized-bed Fenton process
By	Ms. Ladaporn Khunikakorn
Filed of study	Environmental Management
Thesis Advisor	Associate Professor Jin Anotai, Ph.D.
Thesis Co-advisor	Professor Ming-Chun Lu, Ph.D.

Accepted by the Graduate School, Chulalongkorn University in Partial Fulfillment of the Requirements for the Master's Degree

.... Dean of the Graduate School
(Assistant Professor M.R. Kalaya Tingsabadh, Ph.D.)

THESIS COMMITTEE

.... Chairman
(Manaskorn Rachakornkij, Ph.D.)

.... Thesis Advisor
(Associate Professor Jin Anotai, Ph.D.)

.... Thesis Co-advisor
(Professor Ming-Chun Lu, Ph.D.)

.... Member
(Assistant Professor Sutha Khaodhiar, Ph.D.)

.... Member
(Pichaya Rachadawong, Ph.D.)

ลดาพร ชุณิกากรณ์: ปฏิกิริยาออกซิเดชันของอนิลินและไนโตรเบนซินในกระบวนการฟลูอิดไดซ์เบดเฟนตัน. (OXIDATION OF ANILINE AND NITROBENZENE IN FLUIDIZED-BED FENTON PROCESS) อ. ที่ปรึกษา รศ. ดร. จินต์ อโณทัย , อ.ที่ปรึกษาร่วม: Prof. Ming-Chun Lu, Ph.D. 141 หน้า. ISBN 974-53 -2786 -7.

งานวิจัยนี้ศึกษาการเกิดปฏิกิริยาออกซิเดชันของอนิลิน และไนโตรเบนซิน ในกระบวนการฟลูอิดไดซ์เบดเฟนตันโดยใช้ Al_2O_3 และ SiO_2 เป็นตัวกลางซึ่งมีค่า pzc 8.44 และ 6.54 ตามลำดับ ค่า pH ที่เหมาะสมของ อนิลิน และ ไนโตรเบนซิน คือ 3.2 และ 2.8 ตามลำดับ อย่างไรก็ตาม pH 2.8 ถูกเลือกให้ดำเนินการตลอดการทดลอง ภายใต้การศึกษานี้กระบวนการ mineralization ไม่เกิดขึ้น นอกจากนี้ Al_2O_3 นับว่าเป็นตัวกลางที่ดีกว่า SiO_2 ซึ่งความเป็นไปได้เนื่องจาก ณ พื้นผิวของตัวกลางมีค่าประจุเป็นบวกมากกว่าที่ pH 2.8 แม้ว่าการเปรียบเทียบลักษณะปฏิกิริยาออกซิเดชันของสารอินทรีย์ในกระบวนการฟลูอิดไดซ์เบดเฟนตันสามารถกำจัดเหล็กได้ในขณะที่ปฏิกิริยาเฟนตันไม่สามารถทำได้ นอกจากนี้สมการ kinetic ที่ได้จากการศึกษาปฏิกิริยาออกซิเดชันแต่ละตัวสารอินทรีย์ของอนิลิน และไนโตรเบนซินสามารถย่อยสลายได้ดีเช่นเดียวกับการนำสารทั้งสองตัวมาผสมกันภายใต้กระบวนการฟลูอิดไดซ์เบดเฟนตันซึ่งสามารถบ่งชี้และค้นพบว่ามีความไม่สอดคล้องกันกับสมการทางเคมี อนิลินยังถูกพบว่าสามารถถูกออกซิไดซ์ด้วยไฮดรอกซิลเรดิคอล ($OH^{\bullet}$) มากกว่าไนโตรเบนซินเมื่อมีความเข้มข้นเท่ากันโดย 75% จากการเกิด $OH^{\bullet}$ สามารถทำปฏิกิริยากับอนิลินในขณะที่อีก 25% ทำปฏิกิริยากับ ไนโตรเบนซิน จากผลการวิเคราะห์ด้วย EDX พบว่าเหล็กออกไซด์สามารถตกผลึกบนพื้นผิวของตัวกลางอีกทั้งตัวกลางที่มีเหล็กเกาะบนพื้นผิวเหล่านี้ยังคงสามารถนำกลับมาใช้ใหม่ได้อย่างมีประสิทธิภาพ

สาขาวิชา การจัดการสิ่งแวดล้อม (สหสาขาวิชา) ลายมือชื่อนิสิต..

ปีการศึกษา 2548 ลายมือชื่ออาจารย์ที่ปรึกษา..

ลายมือชื่ออาจารย์ที่ปรึกษาร่วม..

4789485220: MAJOR ENVIRONMENTAL MANAGEMENT
KEY WORD: NITROBENZENE / ANILINE / FLUIDIZED-BED FENTON PROCESS

LADAPORN KHUNIKAKORN: OXIDATION OF ANILINE AND
NITROBENZENE IN FLUIDIZED-BED FENTON PROCESS.
THESIS ADVISOR: ASSOC. PROF. JIN ANOTAI, Ph.D.
THISIS CO ADVISOR: PROF. MING-CHUN LU, Ph.D.
141 pp. ISBN 974-53-2786-7.

This research investigated oxidation of aniline (AN) and nitrobenzene (NB) by fluidized-bed Fenton process using Al_2O_3 and SiO_2 as the carriers which have the pzc of 8.44 and 6.54, respectively. Optimum pH for AN and NB oxidation were 3.2 and 2.8, respectively. Al_2O_3 was better than SiO_2 possibly due to higher positive-charged surface at pH 2.8. In spite of comparable performance in organic oxidation, the fluidized-bed Fenton process was able to remove iron whereas the ordinary Fenton process could not. Empirical kinetic equations for the oxidation of individual AN and NB oxidation as well as the combination by fluidized-bed Fenton process were determined and found to be inconsistency with those derived by stoichiometric equations. AN was found to be more vulnerable to $OH^{\bullet}$ oxidation than NB, i.e., when presenting at the same concentration, 72% of the generated $OH^{\bullet}$ reacted with AN whereas the rest of 28% were captured by NB. From the EDX analysis, iron oxide was crystallized onto the surface of the carriers and these iron-coated carriers could be reused successfully.

Field of study: Environmental management Student's signature...
(Inter-Department) Advisor's signature...
Academic year 2005 Co-advisor's signature...

ACKNOWLEDGEMENTS

I would like to express my sincere appreciation to my advisor and co-advisor; Associate. Prof. Dr. Jin Anotai and Prof. Dr. Ming-Chun Lu for encouragements, valuable supporting, opportunity and their guidance. By their kindness can proceed throughout my research freely. Their comments and suggestions do not merely provide valuable knowledge but also broaden perspective in practical applications as well. Special gratitude goes to the chairman of the committee, Dr. Manaskorn Rachakornkij for providing in valuable advice and examining my final work. I also would like to thank other committee member, Chairman of the committee, Assistant Professor Sutha Khaodhiar and Dr. Pichaya Rachadawong members of thesis committee for many valuable comments and their insightful suggestions. I share the pride and joy of completing this dissertation with them. I am glade to all staffs and students at the National Research Center for Environmental and Hazardous Waste Management (NRC-EHWM) Program and Department of Environmental Engineering, King Mongkut's University of Technology Thonburi, Bangkok, Thailand. Special thanks for the worth opportunity, that let me journey to achieve the experiment at CNU; Chia Nan University of Pharmacy and CNU Science, Tainan, Taiwan, which supported living expense, together with the National Science Council of Taiwan supported this research; the grant number is NSC 93-2211-E-041-011.

To every friend of mine from everywhere, thank you for all of your kindness, your friendliness, your patience and many hours all of you have spent working and sharing with me. I will be forever grateful for everything you've done. And to my beloved family, I'm appreciated all of your valuable morale that cheerful me to accomplish my goal. Finally, I'm proud to dedicate this thesis with due respect to my beloved.

CONTENTS

Page

Page

Page

LIST OF TABLES

Table Page

Table Page

LIST OF FIGURES

Figure Page

NOMENCLATURES

OSHA = Occupational Safety and Health Administration

AOPs = advanced oxidation processes

UV = ultraviolet

TOC = total organic carbon

$C_6H_5NH_2$ = aniline (AN)

$C_6H_5NO_2$ = nitrobenzene (NB)

H_2O_2 = hydrogen peroxide

Fe^{2+} = ferrous ion

Fe^{3+} = ferric ion

$OH^{\bullet}$ = hydroxyl radical

OH^- = hydroxide ion

min = minute

M = molar

k = rate constant

r = initial rate

FB = fluidized-bed

FBR = fluidized-bed Fenton reactor

Γ = surface concentration

s = specific surface area

γ = mass concentration

EDX = Energy dispersive X-Ray

SEM = Scanning electron microscopy

AAS = Atomic absorption spectroscopy

CHAPTER I

INTRODUCTION

1.1 Rational

Nowadays, there are several hazardous chemicals which are indeed environmentally persistent. Aniline and nitrobenzene are the organic chemical compounds which consist of a benzene ring but having different functional group and have also been categorized as hazardous wastes. Today, both of these compounds are widely used in several industries such as dye manufacturing, pesticides, rubber chemicals, and pharmaceuticals. Due to their toxicity, reduction of nitrobenzene which is believed to be a human carcinogen (NTP, 2005) to aniline appears to be an important step to prevent methemoglobinemia (a form of anemia) observed in human and experimental animals exposing to nitrobenzene. Advanced oxidation processes (AOPs) are an alternative approach which provides the destruction of hazardous organic compounds. The AOPs generate hydroxyl radical ($OH^\bullet$ which is a strong oxidant with E° of -2.8 v) which can initiate the ring opening of aromatic compound and lead to the mineralization of organic carbon to CO_2 and H_2O (Rodgers et.al, 2001). Fenton's reagent (H_2O_2/Fe^{2+}) is a homogenous oxidant which is one of AOPs and can produce $OH^\bullet$, a non-selective reactant for the oxidation of organic matter in the solution (Rodgers et.al, 2001; Utse et.al, 2000; Lu 1997; Richard, 1992). The conventional Fenton process is not difficult to operate in the field and also cogitated to toxic substances. Although Fenton's reaction can generate high amount of the strong oxidants, Fe^{2+} also can be reduced one electron to transform Fe^{3+}. Nevertheless, the production of substantial amount of $Fe(OH)_3$ precipitates is the major problem of Fenton process (Chou et.al, 2004). To work out this problem, one promising alternative is the use of fluidized-bed reactor in which the carriers can reduce the iron precipitation via crystallization process to form iron oxide species. With very dense formation structure, sludge volume can be significantly reduced. Under an acidic condition and in the presence of H_2O_2, goethite can serve as a iron source to generate ferrous ion which could lead to Fenton reaction (Lu 2000, 2002). At the moment, the fluidized-bed process has just been evolved; its mechanisms and kinetics for contaminant oxidation are under extensive studies. Consequently, this study applies the fluidized-bed reactor to explore the oxidation of nitrobenzene and aniline by Fenton process.

1.2 Objectives

This study intended to investigate the oxidation of nitrobenzene and aniline in fluidized-bed Fenton process. The main objectives of this study are:

1. To investigate on the removal efficiency of aniline and nitrobenzene in fluidized-bed Fenton process.
2. To determine the effects of initial ferrous, hydrogen peroxide, pH, aniline and nitrobenzene in fluidized-bed Fenton process.

3. To investigate on the oxidation kinetics of aniline and nitrobenzene in fluidized-bed Fenton process.
4. To explore the usability of aluminium oxide as the carriers in fluidized-bed Fenton process.

1.3 Hypotheses

1. Coexistence of aniline and nitrobenzene has an impact on the reactions occurred in fluidized-bed Fenton process.
2. The competitive reactions between aniline and nitrobenzene decomposition by fluidized-bed Fenton process depend on system pH and chemical dosages.
3. Aluminum oxide can effectively serve as a medium for iron oxide crystallization.

1.4 Scope of the research

1. Using lab scale reactor of 1.35 liter.
2. Using synthetic aniline / nitrobenzene wastewater.
3. For the fluidized-bed Fenton process, the carriers are the metal oxide (Al_2O_3 , SiO_2).
4. Working at room temperature.
5. Operating in a batch mode.

1.5 Expected Results

1. Effect of pH, H_2O_2 dosage and Fe^{2+} concentration on the degradation of aniline, nitrobenzene, the combination of aniline and nitrobenzene in fluidized-bed Fenton process.
2. The kinetic equation for aniline, nitrobenzene, the combination of aniline and nitrobenzene in fluidized-bed Fenton process.
3. Behavior of oxidation reaction between aniline and nitrobenzene degradation in fluidized-bed Fenton process
4. The reusability of the aluminum oxide

CHAPTER II

THEORIES AND LITERATURE REVIEWS

2.1 Nitrobenzene (NTP, 2005; U.S. EPA, 1995)

2.1.1. General Information

Most nitrobenzene (97%) is used in the manufacture of aniline. Miscellaneous uses include the manufacture of benidine, quinoline, azobenzene, pyroxyline compounds, isocyanates, pesticides, rubber chemicals, pharmaceuticals, and dyes such as nigrosines and magenta. Nitrobenzene is found in soap and shoe and metal polishes and is used as a solvent for cellulose ester, in modifying etherification of cellulose acetate, and in refining lubricating oils. Nitrobenzene will volatilize slowly from soil and surface water and is subject to biodegradation. Adsorption to sediment and bioconcentration are not thought to be significant fate processes in water. Nitrobenzene may leach through the soil and is considered to have intermediate mobility. The formula of nitrobenzene is $C_6H_5NO_2$ with the molecular structure as show in the Figure2.1.

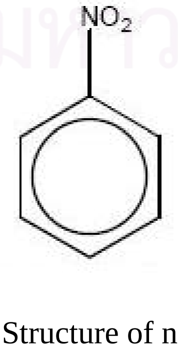

Figure 2.1 Structure of nitrobenzene

2.1.2 Physical and Chemical Properties

Nitrobenzene which is an aromatic compound is widely used in several manufactories. The physical and chemical properties of nitrobenzene are shown in Table 2.1.

Table 2.1 Physical and chemical properties of nitrobenzene

Property	**Value**
Molecular formula	$C_6H_5NO_2$
Molecular weight	123.11 g/mol
Appearance	Pale yellow to brown, oily liquid Almond odor
Odor	4.3
Boiling point	211°C
Melting point	5.7°C
Water Solubility	2.9 g/L @ 25°C
Specific Gravity	1.20 @ 20°C/4°C
Vapor pressure	1.0 mm Hg @ 44.4°C
$\log K_{OC}$	1.56
$\log K_{OW}$	1.85
Reactivity	flammable
Flash point (closed cup)	88°C

2.1.3 Toxicology

Human toxicity effects following acute exposure to nitrobenzene are obvious. Acute nitrobenzene poisoning is characterized by methemoglobinemia with cyanosis, headache, dyspeptics, and coma or death. The primary toxic effect resulting from acute exposure to nitrobenzene by inhalation, oral or dermalroutes is methemoglobinemia and accompanying anoxia and erythrocyte damage. Nervous system effects may also be experienced, but may be partially due to the anoxia from the methemoglobinemia. In human, inhalation exposure to nitrobenzene concentrations equal to or greater than 6 ppm in air (30.72 mg/m^3; 4.4 mg/kg/day) was reported to result in nervous system effects and methemoglobin production. Atmospheric concentrations of nitrobenzene resulting in these effects are well above the odor threshold of 1.9 ppm, which may help limit human exposures. Methemoglobinemia is the primary acute effect following nitrobenzene ingestion. The dose resulting in methemoglobinemia was estimated in one case study at 4.3 to 11 g based on urinary p-nitrophenol levels. Nitrobenzene is rapidly absorbed through the skin and is a contact irritant. Nitrobenzene is reasonably anticipated to be a human based on sufficient evidence of carcinogenicity in experimental animals. The carcinogenicity of nitrobenzene was evaluated in male and female mice, male rats of two strains and in female rats of one strain. When administered to mice and rate by inhalation, nitrobenzene caused significantly increased incidences of tumors at multiple tissue sites in both species. However, in humans, inhalation exposure to nitrobenzene did cause chromosomal aberrations in peripheral blood lymphocytes. Moreover, reduction of nitrobenzene to aniline appears to be an important step in development of methmoglobinemia (a form of anemia) observed in humans and experimental animals exposed to nitrobenzene.

2.1.4 Exposure

The general public potentially is exposed to nitrobenzene in the environment through inhalation of ambient air, ingestion of water, or dermal contact with products or water containing nitrobenzene. Two air surveys, one of almost 600 urban and suburban sites in the United States and one of more than 700 U.S. sites, reported mean concentration of nitrobenzene to be 0.17 ppb and 0.117 ppb, respectively. In a survey of hazardous waste site, nitrobenzene was detected in groundwater at three sites, at a geometric mean concentration of 1.4 ng/L, but was not detected in surface-water wimples from any sites. Occupational exposure to nitrobenzene generally is by inhalation of the vapor or dermal contact with the vapor or liquid. Direct release of nitrobenzene to air during its manufacture is minimized by passage of contaminated air through activated charcoal. Most (97% to 98%) of the nitrobenzene produced is retained in closed systems for use in synthesis of aniline and other substituted nitrobenzene and anilines, thus limiting its release into air.

2.2 Aniline (EPA, 1994; NTP, 2002).

2.2.1. General Information

Aniline, phenylamine or aminobenzene ($C_6H_5NH_2$) is an organic chemical compound which is a primary aromatic amine consisting of a benzene ring and an amino group. The chemical structure of aniline is shown at Figure 2.2. Aniline ignites readily, burning with a large smoky flame. It possesses a somewhat pleasant vinous odor and a burning aromatic taste; it is a highly acrid poison. The great commercial value of aniline is due to the readiness with which it yields, directly or indirectly, valuable dyestuffs. Aniline is manufactured by reducing nitrobenzene with iron and hydrochloric acid and steam-distilling the product (Chemistrydaily.com , 2005).

2.2.2 Physical and Chemical Properties

Aniline is a carcinogen. It is oily and although colorless, it can be slowly oxidized and revivified in air to form impurities which can give it a red-brown tint. The physical and chemical properties of aniline are demonstrated in Table 2.2.

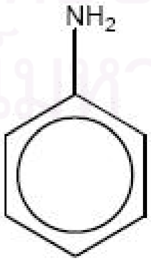

Figure 2.2 Structure of aniline

Table 2.2 Physical and chemical properties of aniline (EPA, 1994).

Property	**Value**
Molecular formula	$C_6H_5NH_2$
Molecular weight	93.12 g/mol
Appearance	Oily and colorless
Vapor Density (Air = 1)	3.22°C @ 101 kPa
Boiling point	184.4°C
Melting point	-6.25°C
Water Solubility	35 g/L @ 25°C
Specific Gravity	1.02173 @ 20/4°C
Vapor pressure	0.67 mm Hg @ 25 °C
K_{OC}	3870 @ pH 6.5 (measured)
Log K_{OW}	0.90
Reactivity	flammable
Flash point (closed cup)	76°C (Close up)

2.2.3 Toxicology

The primary toxic effect resulting from acute exposure to aniline by inhalation, oral or dermalroutes is methemoglobinemia and accompanying anoxia, erythrocyte damage, and spleeneffects. Adverse effects on the liver and spleen have also been reported. The humans were much more sensitive to aniline exposure than rats, judging from methemoglobin formation. Inhalation exposure to 7-53 ppm aniline for several hours resulted in slight symptoms; exposure to 100-160 ppm for 1 hour (6.91-11.06 mg/kg) resulted in (unspecified) serious disturbances. Sitting in a car seat contaminated with aniline resulted in a methemoglobin level of 53% with cyanosis, dyspnea, fatigue, and dizziness in one individual. Recovery occurred within 24 hours following medical treatment. For chronic effect, increased methemoglobin production and adverse spleen effects are the major non-neoplastic effects reported with extended exposure to aniline. Adverse effects on the liver and kidneys have been reported in some studies.

2.2.4 Exposure

Aniline is released into the environment primarily from industrial uses. The largest sources of aniline release are from its primary uses as a chemical intermediate in the production of polymers, pesticides, pharmaceuticals and dyes. The chemical has been detected, but not quantified, in ground water in a shallow aquifer known to be contaminated by coal-tar wastes. Aniline has been found in industrial wastewater and leachates from disposal sites. Aniline in solution adsorbs strongly to colloidal organic matter, which effectively increases its solubility and movement into groundwater. It is also moderately adsorbed to organic material in the soil; adsorption is dependent upon soil pH (pK_a of 4.596). It will slowly volatilize from soil and surface water and is subject to biodegradation. Although rapidly degraded in the atmosphere, aniline can be deposited in the soil by wet and dry deposition, and by adsorption on aerosol particles.

2.3 Advanced Oxidation Processes (AOPs)

AOPs, with the generation of a powerful hydroxyl radical, provide an effective mean of rapidly treating biorefactory compounds with efficient process control. Many AOPs employ hydroxyl radicals, addition of which to aromatic ring initiates ring opening and ultimate mineralization to CO_2 and H_2O. There are various kinds of AOPs such as alkaline ozonation, heterogeneous photocatalytic, Fenton processes, etc. In homogenous photolysis, $OH^{\bullet}$ are generated at the surface of a semiconductor (Usally TiO_2) in the presence of UVA. Homogenous oxidation produces an oxidant and includes methods such as Fenton's reagent (H_2O_2/Fe^{2+}), "peroxone" (H_2O_2/O_3), and hydrothermal (high temperature water oxidation (Rodgers, 2001). AOPs have shown a potential and alternative approach for treating refractory compounds in water.

2.4 Chemistry of Fenton's reagent

Fenton's reagent is known as the mixing of H_2O_2 and Fe^{2+} solution which is frequently used for oxidation and degradation of organic substances owing to its high oxidation power and simplicity. The oxidation of organic matters with Fenton's reagent, which is in fact a induced chain reaction (Lopez-Cueto, 2004).

2.4.1 Hydrogen peroxide

Hydrogen Peroxide (H_2O_2) solutions are clear, colorless, water-like in appearance, nonflammable, and can be mixed with water in any proportion. At high concentrations, it has a slightly pungent or acidic odor. H_2O_2 has a molecular weight of 34.02 g/mole and is nonflammable at any concentrations. The application of H_2O_2, is in the treatment of various inorganic and organic pollutants, is well established. There are the applications of H_2O_2 in the treatment industry involving cleaning, decorating, protecting and etching of metals.

Furthermore, by dissociation into oxygen and water, H_2O_2 can also supply oxygen to microorganism in biological treatment facilities and in the bioremediation of contaminated sites. It can be used as a disinfecting agent in the control of undesirable biofilm growth. Since the oxygen concentration is generally limiting factor during the insitu biodegradation of organic contaminants, many applications using injection of H_2O_2 into the subsurface have been successfully attempted to enhance the biodegradation activity. The decomposition of H_2O_2 can available into water and oxygen by enzymatic and nomenzymatic routes.

The oxidation which is conducted by H_2O_2 is not high by efficient for hazardous chemical compounds, such as highly chlorinated aromatic compounds and inorganic compounds, due to low rates of reaction at reasonable H_2O_2 concentration. H_2O_2 can be activated to form $OH^\bullet$ by transition metal salts, ozone and UV-light.

2.4.2 Hydroxyl radical

Thy hydroxyl radical ($OH^\bullet$) is a strong oxidant ($E° = -2.8$ V) which can degrade rapidly the chemical compounds. $OH^\bullet$ is generated among various AOPs in the reaction mixture has been used for achieve the treatment of a myriad of contaminated waters and industrial wastewater. The $OH^\bullet$ concentration level in turn is affected by the background impurities present in the water stream (Liao et al., 2001). The reaction rate constants for

$OH^{\bullet}$ attack on many organic contaminants are on the order of 10^{9}-10^{10} $M^{-1}s^{-1}$ when sufficient quantities of $OH^{\bullet}$ are generated (Kang and Hua, 2005; Buxton et al., 1988).

The oxidation of Hydroxyl radicals can decompose organic and inorganic substrates (M, R-H) by different types of reactions (equations 2.1 to 2.3) (Hoigné, 1998):

Electron Transfer Reaction:

$$OH^{\bullet} + M^{n} \Rightarrow M^{n+1} + (HO^{-})_{aq} \qquad (2.1)$$

Hydrogen Abstraction:

$$OH^{\bullet} + R\text{-}H \Rightarrow R^{\bullet} + H_2O \qquad (2.2)$$

Electrophilic addition:

$$OH^{\bullet} + R_2C{=}CR_2 \Rightarrow {}^{\bullet}CR_2\text{-}C(OH)R_2 \qquad (2.3)$$

The hydroxyl radical as the power oxidant can be able to decompose the organic chemical by abstraction of proton producing organic radical ($R^{\bullet}$) which are highly reactive as demonstrated equation (2.2). The electron transfer reaction, the oxidized organic is caused electrons of the carbon atoms which the hydrogen abstraction or electrophilic addition could be disapproval by multi halogen or steric hindrance. In the presence of organic substrate, at low pH, $OH^{\bullet}$ can add to the unsaturated bonds lead to initiate ring opening via electrophilic addition also.

There are four types of the chemical reactions of the hydroxyl radical in water (Peres et al., 2004):

a) The addition of $OH^{\bullet}$ to an unsaturated compound, aliphatic or aromatic, to form a free radical product

b) Hydrogen abstraction, where an organic free radical and water are formed

c) Electron transfer, where ions of a higher valence state are formed reducing $OH^{\bullet}$ to hydroxide ions

d) Radical interaction where $OH^{\bullet}$ reacts with another hydroxyl radical to combine or to disproportionate to form a stable product.

2.4.3 Fenton reaction

The hydroxyl radical as the non-selective oxidant can be produced by Fenton's reagent (H_2O_2/Fe^{2+}) which is considerably one kind of the AOPs. Its sequential reactions are very complicated but well specified as shown in equations (2.4) to (2.9) (Pignatello, 1992; Lu et al., 1999; Chen, 2001).

$$Fe^{2+} + H_2O_2 \Rightarrow Fe^{3+} + OH^{\bullet} + OH^{-} \qquad (2.4)$$

$$OH^{\bullet} + Fe^{2+} \Rightarrow OH^{-} + Fe^{3+} \qquad (2.5)$$

$$Fe^{3+} + H_2O_2 \Rightarrow Fe\text{-}OOH^{2+} + H^{+} \qquad (2.6)$$

$$Fe\text{-}OOH^{2+} \Rightarrow Fe^{2+} + HO_2^{\bullet} \qquad (2.7)$$

$$Fe^{3+} + HO_2^{\bullet} \Rightarrow Fe^{2+} + O_2 + H^{+} \qquad (2.8)$$

$$H_2O_2 + OH^{\bullet} \Rightarrow H_2O + HO_2^{\bullet} \qquad (2.9)$$

From equations (2.4) to (2.9) the formation of ferric ion may catalyst hydrogen peroxide causing it to be degraded into water and oxygen. Ferrous ion and some radicals are also occurred in the reaction (Neyens, 2003). The mechanism proposed for the H_2O_2-Fe^{3+} system, know as Fenton-liked reaction, involves $OH^\bullet$ and the hydroperoxyl radical ($HO_2^\bullet$) as shows in equation (2.6). The rate of reaction equation 2.4 (~ 76 $M^{-1}s^{-1}$) is much higher than that corresponding to reaction equation (2.5) (0.01-0.02 $M^{-1}s^{-1}$), therefore in the presence of excess peroxide the Fenton reaction only occurs in the first seconds (or minutes) of the reaction. After this short time, the rate of oxidation is controlled by the Fenton-liked reaction (Lunar et al., 2000).

Hydroxyl radical will react further with organic matters to generate organic radicals which could transform incessantly to other intermediates and finally end products as shown in equation (2.10).

$$OH^\bullet + RH \Rightarrow H_2O + R^\bullet \qquad \text{(chain propagation)} \qquad (2.10)$$

Chen et al. (2001) and Lipczynsk-Kochany et al. (1995) described the mixture of organics and Fenton’s reagent results in addition reaction equations (2.10) to (2.14). $OH^\bullet$ reacts with the organic compounds, H_2O_2, and Fe^{2+} ions in homogeneous phase. It also interacts with other radicals themselves. The reaction rate of hydroxyl radicals are very rapidly much more than the generation of those radicals, which has short-life time. The selectivity of hydroxyl radicals influences to the oxidation of target compounds and availability of these radicals to propagate the reaction.

$$R^{\bullet} + H_2O_2 \Rightarrow ROH + OH^{\bullet} \quad \text{(chain propagation)} \qquad (2.11)$$

$$R^{\bullet} + OH^{\bullet} \Rightarrow ROH \quad \text{(non-chain termination)} \qquad (2.12)$$

$$2R^{\bullet} \Rightarrow \text{R-R (dimmer)} \quad \text{(non-chain termination)} \qquad (2.13)$$

$$R^{\bullet} + Fe^{3+} \Rightarrow Fe^{2+} + \text{product} \quad \text{(chain termination)} \qquad (2.14)$$

2.5 Fluidized-bed Fenton Process

From equations (2.4) to (2.9), the major disadvantage of Fenton's reagent is the production of a substantial amount of ferric precipitation. To overcome and/or ease this problem, the fluidized-bed reactor (FBR) is one of the possible alternatives. In FBR, several important processes occur simultaneously including:

a) Homogeneous chemical oxidation (H_2O_2/Fe^{2+}),
b) Heterogeneous chemical oxidation (H_2O_2/ iron oxide)
c) Fluidized-bed crystallization
d) Reductive dissolution of iron oxides

The emphasis influencing of iron oxide growing on the surfaces of fluidized-bed carrier which are operated in FBR are pH, specific iron loading, H_2O_2/Fe^{2+}, and superical velocity (Chou et al., 2004). As Figure 2.3 illustrates the fluidized-bed Fenton reaction, the Fenton's reagent can produce the non-selective oxidant as $OH^{\bullet}$ via homogeneous reaction (a). Then, this strongly oxidant attacks the aromatic hydrocarbon to initiate ring opening in oxidation reaction (b). After that, the intermediate products from previous reaction appears, these lead into further oxidation (c). Also, Fe^{3+} can be converted from the reducing one electron of Fe^{2+} in Fenton's reaction (d). Some Fe^{3+} can be converted back to Fe^{2+} and initiate Fenton reaction further as in reaction (h). However, in the presence of solid carrier, the ferric hydrolysis product of Fenton's reaction can also crystallize and grow on the surface of the carriers (reaction (e)); hence, decreasing the precipitation in puffy ferric hydroxide forms (Chou et al., 1999). At the same time, the synthesized ferric oxide can also serve as a catalyst for hydrogen peroxide decomposition in a heterogeneous reaction (i) (Chou et al., 2003). When, considering iron oxide on the surface carriers, can re-dissolve via reductive dissolution (g) or heterogeneous reaction (f) also to become Fe^{2+} form. However, these reactions which are similar as equation (2.6) are slower than that equation (2.4) (Pignatello, 1992). In acidic environment, iron species can reform by the way ferric can alter to ferrous form also (d).

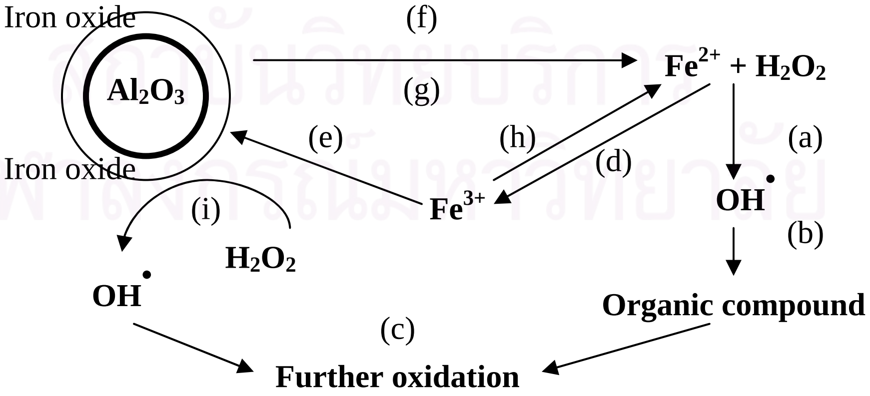

Figure 2.3 Fluidized-bed Fenton reactions

2.6 Point of Zero Charge (pzc)

The complication in contact with aqueous environment happens at the surface of an oxide. The development of a surface charge which can be positive or negative upon the pH surrounding is led by the amphoteric behavior of hydroxylated. The hydrated surface of an oxide presents ion exchange properties and there is a correlation between the exchange capacity and the net surface charge of the oxide. Simple oxides are cation exchangers in environments giving a negative surface charge and are anion exchangers in environments producing a positive surface charge. One of the most important characteristics of an oxide surface is the point of zero charge (pzc) which corresponds to the pH value of the liquid surrounding oxide particles when the sum of surface positive charges balance the sum of surface negative charges. The pzc value characterizes surface acidity when oxide particles are introduced in an aqueous environment their surface charge is positive if pH solution < pzc and is negative if pH solution > pzc (Reymond and Kolenda, 1999).

The protonation (p) and deprotonation (d) of amphoteric surface site are result of surface charge of an oxide in aqueous surrounding which will be denoted by MOH, where M stands for a metal. The corresponding surface reaction may be written as follows (Preocanin et al, 1998; Noh et al, 1988).

$$\mathrm{MOH} + \mathrm{H}^+ \Rightarrow \mathrm{MOH_2}^+ \qquad (2.15)$$

$$\mathrm{MOH} \Rightarrow \mathrm{MO}^- + \mathrm{H}^+ \qquad (2.16)$$

$$\mathrm{OH}^- + \mathrm{H}^+ \Rightarrow \mathrm{H_2O} \qquad (2.17)$$

Moreover, equations (2.15) and (2.16) the association of conversions with surface charge group MOH_2^+ and MO^- may take place. Surface reactions are usually consisting of neutralization in the bulk of the solution. Thus, the amphoteric behavior of hydroxylated sites lead to the development of a surface charge which can be positive or negative charge upon the pH surrounding (Reymond, 1999).

2.7 Literature Reviews

2.7.1 Degradation of nitrobenzene and aniline by various chemical processes

2.7.1.2 Effect of pH

The role of pH optimization is emphasis effect to considering the high removal efficiency of organic matter in every process. High efficiency of the oxidation processes utilizing the activation of H_2O_2 by iron salt is usually obtained when operating under acidic pH condition (Neyens, 2003). As in equation (2.5) and (2.6) in the Fenton's system, when pH is too high and low, the present of proton can cause the formation of Fe-OOH^{2+} then the reaction is let to slow down. Addition, there are many researchers investigating on the degradation of organic compound in acidic range.

Piccinini et al. (1997) investigated on TiO_2 photocatalytic mineralization of nitrobenzene, nitrosobenzene, phenylhydroxylamine, aniline and 4-nitrosophenol in aerated condition. Under slightly acidic condition, all these compounds underwent to carbon dioxide, whereas the nitrogen was converted to nitrate and ammonium ions. The temporal evolution of the $NO^-{}_3/NH^+{}_4$ concentration ratio, besides other experimental conditions (pH, photon flux, reactant concentrations), depends largely on both the initial oxidation state of the nitrobenzene and the nature of the starting organic substrate.

Brillas et al. (1998) studied on the aniline degradation in acidic medium of pH around 3 under photocatalytic and electrochemical conditions. Benzoquinone, hydroquinone, nitrobenzene, phenol and 1,2,4-benenetriol were detected as intermediates by HPLC in both electrochemical and photocatalytic experiments. The proposed reaction pathways for mineralization of aniline at pH 3 by photocatalysis, anodic oxidation, electro-Fenton and phtoelectro-Fenton processes as demonstrate in Figure 2.4.

Utset et al. (2000) conducted a research on the consumption of oxygen during the degradation of aniline by Fenton and photo-Fenton reaction. This study examined the effects of aniline, Fe^{2+} and H_2O_2 initial concentration, pH, temperature, and O_2 flow rate on the ratio O_2 consumed/H_2O_2. The experiment results indicated that this replacement took place in a variable extent, but the presence of H_2O_2 was necessary along the reaction.

Lu et al. (2005) explored the mechanism of chloride ions affecting on aniline oxidation by Fenton's reagent. The results indicated that the inhibition caused by chloride ions can be overcome by increasing the reaction time if the concentration of chloride ions is low.

2.7.1.2 The by-products of aniline and nitrobenzene

With the generation of powerful $OH^{\bullet}$ can lead to destroy double bond of aromatic or unsaturated compound. The aftermath from the initial oxidation reaction, there is a number of intermediates present in the reaction.

Sánchez et al. (1998) attempted to decompose aniline by combined photocatalysis and ozonation. The experimental results showed that the ozonation pretreatment followed by photocatalysis strongly increased the yield of TOC removal in comparison to either ozonation or photocatalysis conducted separately. A mechanism involving the formation of an ozonation anion radical previous to the generation of hydroxyl radicals implied the synergic effect between ozone and TiO_2 under illumination.

Sauleda et al. (2001) studied on the mineralization of aniline and 4-chlorophenol in acidic solution by ozonation catalyzed with Fe^{2+} and UVA light. The initial mineralization rate was enhanced as more oxidizing hydroxyl radical was produced in the medium by the catalyzed ozonations. Each initial pollutant was destructed at similar rate in all processes. *p*-Benzoquinone and nitrobenzene were identified as intermediates of aniline oxidation. Nitrate ion attained maximum production under UVA irradiation, indicating that the generation of nitrobenzene from selective attack of O_3 on the amino group of aniline was photocatlyzed.

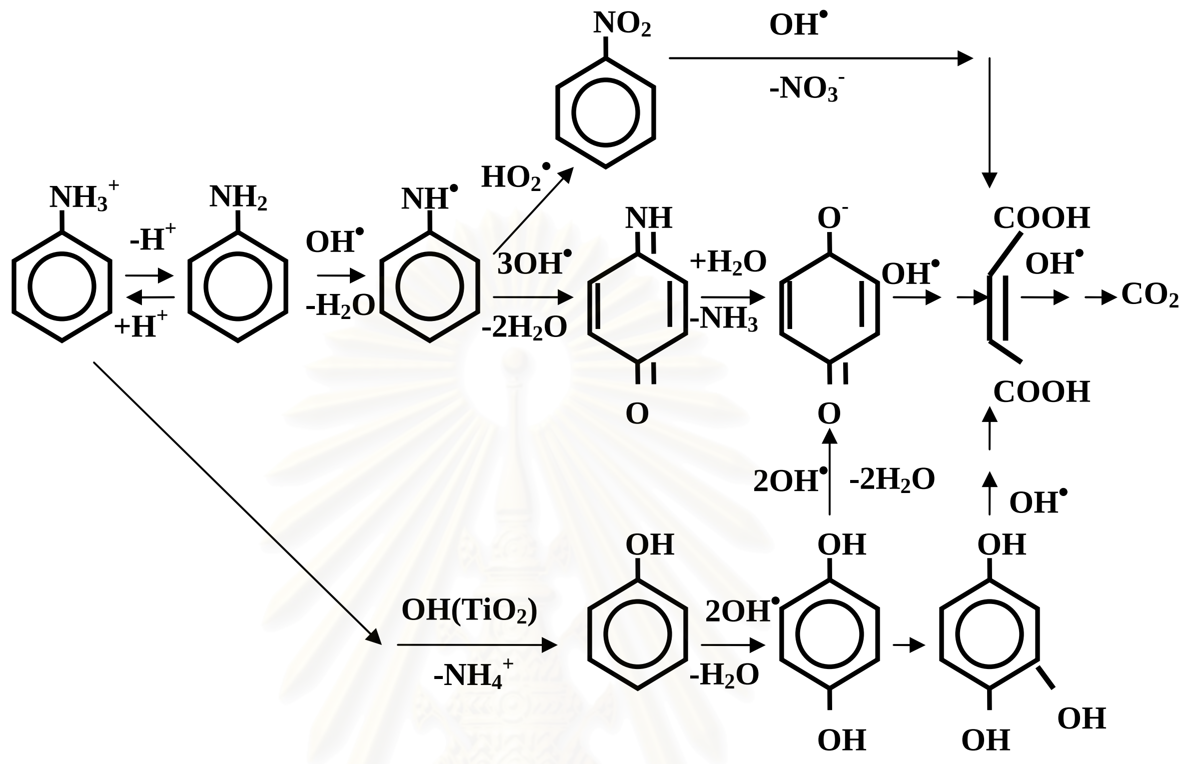

Figure 2.4 Proposed reaction pathway for aniline mineralization at pH 3 following (Brillas et al., 1998)

Sarasa et al. (2002) treated aqueous solution of aniline and *p*-chloroaniline with ozone in order to investigate the reaction and oxidation by-products. The main examined aromatic by-products were nitrobenzene and azobenzene when the experiment was performed at acidic pH. All the aromatic by-products found were less toxic than the raw materials.

Rodriguez et al., (2003) described the effect of temperature and initial concentration of H_2O_2, Fe^{2+}, $PhNO_2$ and dissolved oxygen on the degradation rate of nitrobenzene by Fenton-like reagent [H_2O_2 » [Fe^{2+}]$_0$). This experimental reaction was addressed in a completely mixed-batch reactor under a wide range of experimental conditions; pH ~3.0; 278-318 K; $1.5 < [H_2O_2]_0 < 26.5$ mM; $0.04 < [Fe^{2+}]_0$, 1.1 mM; $0.3 < [PhNO_2]_0 < 2.5$ mM; and $0 < [O_2]_0 < 1.4$ mM. As results, the degradation rate of $PhNO_2$ behaved as pseudo-first order kinetics. The second-order rate constant for the overall rate of H_2O_2 decomposition by Fe^{3+} was found to be 0.83 $M^{-1}s^{-1}$ at 298 K. Also, they found that there were the oxidation product *o*-, *m*-, and *p*-nitrophenols as intermediates in the ratio of 1:1.3 – 2.8:1.4 – 2.7 as compared with $PhNO_2$ when conversion of the latter was less than 25%. The isomeric distributions of nitro-phenol appeared during the degradation of $PhNO_2$ by 'Fenton-like' reagent, photolysis and radiolysis are presented in Table 2.3.

2.7.2 The removal oxidation of organic compound in heterogeneous catalysis by hydrogen peroxide

Lopez et al. (1994) investigated the effectiveness of Fenton's reagent for the pre-treatment of municipal landfill leachate with biological treatment was investigated. The municipal landfill leachate in southern was primary explored for its main characteristics. At the optimum conditions of Fe^{2+} = 275 mgl^{-1}; H_2O_2 = 3300 mgl^{-1}; initial pH =3; reaction time = 2 H the BOD_5/COD of the treated effluent was greater than 0.5 as desired results. To permit a subsequent biological treatment, residual ferric ions were eliminated by increasing the pH up to 8.5 by adding 3 g/l^{-1} of $Ca(OH)_2$ and 3 mg/l^{-1} of cationic polyelectrolyte, the later as aid to coagulation at the end of the Fenton's pretreatment.

Table 2.3 The isomeric distribution of nitrophenols formed during the action of Fenton reagent, photolysis and radiolysis on the aqueous solutions of $PhNO_2$

Solutions of $PhNO_2$ Source of the attacking species	Ratio of the *o*-, *m*- and *p*-isomers	Reference
'Fenton-like' reagent[a]	1:1.3–2.8:1.4–2.7	Rodriguez et al., 2003
'Fenton-like' reagent[b]	1:0.6–1.0:0.8–1.2	Rodriguez et al., 2003
'Fenton-like' reagent	1:1.3:1.9	Norman and Radda, 1962
'Fenton-like' reagent	1:0.8:1.8	Loble et al., 1949
Photolysis[c]	1:0.6:0.7	Lipczynska-Kochany, 1992
Radiolysis		Radiolysis Loebl et al., 1950
pH 2	1:0.9:1.0	
pH 6	1:1.0:1.0	
Radiolysis (pH 5.5)		Matthews and Sangster, 1967
Air	1:0.6:0.7	
Nitrogen	1:0.7:1.8	

[a] Conversion of $PhNO_2$ was 15–25%.
[b] Conversion of $PhNO_2$ was 80–90%.
[c] In the presence of H_2O_2
Available from Rodriguez et al., (2003). Advances in environmental research, 7.

Lin et al. (1996) investigated on the possibility of using mixture of hydrogen peroxide and iron oxide (goethite, α-FeOOH) particles as a chemical oxidant for wastewater treatment by using BuCl as a studied compound. The oxidation rate of BuCl was closely related with degradation rate of hydrogen peroxide. The results showed that BuCl was oxidized effectively by hydroxyl radical generated from the interaction of hydrogen peroxide with FeOOH particles.

Kang et.al. (2000) studied on that the effect of reaction conditions on the oxidation efficiency on non-biodegradable landfill leachate in the Fenton process. The results indicated that the COD removal with hydrogen peroxide was most efficient in the pH range of 2.5-4. The organic oxidation drastically decreased at pH value above 5. The increasing of ferrous dosage can increased the COD removal efficiency by coagulation, but up to a minimum dosage of 500 mg/l lead to change scarcely efficiency.

Lu (2000) investigated the effect of goethite particle size, goethite concentration, Fe^{2+} and Fe^{3+} on the 2-chlorophenol oxidation. It was found that 2-chlorophenol degradation could be decomposed with hydrogen peroxide catalyzed by goethite and the oxidation rate increased with decreasing goethite particle size. In addition, the essential mechanisms of goethite catalyzing hydrogen peroxide to decompose 2-chlorophenol maybe due to the catalysis of ferrous ions and goethite surface.

Lunar et al. (2000) examined degradation of metol [N-methyl-p-aminophenol] by Fenton's reagent under optimal dark condition with 0.2 M, H_2O_2 9.0 x 10^{-4} M Fe^{2+}, pH 3 -5, at room temperature and the initial COD of a 5 x 10^{-3} M. The experimental results demonstrated that the metol was reduced by approximately 50% within 2 h. After that, the COD reduction was very slow (about 20% in five days). The detection of aromatic compound can not found within the first 4 h of reaction indicating that residual organic matter was mainly made up of ring cleavage products. Metol conversion performed as a first-order reaction with respect to metol and Fe^{2+}. Complete destruction of residual organic matter could be achieved at high temperature (about 60°C) or by using the photo-

Fenton reaction, which thus opens up prospects for an effective treatment of paminophenols in effluent from photographic processes.

Huang et al. (2001) examined the catalyzed decomposition of hydrogen peroxide and 2-choropheno (2-CP) in the presence of iron oxides. The catalytic activity for hydrogen peroxide decomposition followed the following sequence: granular ferrihydrite > goethite > hematite. The strong diffusion resistance for granular ferrihydrite was ascribed either to its microporous structure or to the formation of oxygen in the pores of the iron oxide leading to the unexpected catalytic activity of granular ferrihydrite to hydrogen peroxide and 2-CP.

Panizza et al. (2001) explored the removal of organic pollutants mainly containing naphthalene and anthraquinone-sulphonic acid from industrial wastewater by electrogenerated Fenton’s reagents. They found that the reduction of oxygen to H_2O_2 on graphite felt occurred at -1 V. Also, the greatest COD removal (87%) and color fading (89%) were obtained with a Fe^{2+} concentration of 3 mM for the electro-Fenton treatment process. The COD removal kinetic acted a pseudo-first order reaction. And, the chemical or electrochemical surface pre-treatment had no benefit influence in organics oxidation.

Teel et al (2001). studied the comparison of mineral and soluble iron Fenton’s catalysts for the treatment of trichloroethylene (TCE). The experimental results, using hydroxyl radical scavengers, indicated that the standard Fenton’s system decomposed TCE entirely by hydroxyl radical mechanisms whereas approximately 10-15% of the degradation completed in the modified soluble iron and goethite-catalyze system at pH 3 was mediated by non-hydroxyl radical mechanisms.

Lu (2002) explored how surface dissolution of goethite affects 2-chlorophenol oxidation in the goethite/H_2O_2 process. The results show that ligand and reductant could enhance the dissolution rate of goethite which was surface-controlled mechanism. Furthermore, a mechanism proposed therein revealed that the contaminant and its intermediate species affected the oxidation rate as well.

2.7.3 The application in fluidized-bed Fenton reactor (FBR)

Chou and Huang (1999a) investigated on the effect of Fe^{2+} on the catalytic oxidation of benzoic acid in the FBR applying supported γ-FeOOH as the carrier. They found that both mineralization of organics and crystallization of Fe^{3+} were simultaneously well performed under proper condition. Moreover, the reductive and the crystallization of γ-FeOOH as well as the oxidation of benzoic acid was proposed based on the experiment results. The reaction mechanism is shown in Figure 2.5.

Chou and Huang (1999b) demonstrated that the treatment efficiency of benzoic acid at an initial pH of 3.2 was higher than at initial pHs of 6.0 and 10.0 which could be party explained by reductive dissolution of γ-FeOOH. Beside, the majority of oxidation occurred on the catalyst surface with some occurred in the solution due to iron dissolution of the catalyst.

Tai (1999) studied on the crystal growth kinetics of two-step growth process in liquid fluidized-bed crystallizers. A reliable method has been proposed to determine the parameters of the two-step growth. For sparingly soluble salts, the growth process wais more complicated, but the two-step model could still be applied successfully under a similar environment of pH, ionic strength, and species ratio.

Chou et al. (2004) applied a novel supported iron oxyhydroxide (FeOOH) catalyst to treat benzoic acid by hydrogen peroxide using a fluidized-bed crystallization reactor. The crystallization reached the maximum between pH 3.0 and 4.0 and the crystallization increased with increasing H_2O_2/Fe^{2+} ratio, and then attained a plateau. The results indicated that, significant removal of benzoic acid (i.e. 95%), TOC (i.e. 49-59%) and Fe (III) (i.e. 70-90%) was attained within pH 3.4-3.7 and C_{Fei} of 28-130 mg/l.

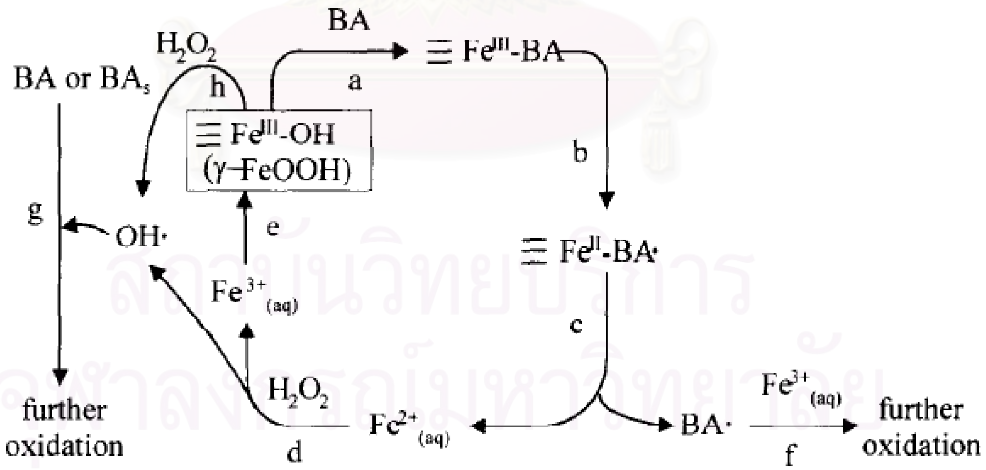

Figure 2.5 the reaction mechanism of benzoic acid (BA) in FBR-Fenton process: (A) reductive dissolution: reactions a, b, and c; (B) systhesis of Fe(III)hydroxide; reactions d and e; (C) oxidation of BA: reactions f, g, and h; BAx (5) denotes the surface complex of BA and γ-FeOOH. (Chou, 1999a).

CHAPTER III

METHODOLOGY

3.1 Materials

3.1.1 Chemicals

Nitrobenzene, aniline, ferrous sulfate, hydrogen peroxide (35%) were acquired from the Merck Company. All chemical substances are reagent grade. Two types of metal oxide i.e Al_2O_3 and SiO_2, was used in this study. Al_2O_3 serving as the main carrier in the FBR has white color, circle shape with 2.5 mm of average particle diameter. SiO_2 has a grain shape with 0.50 mm. of average particle diameter.

3.1.2 Fluidized-bed Reactor

A 1.35-litre fluidized-bed reactor (FBR) was operated in all experiments performed. The FBR is a cylinder vessel which consists of outlet, inlet and recalculate sections as shown in the Figure 3.1. The carriers are fluidized by adjustment the internal circulation at the optimum bed expansion.

3.2 Experiment Procedures

3.2.1 Point of zero chare of metal oxide

De-ionized water having very low ionic strength is used to make suspensions. The use of aqueous solutions containing monovalent ions is worthwhile; provides that added ions are not specifically adsorbed on the surface oxide. It is important to select the electrolyte nature as a function of the studied oxide. In this research, the solution containing 0.01 M of aniline and 0.025 M of Na_2SO_4 which stand for the experimental solutions was used to determine the pzc and compared to that of pure water.

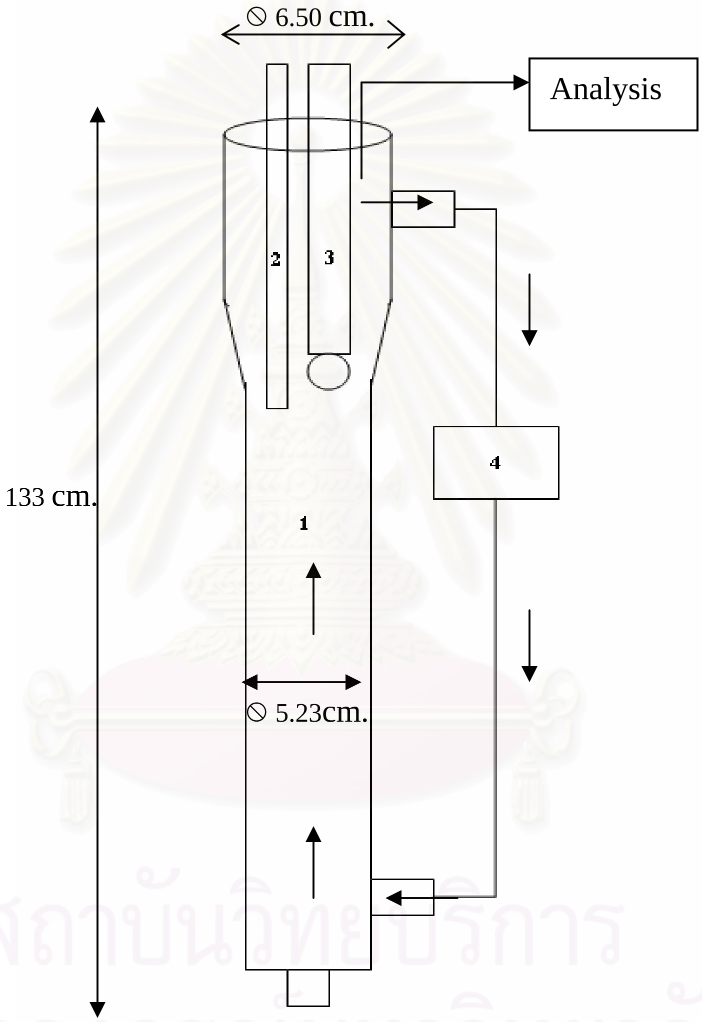

1. glass cylinder reactor
2. thermometer
3. pH meter
4. re-circulated pump

Figure 3.1 Fluidized-bed reactor (FBR) compartments

Predetermine amounts of metal oxide particles were put into the flasks containing either DI water or experiment solution to yield 0, 0.2, 0.4, 0.6, 1.2, 2.4, 5, 10, 20, 30, 40, 50 g/l. Both DI water or experiment solutions were used after bubbling with nitrogen gas. The flasks of metal oxide/water were purged with nitrogen gas, sealed, and placed on a shaker for 24 hours, which was found to be sufficient to allow the mixture to reach equilibrium. Then, pH of the mixture was measured. The experimental procedure chart is mentioned in Figure 3.2.

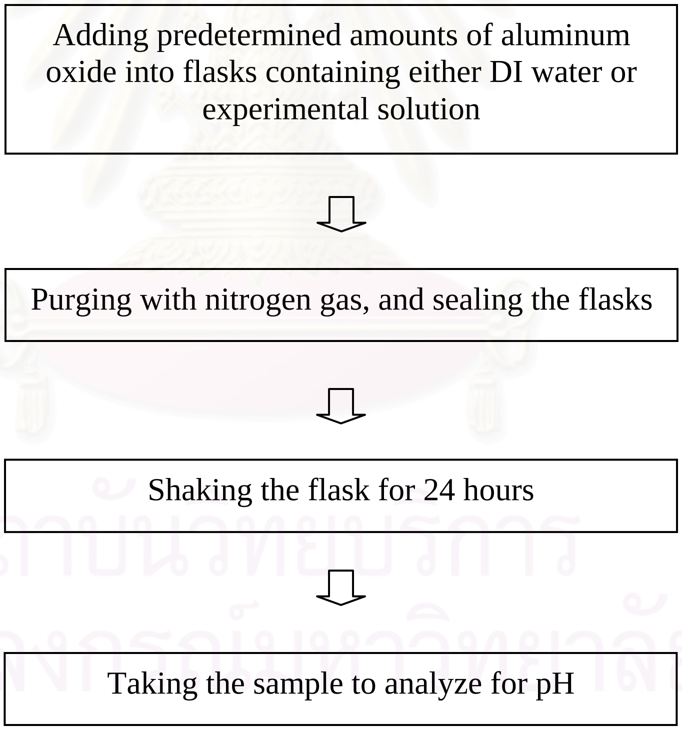

Figure 3.2 Experimental procedure chart of point of zero charge

3.2.2 Fluidized-bed Fenton Experiment

At the beginning, the synthesis wastewater containing nitrobenzene and/or aniline was poured into the FBR. Next, the recycle pump was turned on to mix the solution at the desired bed expansions. After that, the desire pH was adjusted by 1:4 H_2SO_4 which took approximately 10 minutes before the pH reading was stable. Pre-calculated ferrous solution was purred at the 5th minute after the recycle pump had been switched on. The solution was rechecked again before adding H_2O_2 solution and the reaction was simultaneously started. At selected time interval of 0, 2, 5, 10, 20, 30 and 60 minutes, 4 ml aliquot was taken from the FBR and analyzed immediately for residual H_2O_2, nitrobenzene, aniline, ferrous, total iron, and TOC. All experimental activities are as shown in Figure 3.3.

3.2.3. Fenton experiment

In this experiment, the procedures are all the same as previous section for fluidized-bed Fenton process, except for there is no metal oxide inside the reactor. Analysis parameters are also similar to those shown in Figure 3.3.

3.2.4. Reusability of Aluminum oxide

All procedures were carried out as the fluidized-bed Fenton experiment, only that, the aluminum oxide particles were reused again in every experimental cycle required. At the end of each cycle, 1 g of the metal was withdrawn from the reactor for analysis later.

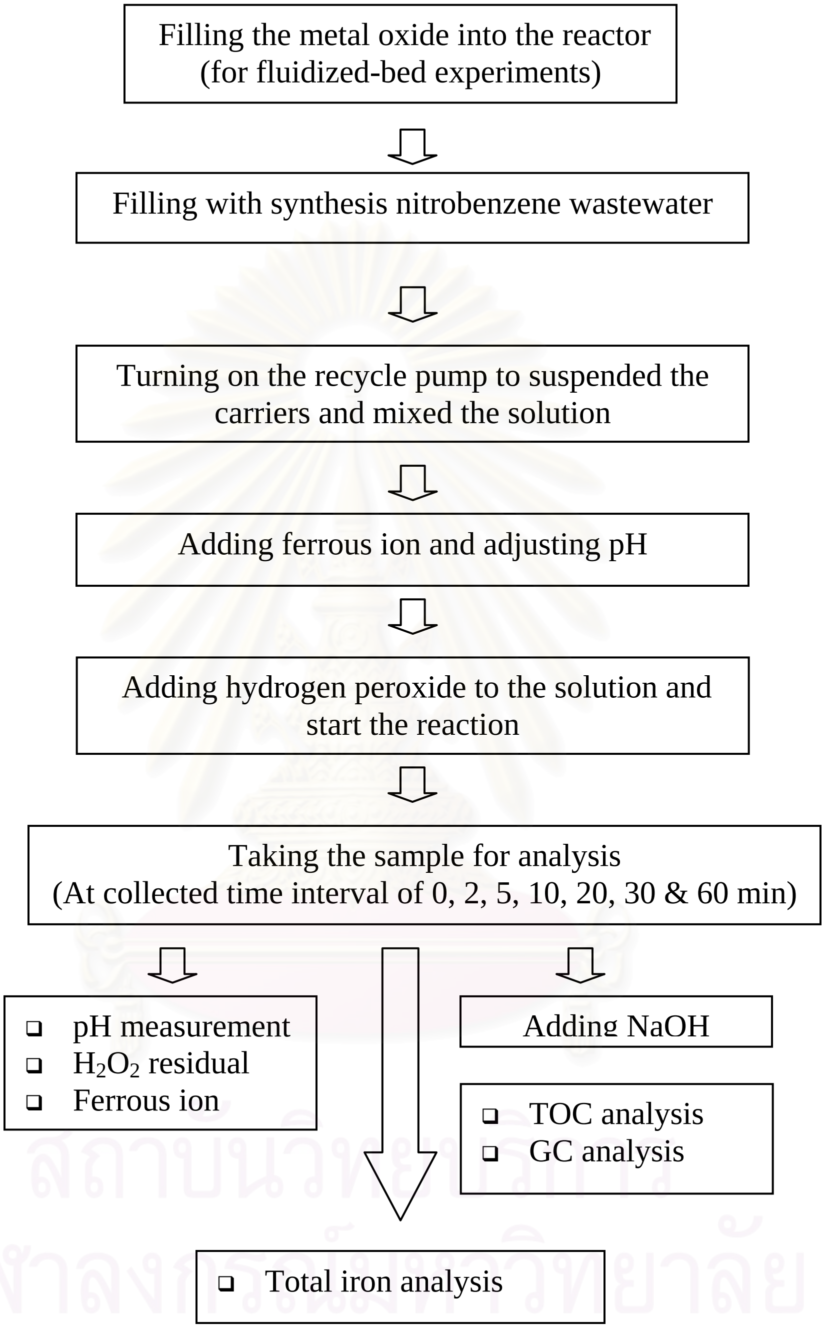

Figure 3.3 Experiment for Fenton and fluidized-bed Fenton process

3.3 Experimental Scenarios

The mainly conditions; 0.01 M of AN or NB, 0.05 M of H_2O_2, 0.001 M of Fe^{2+} and 100 g of metal oxide in FBR was referred from the investigation of oxidation of NB in FB-Fenton as the previous study of Sakulkitimasak (2004).

A. Investigation of the degradation of individual target chemical compound

A 1. Aniline

Table 3.1 Effect of individual component

Aniline (M)	pH	Metal oxide (100 grams)		Control parameter
0.01	3.2±0.2	Al_2O_3	SiO_2	H_2O_2
				Adsorption

Table 3.2 Comparison of the nitrobenzene removal efficiency in Fenton, and FB-Fenton

Aniline (M)	H_2O_2 (M)	pH	Fe^{2+} (mM)	Metal oxide in FBR (grams)
0.01	0.05	2.8±0.2	1	0
				100

Table 3.3 Effects of pH on the removal efficiency in FBR

Aniline (M)	Fe^{2+} (mM)	H_2O_2 (M)	Metal oxide (grams)	pH
0.01	1	0.05	100	2.4±0.2
				2.8±0.2
				3.2±0.2
				3.6±0.2
				4.0±0.2

A2 Nitrobenzne

Table 3.4 Effect of individual component

Nitrobenzene (M)	pH	Metal oxide (100 grams)		Control parameter
0.01	3.2±0.2	Al_2O_3	SiO_2	H_2O_2
				Adsorption

Table 3.5 Comparison of the aniline removal efficiency in Fenton, and FB-Fenton processes

Nitrobenzene (M)	H_2O_2 (M)	pH	Fe^{2+} (mM)	Metal oxide in FBR (grams)
0.01	0.05	3.2±0.2	1	0
				100

Table 3.6 Effects of pH on the removal efficiency in FBR

Nitrobenzene (M)	Fe^{2+} (mM)	H_2O_2 (M)	Metal oxide (grams)	pH
0.01	1	0.05	100	2.4±0.2
				2.8±0.2
				3.2±0.2
				3.6±0.2
				4.0±0.2

B. Optimization for combined aniline and nitrobenzene oxidation

Table 3.7 Effect of pH on the removal efficiency

Aniline (M)	Nitrobenzene (M)	Fe^{2+} (mM)	H_2O_2 (M)	Metal oxide (grams)	pH
0.005	0.005	1	0.05	100	2.4±0.2
					2.8±0.2
					3.2±0.2
					3.6±0.2

Table 3.8 Performance comparison between Fenton and FB-Fenton processes

Aniline (M)	Nitrobenzene (M)	H_2O_2 (M)	pH	Fe^{2+} (mM)	Metal oxide in FBR (grams)
0.005	0.01	0.05	2.8±0.2	1	0
					100

C. Determination of kinetic information for aniline and nitrobenzene oxidation by FBR

C 1. Aniline

Table 3.9 Reaction order with respect to aniline

H_2O_2 (M)	Fe^{2+} (mM)	pH	Metal oxide in FBR (grams)	Aniline (M)
0.05	1	2.8±0.2	100	0.0100
				0.0080
				0.0060
				0.0040
				0.0020

Table 3.10 Reaction order with respect to H_2O_2

Aniline (M)	Fe^{2+} (mM)	Metal oxide (grams)	pH	H_2O_2 (M)
0.01	1	100	2.8±0.2	0.1000
				0.0500
				0.0250
				0.0150
				0.0050

Table 3.11 Reaction order with respect to Fe^{2+}

Aniline (M)	H_2O_2 (M)	Metal oxide (grams)	pH	Fe^{2+} (M)
0.01	0.0500	100	2.8±0.2	0.00200
				0.00100
				0.00075
				0.00050
				0.00025

C 2 Nitrobenzene

Table 3.12 Reaction order with respect to nitrobenzene

H_2O_2 (M)	Fe^{2+} (mM)	pH	Metal oxide in FBR (grams)	Nitrobenzene (M)
0.05	1	2.8±0.2	100	0.0100
				0.0080
				0.0060
				0.0040
				0.0020

Table 3.13 Reaction order with respect to H_2O_2

Nitrobenzene (M)	Fe^{2+} (mM)	Metal oxide (grams)	pH	H_2O_2 (M)
0.01	1	100	2.8±0.2	0.1000
				0.0500
				0.0250
				0.0150
				0.0050

Table 3.14 Reaction order with respect to Fe^{2+}

Nitrobenzene (M)	H_2O_2 (M)	Metal oxide (grams)	pH	Fe^{2+} (M)
0.01	0.0500	100	2.8±0.2	0.00200
				0.00100
				0.00075
				0.00050
				0.00025

C.3 Oxidation of combined nitrobenzene and aniline

Table 3.15 Effect of aniline and nitrobenzene combination

Nitrobenzene (M)	Fe^{2+} (mM)	Metal oxide (grams)	H_2O_2 (M)	pH	Aniline (M)
0.002 (4:1)	1	100	0.05	2.8±0.2	0.008 (4:1)
0.004 (3:2)					0.006 (3:2)
0.005 (1:1)					0.005 (1:1)
0.006 (2:3)					0.004 (2:3)
0.008 (1:4)					0.002 (1:4)

Table 3.16 Effect of H_2O_2

Nitrobenzene (M)	Aniline (M)	Fe^{2+} (mM)	Metal oxide (grams)	pH	H_2O_2 (M)
0.005	0.005	1	100	2.8±0.2	0.1000
					0.0500
					0.0250
					0.0150
					0.0050

Table 3.17 Effect of Fe^{2+}

Nitrobenzene (M)	Aniline (M)	H_2O_2 (M)	Metal oxide (grams)	pH	Fe^{2+} (M)
0.005	0.005	0.0500	100	2.8±0.2	0.00200
					0.00100
					0.00075
					0.00050
					0.00025

D. Comparison between different media

Table 3.18 Effect of media type on aniline oxidation in FBR

Aniline (M)	H_2O_2 (M)	Fe^{2+} (mM)	pH	Media
0.005	0.0500	1	2.8±0.2	Al_2O_3
				SiO_2

Table 3.19 Effect of media type on nitrobenzene oxidation in FBR

Nitrobenzene (M)	H_2O_2 (M)	Fe^{2+} (mM)	pH	Media
0.005	0.0500	1	2.8±0.2	Al_2O_3
				SiO_2

E. Investigation on the effect of stepwise addition of Fenton's reagent

Table 3.20 The effect of stepwise at the pH 2.8

Nitrobenzene (M)	Aniline (M)	pH	Metal oxide (grams)	H_2O_2 (M)		Fe^{2+} (mM)	
				Initial	After 30min	Initial	After 30min
0.005	0.005	2.8±0.2	100	0.05	-	1	-
				0.05	0.005	1	0.1
				0.05	0.025	1	-

Table 3.21 The effect of stepwise at the pH 3.6

Nitrobenzene (M)	Aniline (M)	pH	Metal oxide (grams)	H_2O_2 (M)		Fe^{2+} (mM)	
				Initial	After 30min	Initial	After 30min
0.005	0.005	3.6±0.2	100	0.05	-	1	-
				0.05	0.005	1	0.1
				0.05	-	1	0.5
				0.05	0.025	1	0.5

F. Determination of the reusability of metal oxide (Al_2O_3)

Table 3.22 determination of the reusability of metal oxide (Al_2O_3)

Nitrobenzene (M)	Aniline (M)	H_2O_2 (M)	Fe^{2+} (mM)	pH	Al_2O_3 100g
0.005	0.005	0.0500	1	2.8±0.2	Cycle 1st
					Cycle 2nd
					Cycle 3rd
					Cycle 4th
					Cycle 5th

3.4 Analytical Methods

3.4.1. Measurement of nitrobenzene and aniline

First of all, the liquid samples were filtered through 0.45 μm syringe microfilters to separate precipitated iron from the solutions. Next, the analysis of residual sample were addressed by using a HP4890 gas chromatograph equipped with a frame ionization detector and HP-5 (Hewlett-Packard) capillary column (0.53 mm x 15 m length). The chromatographic conditions for nitrobenzene were as follows 1st level ; initial oven temperature at 85 ˚C increased to 110 ˚C of final oven temperature with 12 ˚C /min.: 2nd level: initial oven temperature at 110 ˚C was reached to 200 ˚C of final oven temperature for 1 minute with 20 ˚C / minutes. And, the initial oven temperature at 85 ˚C for 1.50 minutes, final oven temperature was 200 ˚C with and increasing rate of 65 ˚C/ minutes were operated for the chromatographic condition of aniline. Operation also included injector temperature of 250 ˚C, detector temperature of 250 ˚C, and nitrogen carrier gas, flow rate at 14.6 ml/minutes.

3.4.2 Analysis of total organic carbon

The SHIMADZU TOC-V_{CPH} was used for analyzing of total organic carbon. Before the analysis, all supernatants were diluted 10 times by NaOH, and then the solutions were filtered with 0.45 μm. microfilters to separate iron sludge from the solutions.

3.4.3 Analysis of total iron concentration

The samples were digested by nitric acid and diluted 8 times by RO water. Then, the samples were filtered with 0.45 μm microfilters to separate small particles from the solutions. Next, the total iron concentration was analyzed using a HITACHI Z6100 polarized Zeeman atomic absorption spectrophotometer.

3.4.4 Analysis of ferrous concentration

The samples were analyzed by phenanthroline method in Appendix A. The RO water was added to making up to volume to 50 ml. The RO water mixed with the sample but no phenanthroline was used as a blank for every sample

3.4.5 Other measurements

The concentration of hydrogen peroxide was determined by standard iodometric method which potassium iodie was used as a reactant as described in Appendix B. The pH measurement was carried out by a SUNTEX TS-1 Digital pH/MV meter. COD was measured by closed reflex titrimetric method (Kingzett, C.T., 1880).

CHAPTER IV

RESULTS AND DISCUSSIONS

4.1 Media Characterization

4.1.1 Point of zero charge (pzc) of Aluminum oxide and Silica Oxide

Mass titration method was selected to determinate the pzc of metal oxide. The addition subsequent portions of metal oxide to the water or an aqueous electrolyte solution might be acidified or contain a base were carried out. The pH of the system changes gradually and approaches a constant value, which is the pzc in the case of pure oxide. This method is based on the postulate that pzc value is associated with pH of minimal solubility that allows to deduce pzc value from equilibrium pH of a concentration (Reymond, 1999). Also, Preocanin (1998) described the relationship between the change in H^+ and OH^- concentrations in the bulk of the solution and the mass concentration of the suspension as shown in equations (4.1) and (4.2).

$$\Delta c(H^+) - \Delta c(OH^-) = \gamma(k-b) - \gamma s(\Gamma(MOH_2^+) - \Gamma(MO^-) \qquad (4.1)$$

Equation (4.1) is based on equations (2.15) to (2.17) where Γ and s stand for surface concentration and specific surface area, respectively. The portions of acidic or basic impurities (if any are present) are expressed as tractions (k or b) and γ is the mass concentration of the solid phase. In Addition, the changes in the concentration of

H^+ and OH^- ions maybe obtained from pH measurements where y stand for the activity co-efficient as shown in equations (4.2) and (4.3).

$$\Delta c(H^+) = \frac{c^\circ}{y}\left(10^{-pH_\gamma} - 10^{-pH_0}\right) \qquad (4.2)$$

$$\Delta c(OH^-) = \frac{c^\circ}{y}\left(10^{pH_\gamma - pK_w} - 10^{pH_0 - pK_w}\right) \qquad (4.3)$$

From the experimental results, the pzc of media, i.e., Al_2O_3 and SiO_2, are shown in the Figure 4.1(a) and (b). The pH of suspensions was measured after 24 hr of contact time. Experiments with de-ionized water (DI) represented the situation of no ionic strength whereas those with synthetic wastewater referred to the real situation. In case of Al_2O_3 (Figure 4.1(a)), the pH increased with increasing Al_2O_3 dosage. Regardless of the ionic strength, pH of both solutions increased rapidly at the first stage and was asymptote at 8.44. On the other hand, the pH of SiO_2 suspensions with and without ionic strength dropped rapidly at the initial stage and leaned toward 6.54. This implies that the ionic strength causing by aniline and 0.025 M of Na_2SO_4 had no significant impact on pzc of the media. Reymond (1999) stated that various ions could cause a screen effect on the surface charge but the pzc might not be altered if the ions were not specifically adsorbed on the carriers. These results indicated that the surfaces of both media were positively charged since the working pH range was 2.4-4.0 which was lower than the pzc. The table 4.1 compares the pzc of metal oxide obtained in this study with those from other studies. It can be seen that the pzc of metal oxide obtained from this study was within the range reported by other researchers.

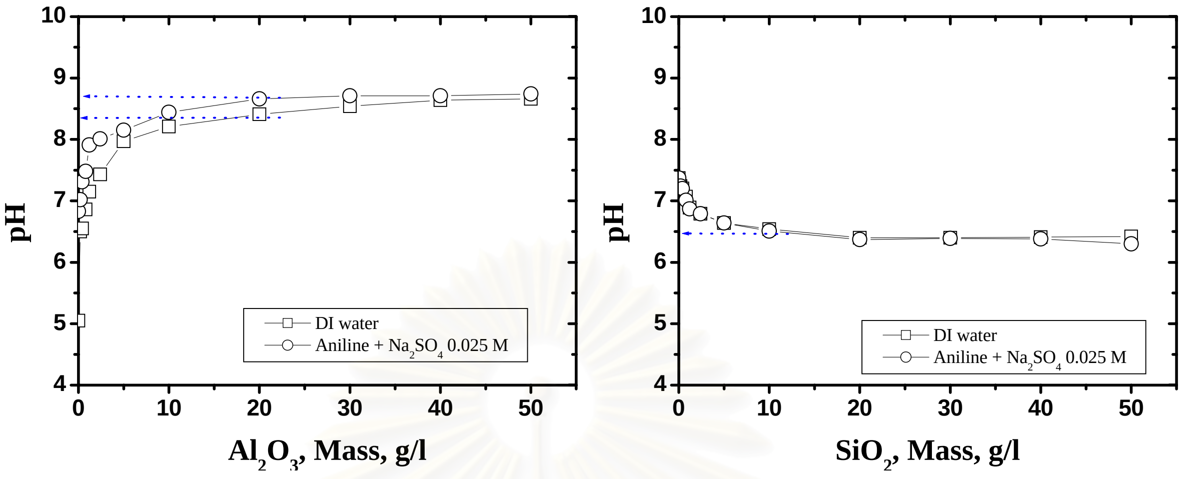

(a) pH of experimental solution in Al_2O_3 (b) pH of experimental solution in SiO_2

Figure 4.1 Measurement of point of zero charge of the carriers by mass titration

Table 4.1 Comparison point of zero charge of metal oxide

Metal oxide	Description	Salt	pH_{pzc}	Source
Al_2O_3 SiO_2	0.01 AN	0.025 M Na_2SO_4	8.4 6.5	This study
γ- Al_2O_3 SiO_2	American Cyanameid Cabot L90	- -	7.4 3.2	Noh and Schwarz (1988)
γ- Al_2O_3	-	KNO_3	7.5	Mustafa et al. (1998)
γ- Al_2O_3	Degussa	-	6.9	Remond et al. (1999)
	Procatayse	-	8.4	
SiO_2 (Aerosil)	Degussa	-	3.5	
SiO_2 (Silica gel)	Rhône-Poulene	-	6.2	
SiO_2 (Tixosil)	Rhône-Poulene	-	6.7	
SiO_2 (Silica)	Lobo	-	10.6	
γ- Al_2O_3 (gibbsite)	-	-	8.1-9.6	Jodin (2005)

4.1.2 Surface Property of Media

In this study, Al_2O_3 was used principally through out the experiments. From visual observation, Al_2O_3 had white color with ragged circle shape and average diameter of 2.5 mm. The results from BET analysis revealed the surface area and average aperture information were 314 m^2/g and 10.89° respectively. From EDX analysis, this carrier consists of 49.97% of aluminum and 50.03% of oxygen by weight. SiO_2 was a light-brown grain shape with the average diameter of 0.5 mm.

4.2 Control Experiments

This experimental part aimed to determine the degradation of target compounds in FBR deriving from each individual constituent via non-Fenton reaction as specified in Tables 3.1 and 3.4 in Chapter 3. Figure 4.2 exhibits that nitrobenzene (NB) and aniline (AN) concentrations were not significantly reduced in all control tests, i.e., only 18% or less for NB and 12% or less for AN. The disappearance of NB and AN could be derived from many reasons. Oxidation by H_2O_2 should be insignificant since both NB and AN reaching a plateau while more 86% of H_2O_2 of still presented in the solution. Volatilization to the atmosphere could be a minor leak of NB and AN due to their low vapor pressure of 1.0 and 0.67 mm Hg, respectively. It is believed that the adsorption onto the surface of carriers and apparatus was the major reason for the NB and AN depletion. From these results, it implies that both of these target compounds could not be degraded effectively and rapidly without an involvement of hydroxyl radicals under the studied conditions.

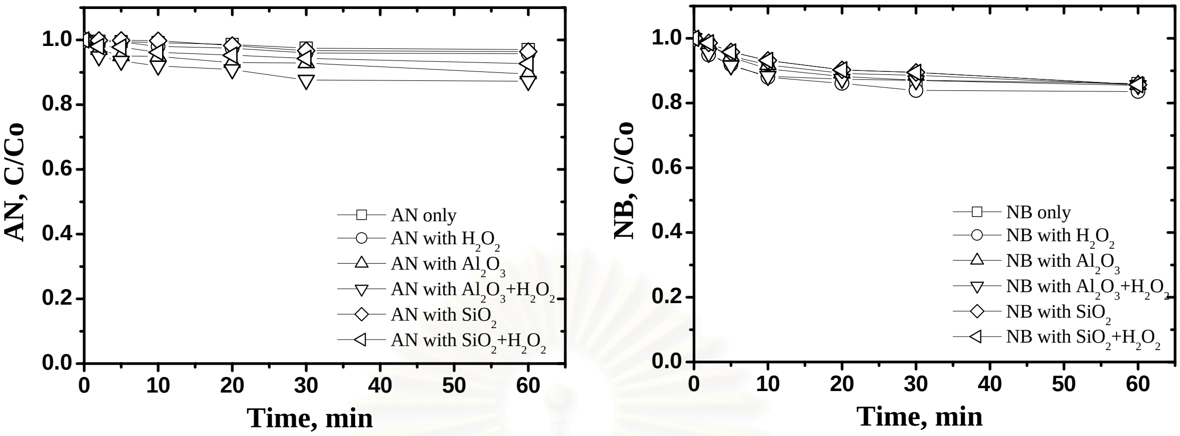

(a) Aniline remaining (b) Nitrobenzene remaining

Figure 4.2 The control experiment in FBR; 0.01 M of AN, 0.01 of NB, 0.05 M of H_2O_2 and initial pH 2.8

4.3 Media Comparison

Effects of carriers (Al_2O_3 and SiO_2) on the degradation of NB, AN and AN/NB were investigated. Interested parameters were removal efficiency and iron pelletization in order to reduce the amount of iron oxide which is the major drawback of Fenton process. The carriers which have different elements were operated in this scenario. The properties of the solid particles have major influence on fluidization (Rodriguez et al., 2000a). The dissimilar media properties could induce the different removal efficiency behavior of target compounds.

Figure 4.3 compares the characteristics of the FBR regarding on system performance using Al_2O_3 or SiO_2 as the media. Within the first 5 min, the characteristics of both systems including AN, H_2O_2, Fe^{2+}, and TOC were quite similar. With the generation of $OH^{\bullet}$ via Fenton regent, AN was oxidized much more efficiently than in the presence of H_2O_2 alone. However, the system with Al_2O_3 showed a better removal of AN (Figure 4.3(a)) and Fe^{2+} (Figure 4.3(c)) in the later stage than SiO_2, i.e., 95.8 versus 44.6% and 93.4 versus 65.7%, respectively. This means more Fe^{2+} was converted to Fe^{3+} in the presence of Al_2O_3 than SiO_2. H_2O_2 consumption was also higher in Al_2O_3 system than in SiO_2 system as shown in Figure 4.3(b) which corresponded very well with AN degradation. This implies that might be due to the difference in pzc of both media, i.e., 8.21 for Al_2O_3 and 6.54 for SiO_2; hence, at working pH of 2.8, surface of Al_2O_3 was more positively charged than those of SiO_2. This might somehow effect on the formation of $OH^{\bullet}$. Nonetheless, it is interesting to observe that the TOC in both systems was comparable through out the experimental period of 60 min (Figure 4.3(d)). With only 13% removal within the reaction period of 60 min, it implies that complete mineralization did not occur in the FBR under the studied conditions. Most of the intermediate organics still remained in the solution.

Similarly, Figure 4.4 compared the characteristics for NB removal between Al_2O_3 and SiO_2. It was interesting in the scenario that the degradations of NB (Figure 4.4(a)) and H_2O_2 (Figure 4.4(b)) were comparable for both carriers. The disappearance of NB was more rapid than AN which implies that NB is more susceptible to $OH^{\bullet}$ than AN. Another important point is the profile of H_2O_2 which was much lower than in the case of AN implying that NB may involve or accelerate the decomposition of H_2O_2. Again, Al_2O_3 could remove Fe^{2+} better than SiO_2, i.e., 83.1 and 65.7%, respectively. The phenomenon in the FBR system was very complicated since the surface area of the media of SiO_2 was much more than those of

Al_2O_3 but the pelletization became poorer. Considering on TOC removal (Figure 4.4(d)), the efficiency was better with Al_2O_3 (29.3%) than with SiO_2 (27.9%); nonetheless, these numbers were higher than in the case of AN. This is because NB is one of the intermediates of AN oxidation; therefore, the mineralization pathway of NB is shorter or simpler than AN (Brillas et al, 1998).

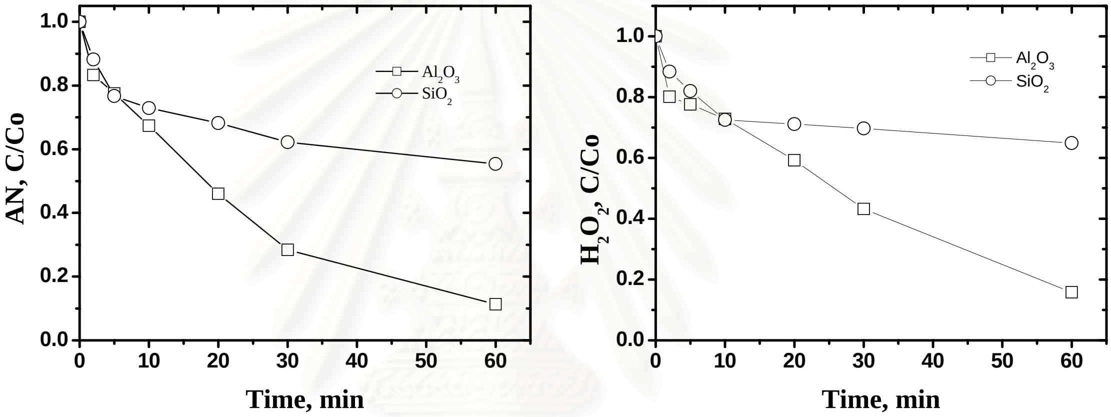

(a) Aniline remaining (b) H_2O_2 remaining

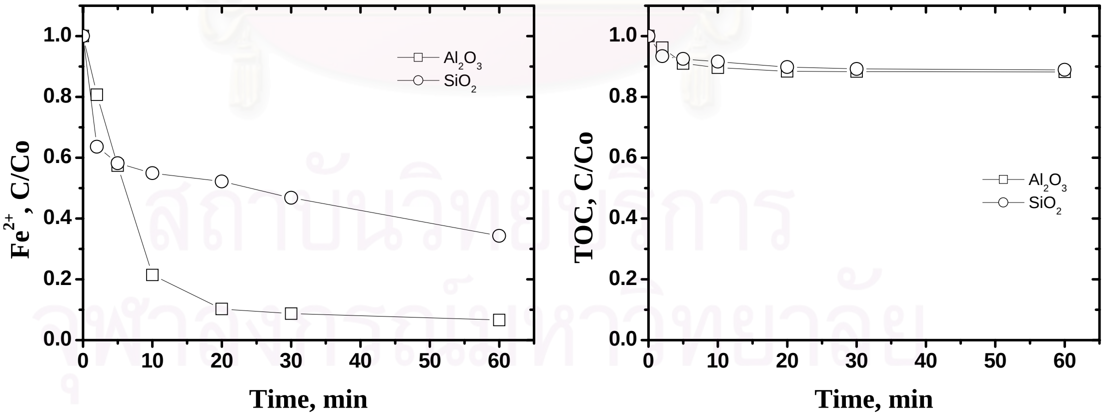

(c) Fe^{2+} remaining (d) TOC remaining

Figure 4.3 Effect of media: 0.01 M of AN, 0.05 M of H_2O_2, 0.001 M of Fe^{2+}, 74.07 g/l of the media and initial pH 2.8.

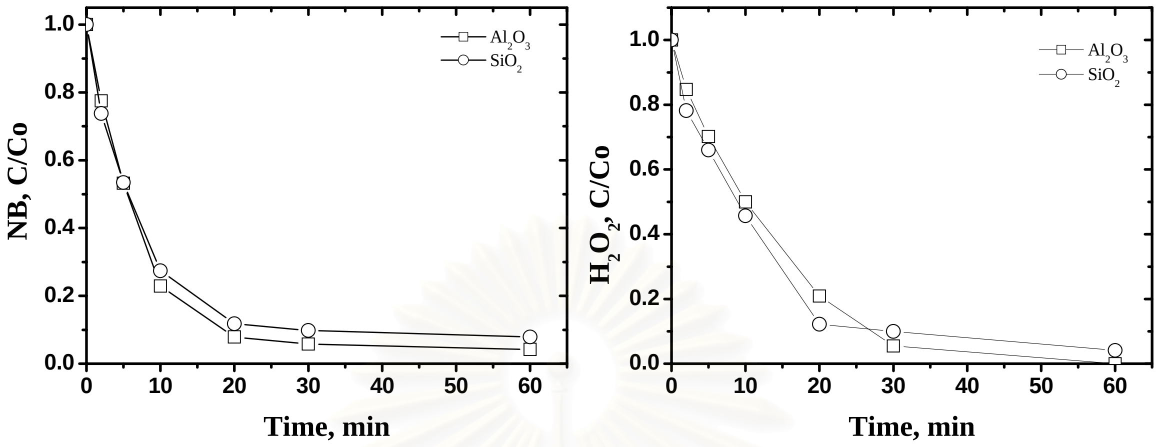

(a) Nitrobenzene remaining (b) H_2O_2 remaining

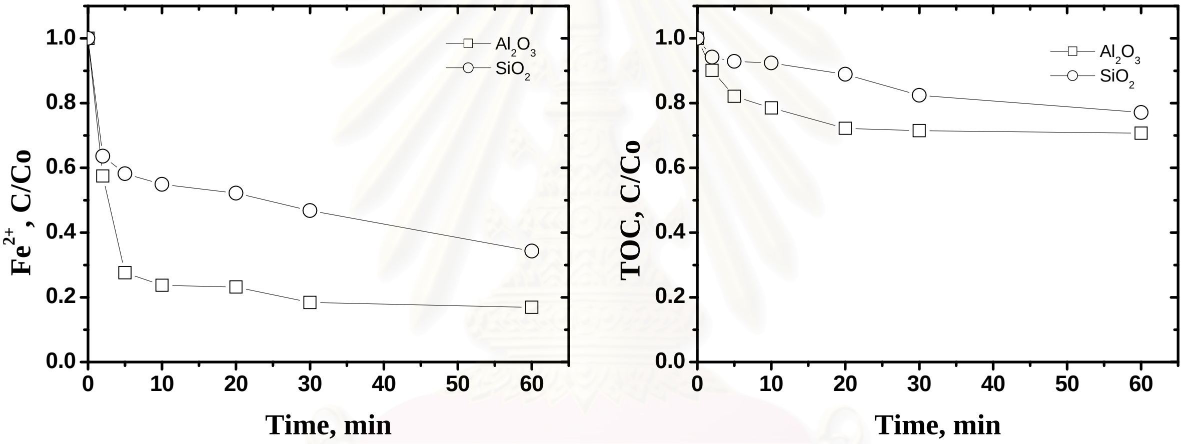

(c) Fe^{2+} remaining (d) TOC remaining

Figure 4.4 The media comparison onto nitrobenzene oxidation; 0.01 M of NB, 0.05 M of H_2O_2, 0.001 M of Fe^{2+}, 74.07 g/l of the media and initial pH 2.8.

In conclusion, Al_2O_3 proved to be a better carrier for AN and NB oxidation in the FBR system than the SiO_2. It is believed to be due to the higher pzc of Al_2O_3 which created more positive charged surface than SiO_2. This not only involved with the compound oxidation but also related to Fe^{2+} removal.

4.4 pH optimization for Fluidized-bed Fenton process

In this experiment, the optimization of pH for fluidized-bed Fenton process was examined for AN, NB, and AN/NB. Typical range for Fenton process is in the acidic range in which abundant protons are available or the decomposition of H_2O_2 to produce the maximum amount of $OH^{\bullet}$. Consequently, it is essential to determine the optimum pH for the FBR process which can provide the best performance.

4.4.1 Effect of pH on Aniline Degradation

In this scenario, the solution pH was operated initially at 2.4, 2.8, 3.2, 3.6 and 4.0. In the Figures 4.5(a) and (e), the degradation rate of AN increased from 2.1 to 2.9 mM/min as the pH decreased from 4 to 3.6, respectively, and remained comparably at 3.1 mM/min at pH 3.2. However, as pH is at 2.8 and 2.4, the rate became slower particularly i.e., 0.8 and 0.3 mM/min, respectively. All experiments except at pH 2.4 AN could be removed up to 90% within 60 min. As a result, optimum pH for AN oxidation by FBR Fenton process with Al_2O_3 as a carrier was 3.2 to 3.6. Consumption of H_2O_2 followed closely with the decomposition of AN as shown in Figure 4.5(b). However, Fe^{2+} was consumed largely between pH 2.8 and 3.2 with the maximum usage of greater than 95%. Figure 4.5(d) shows the crystallization performance of Al_2O_3 with respect to pH. The optimum pH for iron crystallization was found to be at 2.8 with more than 40% of removal efficiency.

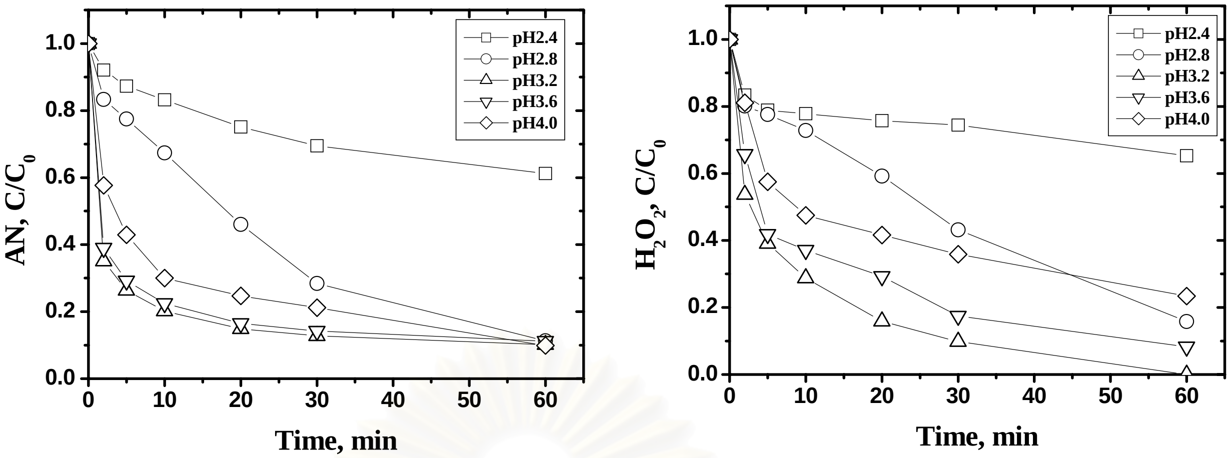

(a) Aniline remaining (b) H_2O_2 remaining

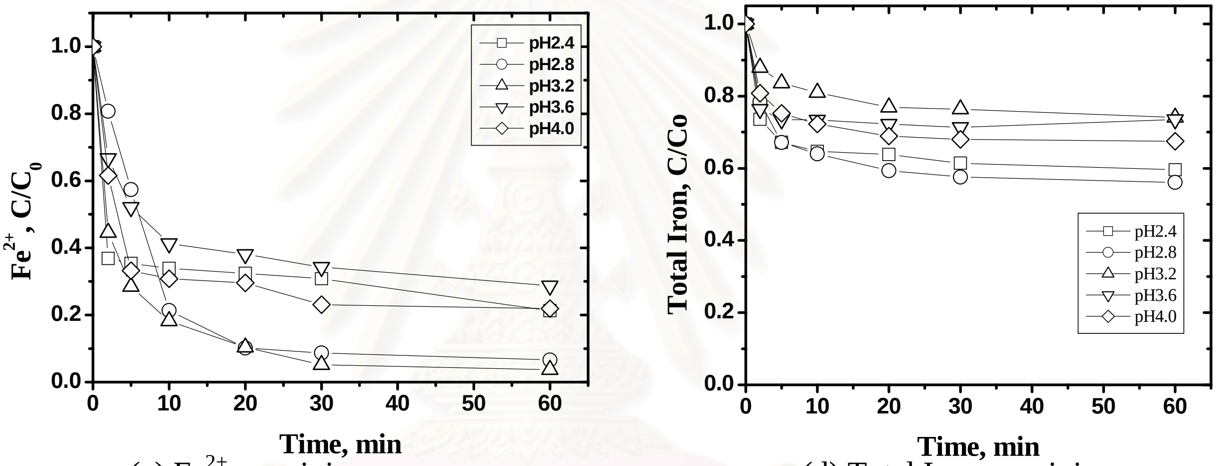

(c) Fe^{2+} remaining (d) Total Iron remaining

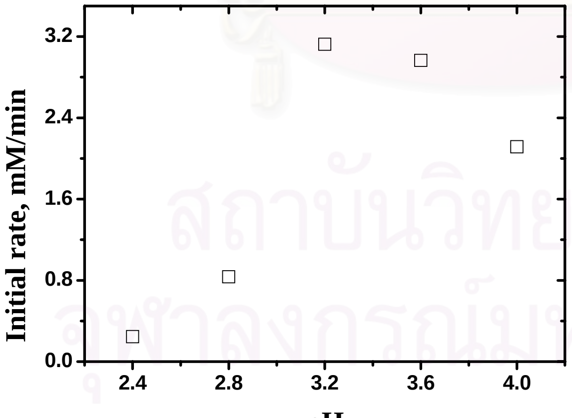

(e) Initial rate of Aniline

Figure 4.5 The optimization pH oxidation of the individual compound in FBR; 0.01 M of AN, 0.05 M of H_2O_2 , 0.001 M of Fe^{2+}, 74.07 g/l of Al_2O_3.

4.4.2 Effect of pH on Nitrobenzene Degradation

Similar to previous scenario, the pH was varied from 2.4 to 2.8, 3.2, 3.6 and 4.0 and the results were summarized in Figure 4.6. Optimum pH for NB oxidation was 2.8 with the maximum efficiency of 95.2%. Removal of iron via surface crystallization was comparable in all pHs.

4.4.3 Effect of pH on Combined Aniline and Nitrobenzene Degradation

Figure 4.7 shows profiles of all important parameters obtained from this part. Optimum pH for AN was still at 3.2 whereas for NB degradation was slightly changed from 2.8 to 3.2. Consumptions of H_2O_2 and Fe^{2+} were quite steady regardless on pH except for the Fe^{2+} at pH 3.6 which was consumed intensively as compared to the other pH.

As a result, pH 2.8 was selected for the optimum conditions for both AN and NB oxidation as well as iron crystallization. All experiments afterward were conducted at the initial pH 2.8.

4.5 Comparison between Traditional Fenton and Fluidized-bed Fenton Processes

To compare the performance of traditional and fluidized-bed Fenton processes, the optimum conditions from previous sections have been employed, i.e., using Al_2O_3 as the carrier and working at the optimum pH of each scenario (3.2, 2.8, and 2.8 for AN alone, NB alone, and combined AN/NB, respectively).

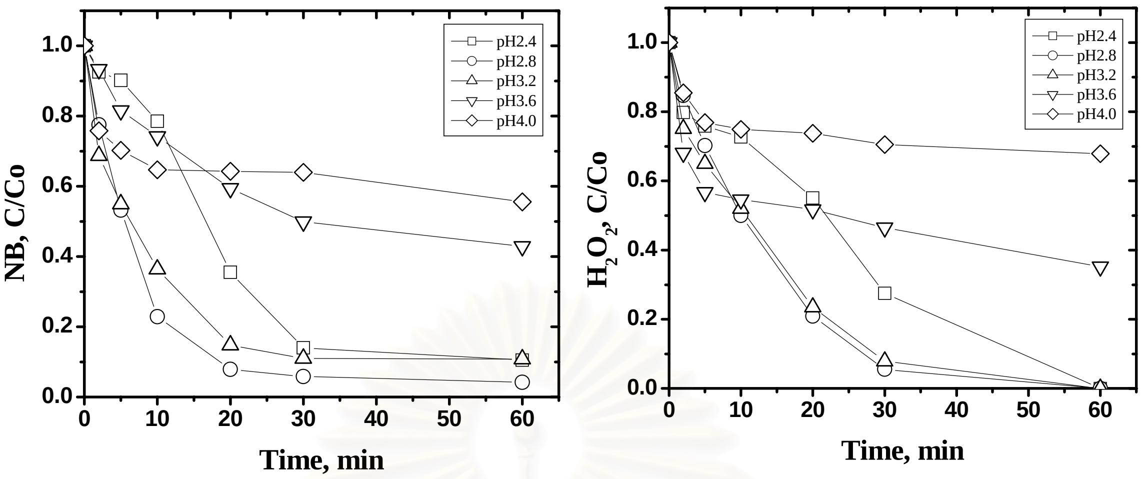

(a) Nitrobenzene remaining (b) H_2O_2 remaining

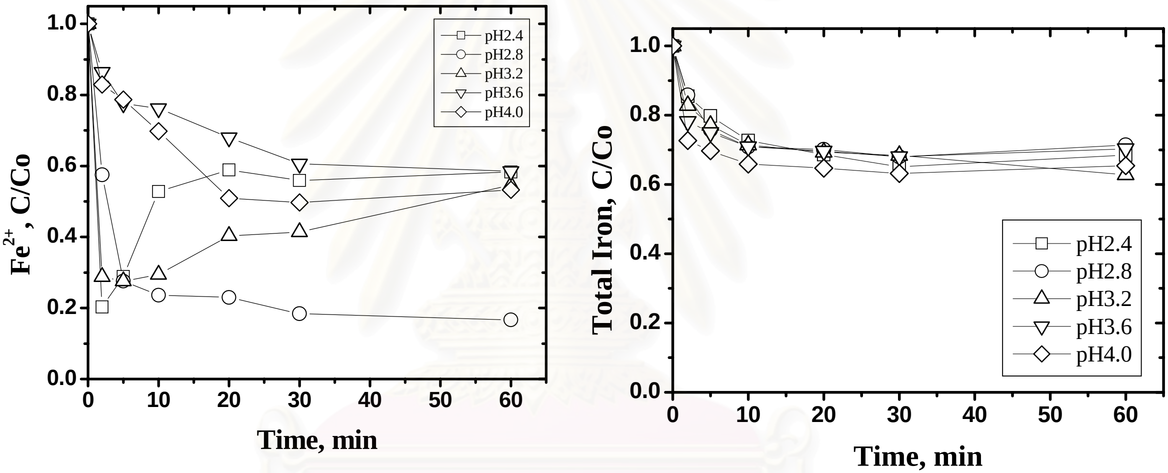

(c) Fe^{2+} remaining (d) Total Iron remaining

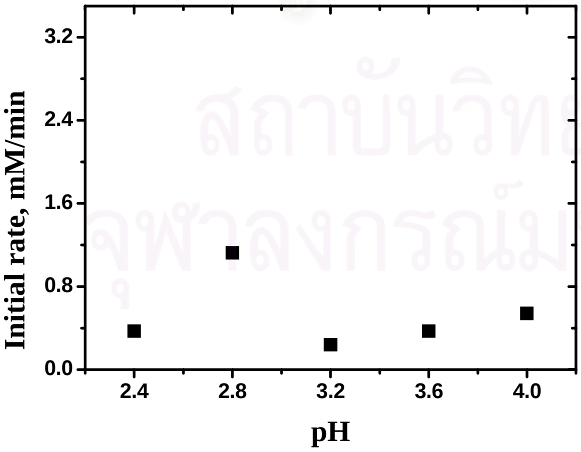

(e) Initial rate of Nitrobenzene

Figure 4.6 The optimization pH oxidation of the individual compound in FBR; 0.01 M of NB, 0.05 M of H_2O_2 , 0.001 M of Fe^{2+}, 74.07 g/l of Al_2O_3.

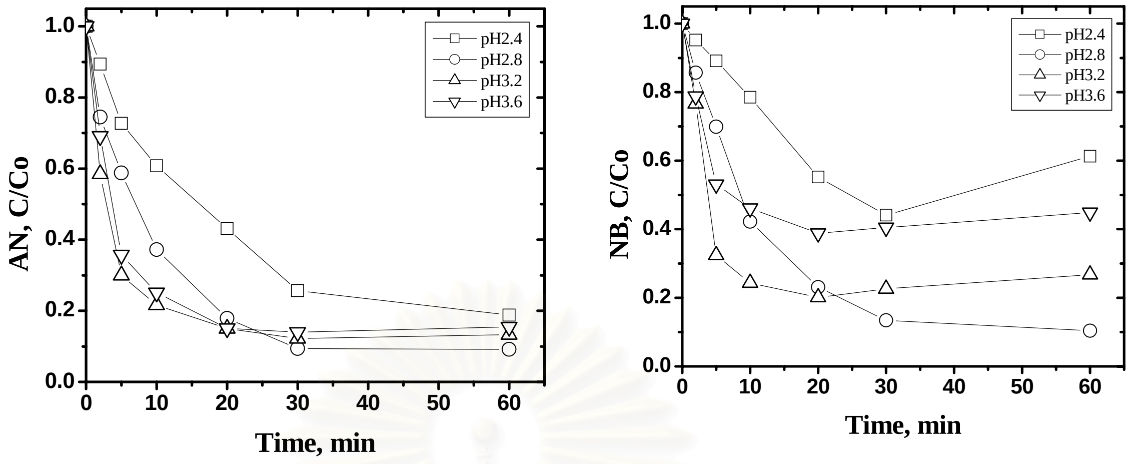

(a) Aniline remaining (b) Nitrobenzene remaining

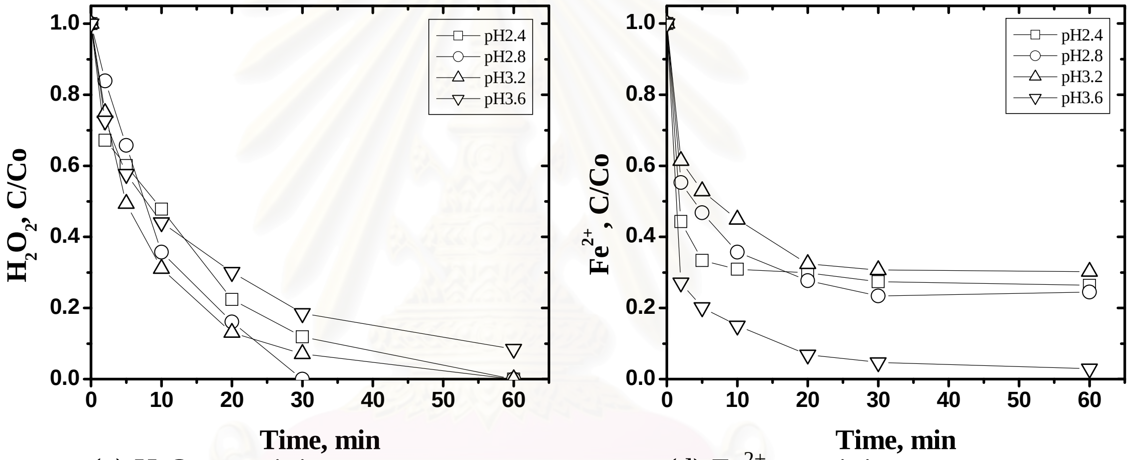

(c) H_2O_2 remaining (d) Fe^{2+} remaining

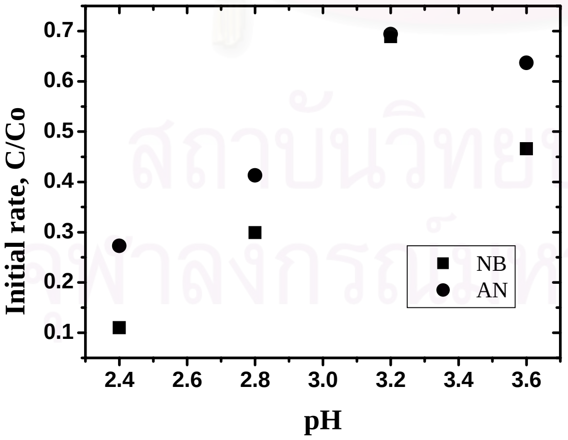

(e) Initial rate of the combination target compounds

Figure 4.7 The optimization pH oxidation of the combination compound in FBR; 0.005 M of AN, 0.005 M of NB, 0.05 M of H_2O_2 , 0.001 M of Fe^{2+}, 74.07 g/l of Al_2O_3.

4.5.1 Oxidation of aniline in Fenton and FB-Fenton processes

Figure 4.9 summarizes the results for AN decomposition by both traditional and fluidized-bed Fenton processes. Under this scenario, the data repeatability and reliability were also determined as shown in Figure 4.8 (a) as an example case in which the Fenton experiment was triplicate. It can be seen from the figure that data obtained from three different runs with similar conditions were almost the same; hence, verified the consistency of experimental set up and procedure. Considering on AN removal from Figure 4.8(a), it can be seen that initial AN removal rates of 3.38 mM/min for Fenton and 3.13 mM/min for FBR and efficiencies of 83.25% for Fenton and 89.54% for FBR were comparable. This is expected in the system with abundant Fe^{2+} since the major function of FBR is to crystallize the Fe^{3+} onto the carrier rather than to improve the performance of organic oxidation. This finding is in agreement with the study of Sakunkitmasak (2004) who found that the removal rate of NB by ordinary Fenton process was better than FBR at Fe^{2+} dosage of 0.5 mM. However, as the Fe^{2+} dosage increased to 0.667 mM, the rates between the two processes became closer and were not distinguishable between the two as the Fe^{2+} increased to 1 and 2 mM. With the conditions used in this study, complete oxidation of AN could not be achieved within 60 min. This might be due to the insufficient of Fenton reagents particularly the H_2O_2 remaining in the solution. Oxidation rate in the second stage was very slow via Fenton-like reaction similar to the study of Lu et al. (1999). Major differences between ordinary and FBR Fenton processes were the consumption of H_2O_2 and Fe^{2+} as well as the iron removal as shown in Figure 4.8 (b), (c), and (d), respectively. With the presence of carrier in FBR, the heterogeneous reactions became more complicated than those in homogeneous solution. Chou et al. (1999a) synthesized γ-FeOOH on a brick grain support via the oxidation of Fe^{2+} and H_2O_2 as shown in equation (4.4)

$$H_2O_2 + 2Fe^{2+} + H_2O \leftrightarrow 2\,\gamma\text{-FeOOH} + 4H^+ \qquad (4.4)$$

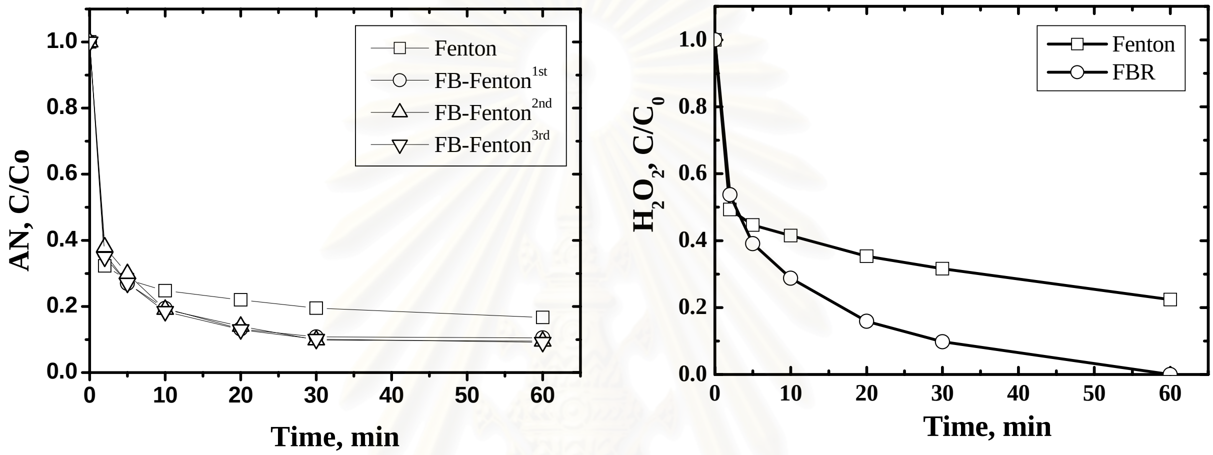

(a) Aniline remaining

(b) H_2O_2 remaining

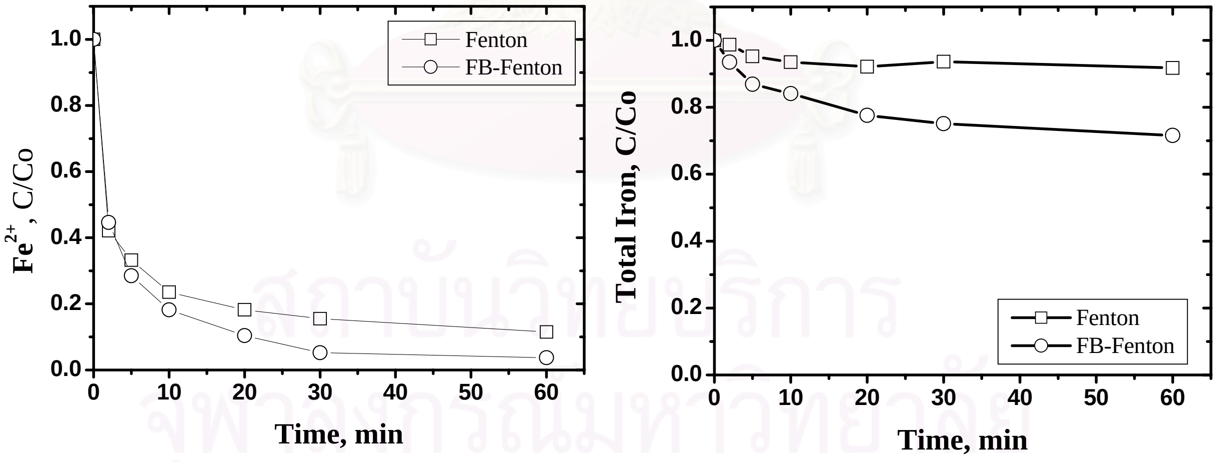

(c) Fe^{2+} remaining

(d) Total iron, remaining

Figure 4.8 The comparison between traditional Fenton process and Fluidized-bed Fenton process at the optimization pH; 0.01 M of AN_{only}, 0.05 M of H_2O_2 , 0.001 M of Fe^{2+}, 74.07 g/l of Al_2O_3, at initial pH 3.2.

Hence, H_2O_2 reacted with Fe^{2+} reacted in more variety ways in the presence of Al_2O_3 resulting that extra H_2O_2 and Fe^{2+} were consumed. As a result from equation (4.1), more iron was removed from the solution by adsorbing and/or crystallizing onto carrier and equipment surfaces (Figure 4.9(d)). Only 8.26% of iron were removed in the ordinary Fenton experiment as compared with 28.4% in FBR experiment.

4.5.2 Oxidation of Nitrobenzene in Fenton and FB-Fenton Processes

Changing the target compound from AN to NB did not make any differences between ordinary and FB Fenton processes in term of organic oxidation as shown in Figure 4.9 (a). NB could not be removed completely within the studied conditions. Lack of H_2O_2 might be the major reason that stopped Fenton-like process. However, the presence of NB led to similar consumption of H_2O_2 and Fe^{2+} (Figure 4.9 (b) and (c)) between ordinary and FB Fenton processes. This differs from the results obtained in the case of AN. According to Figure 2.4, NB is the 2nd generation product of AN oxidation; therefore, the reaction pathways between AN and NB oxidations are slightly different. Although the amount of $OH^{\bullet}$ being generated in AN and NB experiments should be equivalent since the Fenton reagents being added were the same. Most of $OH^{\bullet}$ in AN experiment would react intensively with AN and $C_6H_6N^+$ whereas those in NB experiment would counter with NB, benzoquinonimine, and phenol which are the 3rd-generation intermediates. As a result, the reaction rates of $OH^{\bullet}$ among these compounds were different and led to the variation in H_2O_2 and Fe^{2+} consumptions. Iron removal increased slightly from 28.4% in AN experiment to 32.5% in the presence of NB. This might be due to the involvement of organic radicals in the iron crystallization process.

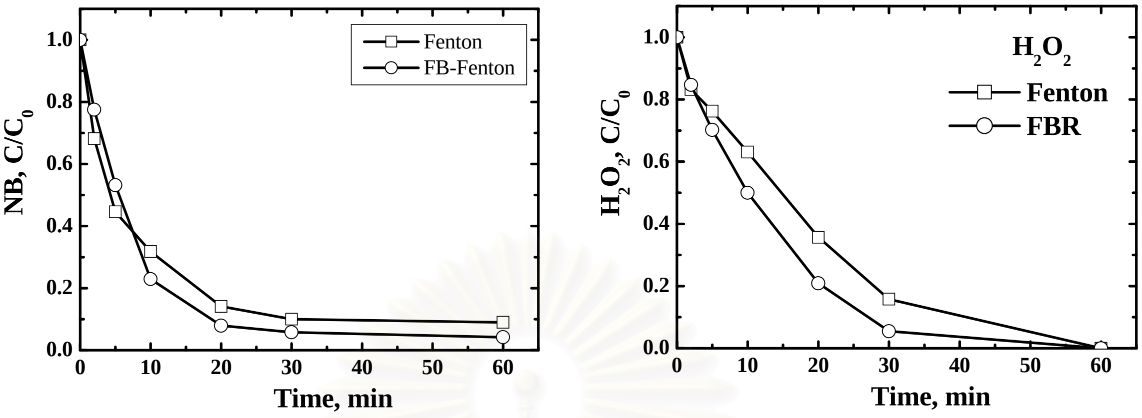

(a) Nitrobenzene remaining

(b) H_2O_2 remaining

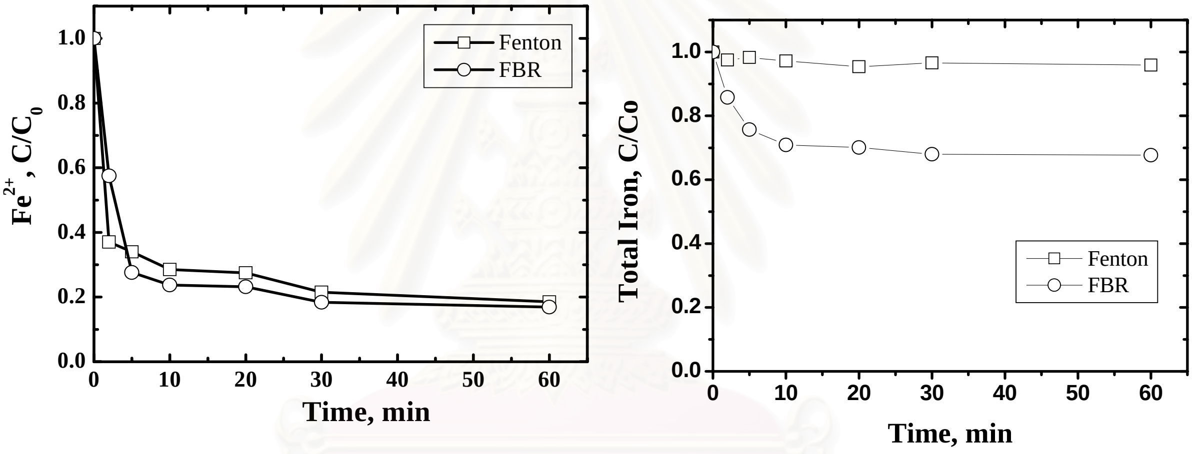

(c) Fe^{2+} remaining

(d) Total iron, remaining

Figure 4.9 The comparison between traditional Fenton process and Fluidized-bed Fenton process at the optimization pH; 0.01 M of NB_{only}, 0.05 M of H_2O_2 , 0.001 M of Fe^{2+}, 74.07 g/l of Al_2O_3 at initial pH 2.8.

4.5.3 Oxidation of Combined Aniline and Nitrobenzene in Fenton and FB-Fenton processes

Again, the removal of AN and NB by both ordinary and FB Fenton processes were quite similar as shown in Figure 4.10 (a) and (b). These results repeatedly confirm that the presence of carriers posed no impact on organic oxidation providing that enough Fe^{2+} has been added. Profiles of H_2O_2 and Fe^{2+} in Figure 4.10 (c) and (d) were similar to those in AN only scenario, i.e., H_2O_2 and Fe^{2+} were consumed to a greater extent in the presence of Al_2O_3. Certain amount of iron was removed from the solution by crystallization onto Al_2O_3 surface (Figure 4.10 (e)). It is interesting to observe that the total iron profiles in either AN only, NB only, and AN/NB scenarios were analogous to Fe^{2+} profiles and not directly related to H_2O_2 profiles. This implies that the crystallization of iron oxide onto carrier surface may require $OH^{\bullet}$ involvement in certain way. Figure 4.10 (f) which is the TOC profile indicates that only 20% of AN and NB was completely mineralized to carbon dioxide gas.

4.6 Kinetic Determination for Fluidized-bed Fenton Process

In this part, the degradation kinetic information of AN, NB and AN+NB by fluidized-bed Fenton process was determined. Initial rate technique was used in order to eliminate any interference from intermediate competitions. For this method, a series of different concentrations for one reactant at a time were performed. The effect of such reactant on the target compound oxidation could be determined by the initial slope on the “target compound concentration” versus “time” plot. The reaction order with respect to each reactant could be determined as a slope on a log-log scale plot between “obtained initial rate” and “reactant concentration”.

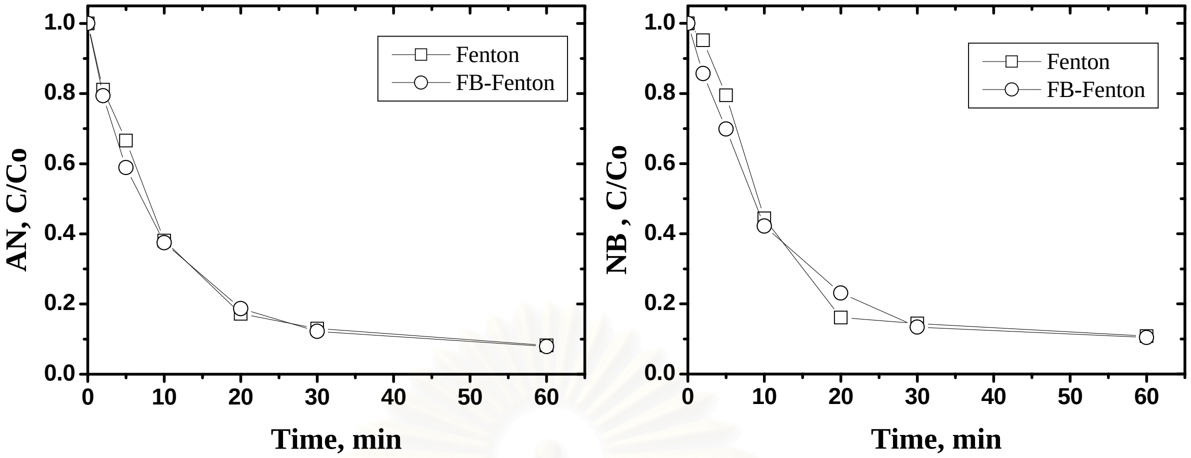

(a) Aniline remaining (b) Nitrobenzene remaining

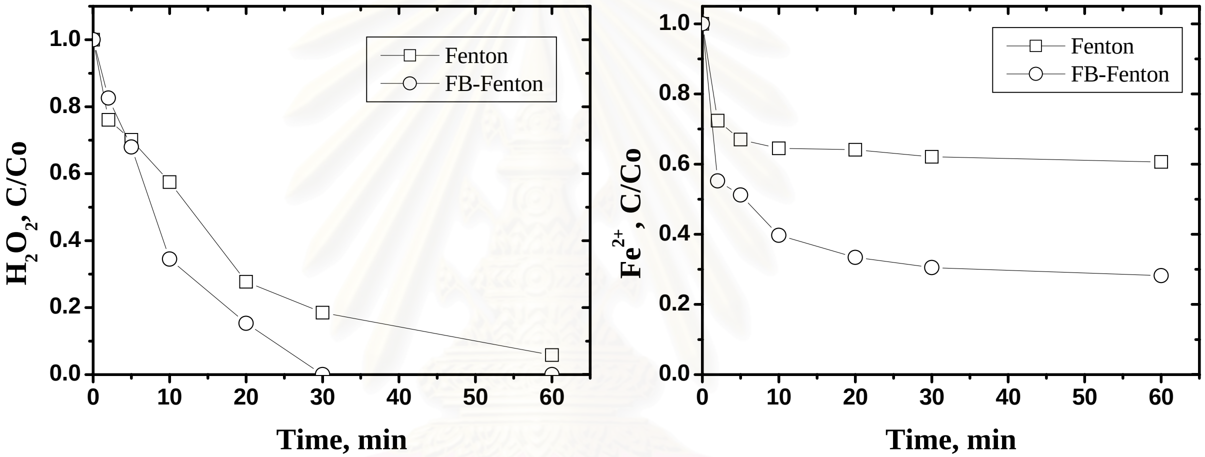

(c) H_2O_2 remaining (d) Fe^{2+} remaining

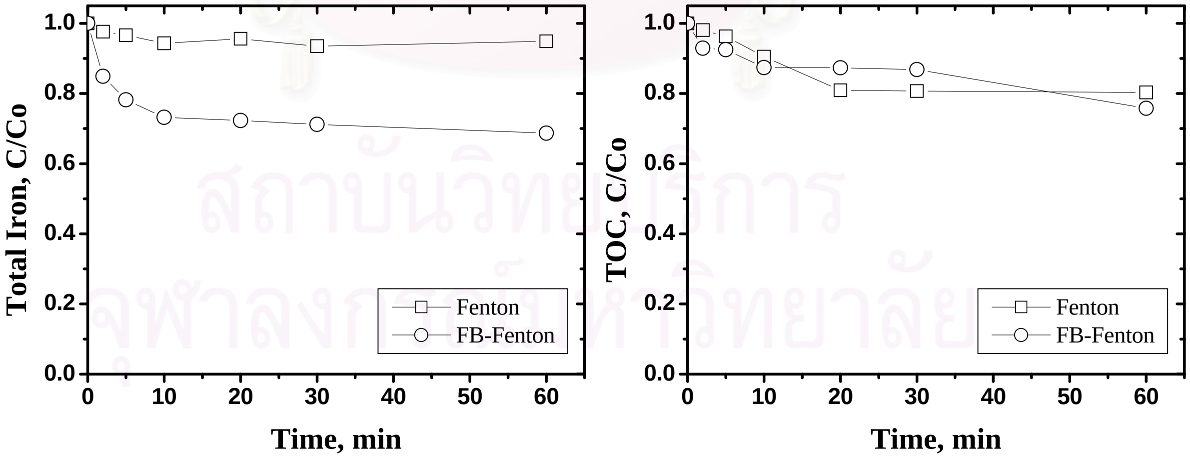

(e) Total iron remaining (f) TOC remaining

Figure 4.10 The comparison between traditional Fenton process and Fluidized-bed Fenton process at the optimization pH; 0.005 of AN_{cb}, 0.005 M of NB_{cb}, 0.05 M of H_2O_2 , 0.001 M of Fe^{2+}, 74.07 g/l of Al_2O_3 at initial pH 2.8.

4.6.1 Effect of Organic Concentration

To determine the effect of AN on the oxidation rate, various AN concentrations of 0.002, 0.004, 0.006, 0.008 and 0.01 M were used with 0.05 M of H_2O_2, 0.001 M of Fe^{2+}, 74.07 g/l of Al_2O_3 at pH 2.8. The results are shown in Figure 4.11. The initial rates increased slightly as the AN concentration increased from 0.002 to 0.01 M. Further analysis in Figure 4.11(e) revealed that these rates had a linear relationship with AN concentration with the R^2 of 0.9856. Hence, the rate equations as a function of AN can be written as

$$-\frac{d[AN_{only}]}{dt} = k_{ANonly}[AN_{only}]^{0.50} \qquad (4.5)$$

where, “k_{ANonly}” is the constant in the system with only AN presence.

Similar to the AN case, the concentrations of NB were varied from 0.002 M to 0.004, 0.006, 0.008 and 0.01 M, respectively, in order to evaluate the impact of NB on the oxidation rate. The results were summarized in Figure 4.12. Linear relationship between initial rate of NB oxidation and NB concentration was also established; hence, the rate equations became:

$$-\frac{d[NB_{only}]}{dt} = k_{NBonly}[NB_{only}]^{0.15} \qquad (4.6)$$

Where “k_{NBonly}” is the apparent rate constant in the system with only NB presence.

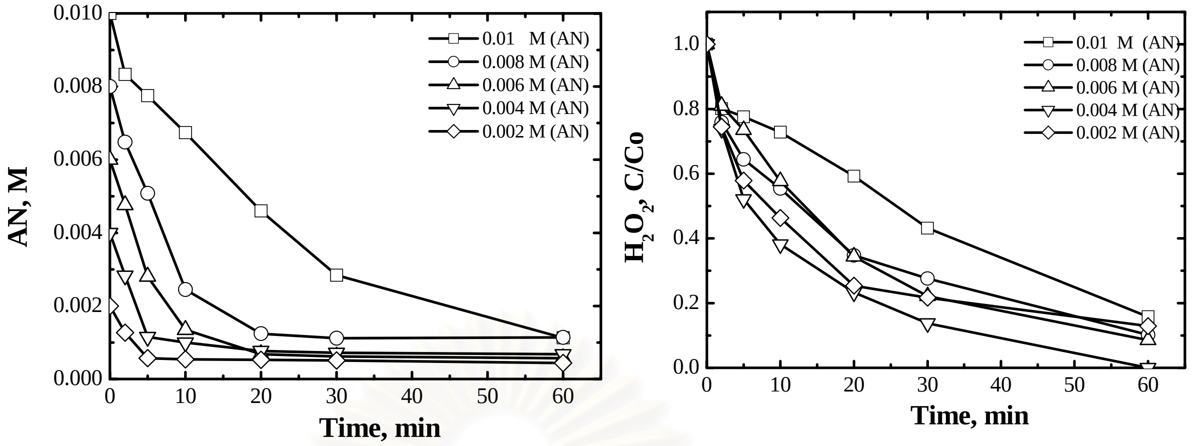

(a) Aniline remaining (b) H_2O_2 remaining

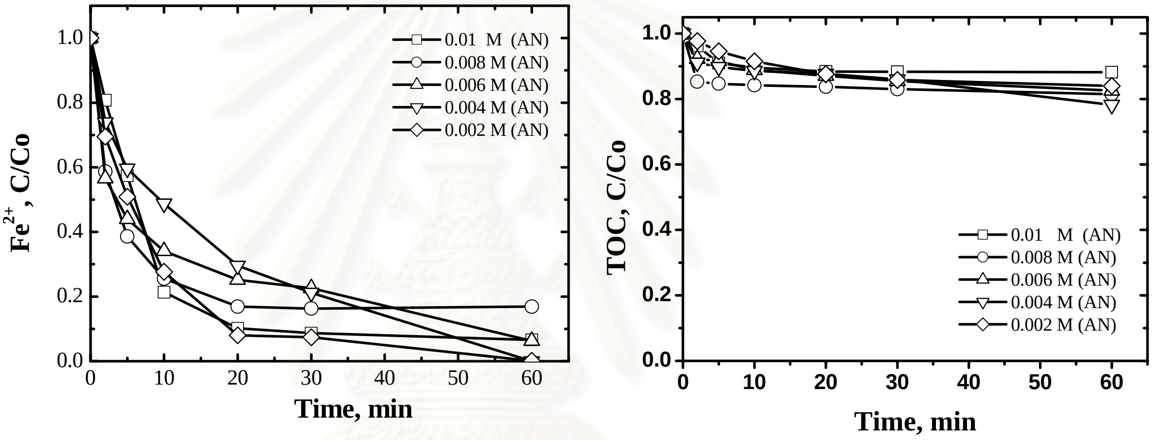

(c) Fe^{2+} remaining (d) TOC remaining

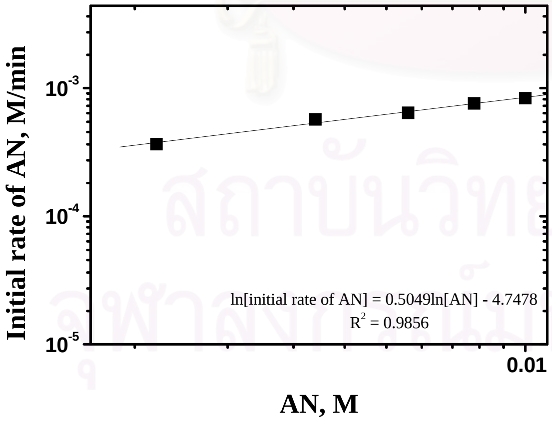

(e) Initial AN removal rate (M/min)

Figure 4.11 Effect of AN concentration; 0.002, 0.004, 0.006, 0.008 and 0.01 M on FB-Fenton process; 0.01 M of AN, 0.05 M of H_2O_2, pH 2.8 and Al_2O_3 of 74.07 g/l.

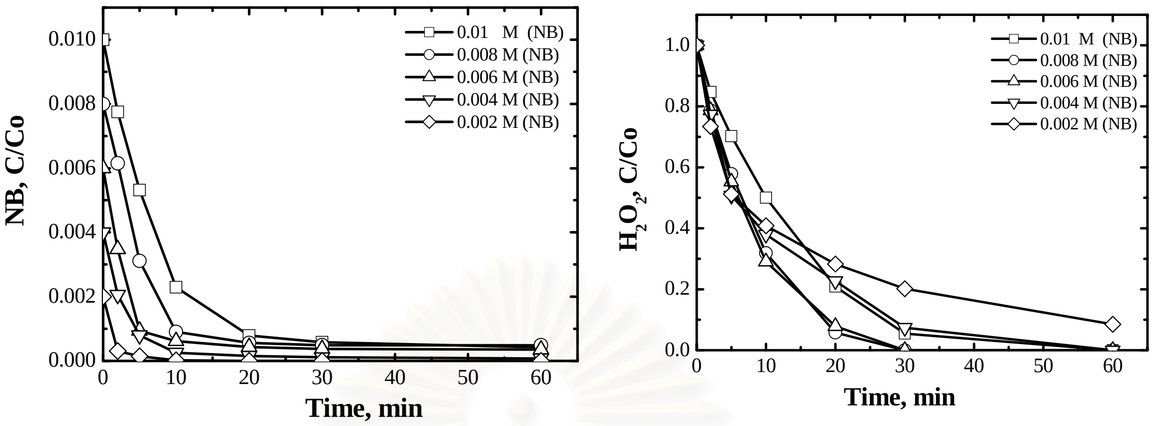

(a) Nitrobenzene remaining (b) H_2O_2 remaining

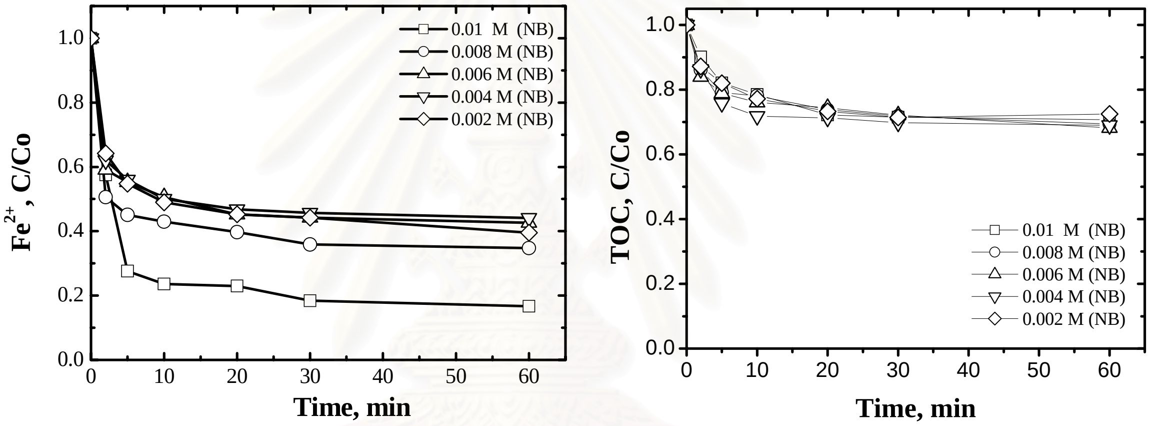

(c) Fe^{2+} remaining (d) TOC remaining

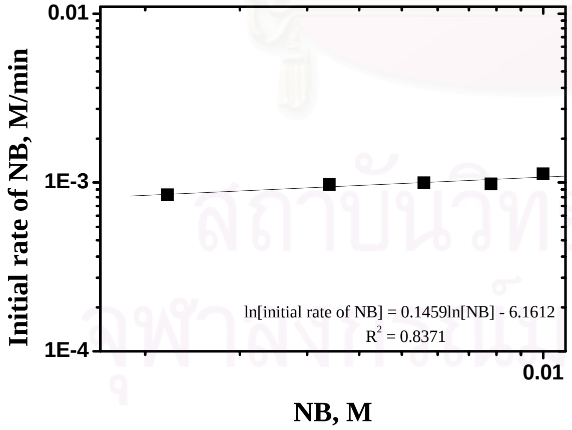

(e) Initial NB removal rate (M/min)

Figure 4.12 Effect of NB concentration; 0.002, 0.004, 0.006, 0.008 and 0.01 M on FB-Fenton process; 0.01 M of AN, 0.05 M of H_2O_2, pH 2.8 and Al_2O_3 of 74.07 g/l.

To better understand the competition between AN and NB in $OH^{\bullet}$ oxidation, several molar ratios of AN and NB were also tested in the FBR and the results are shown in Figure 4.13. It was still found that the initial degradation rates of AN and NB still had the linear relationship with their initial concentrations. As a result, the rate law for each compound can be written as follows:

$$-\frac{d[AN_{cb}]}{dt} = k_{ANcb}[AN_{cb}]^{0.54} \qquad (4.7)$$

$$-\frac{d[NB_{cb}]}{dt} = k_{NBcb}[NB_{cb}]^{1.99} \qquad (4.8)$$

where k_{ANcb} and k_{NBcb} are the constant of AN and NB, respectively, in the system with both AN and NB presence.

4.6.2 Effect of H_2O_2

Fenton's chemistry involved a complex collection of reaction pathways. Its utility as an oxidizing system relied on the formation of hydroxyl radical ($OH^{\bullet}$) from H_2O_2, through the reduction and oxidation (redox) cycles of iron (Fe) and a series of radicals propagation and termination reactions. In this part, various H_2O_2 concentrations of 0.1, 0.05, 0.025, 0.015 and 0.005 M were employed to observe the effect on degradation rate of target compounds. The effects of H_2O_2 dosage on the degradation of AN were shown in Figure 4.14. The results show that initial degradation rates of AN increased with increasing H_2O_2 which were similar to many other studies.

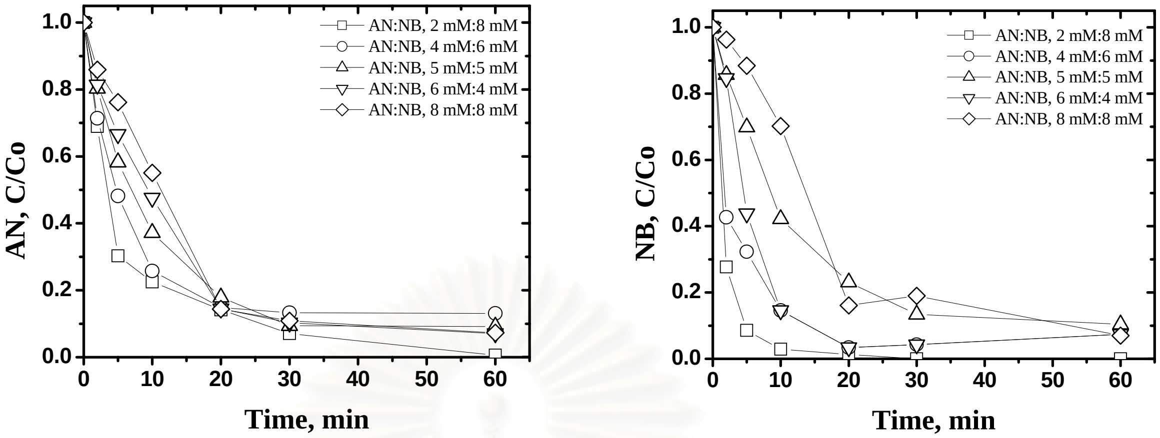

(a) Aniline remaining (b) Nitrobenzene remaining

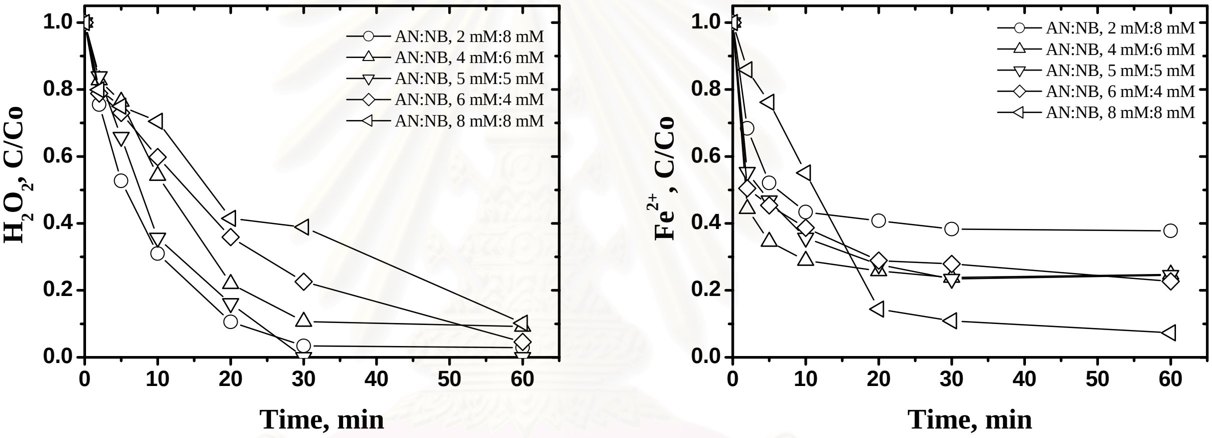

(c) H_2O_2 remaining (d) Fe^{2+} remaining

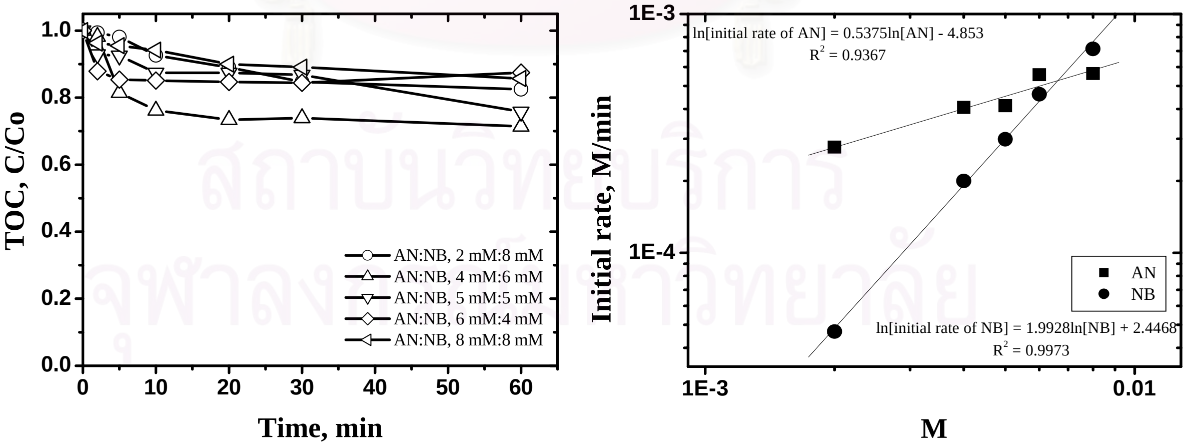

(e) TOC remaining (f) Initial rate of the combination AN/NB

Figure 4.13 Effect of combination AN/NB on molar basis at; 2:8, 4:6, 5:5, 6:4, and 8:2 on FB-Fenton process; 0.001 M of Fe^{2+}, 0.05 M of H_2O_2, pH 2.8 and Al_2O_3 of 74.07 g/l.

Kang et al. (2000) found Fenton process could remove color of the synthetic dye wastewater better when the H_2O_2 dosage increased. Lu et al. (1999) also reported that the oxidation of DDVP by Fenton process proceeded to a greater extent when H_2O_2 increased. Further analysis as shown in Figure 4.14(f) reveals that the initial rates were linearized with H_2O_2 concentration; hence, the rate law became:

$$-\frac{d[AN_{only}]}{dt} = k_{H,ANonly}[H_2O_2]^{0.39} \tag{4.9}$$

Where "$k_{H,\ ANonly}$" is the constant for AN degradation with respect to H_2O_2.

The H_2O_2 dosages affecting on the degradation of NB had also been explored as shown in the Figure 4.15 which was quite similar to that of AN experiment. Initial rate for NB degradation had a linear relationship with respect to H_2O_2 concentration and the rate law can be written as:

$$-\frac{d[NB_{only}]}{dt} = k_{H,NBonly}[H_2O_2]^{0.22} \tag{4.10}$$

Where "$k_{H,\ NBonly}$" is the constant for NB degradation with respect to H_2O_2 concentration.

Effect of H_2O_2 on fluidized-bed Fenton process performance in the presence of both AN and NB was also determined. From Figure 4.16, initial degradation rates of both AN and NB increased sequentially as the H_2O_2 increased from 0.005 to 0.1 M. The plot in Figure 4.16 (f) shows a linear relationship between H_2O_2 and both AN and NB; hence, the equations became:

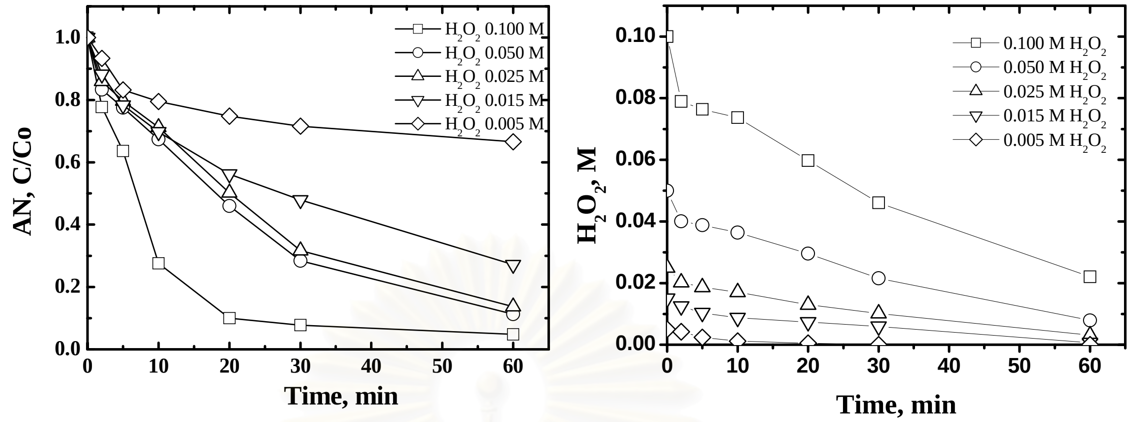

(a) Aniline remaining (b) H_2O_2 remaining

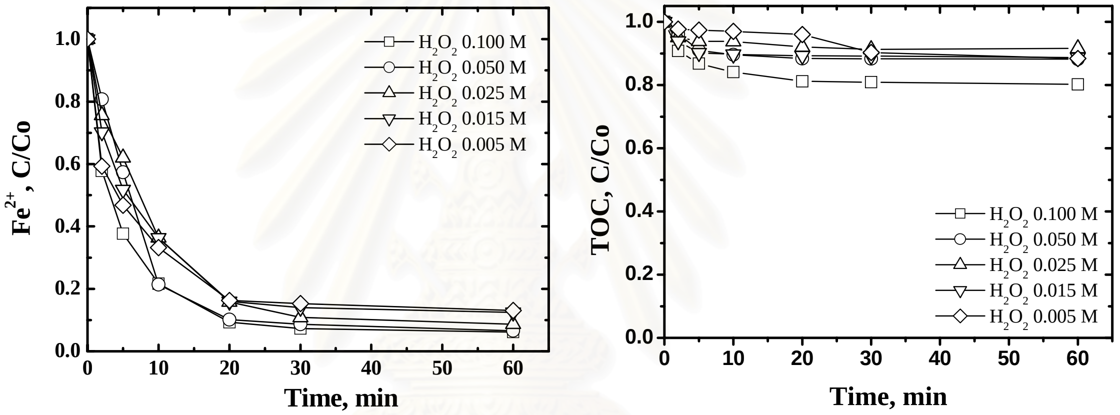

(c) Fe^{2+} remaining (d) TOC remaining

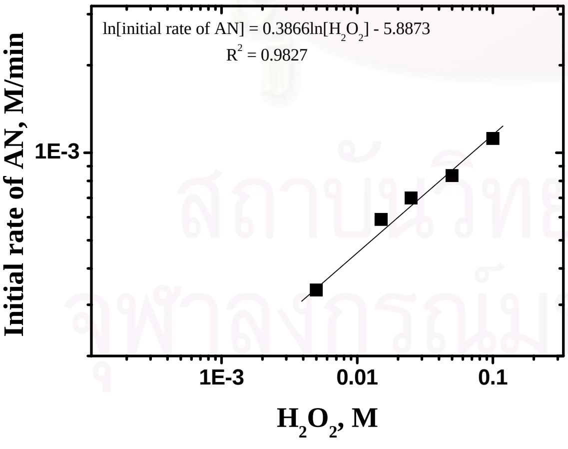

(e) Initial rate of AN vs. H_2O_2

Figure 4.14 Effect of H_2O_2 on oxidation of AN_{only} in FB-Fenton process; H_2O_2 dosage: 0.1, 0.05, 0.025, 0.015 and 0.005 M with parameter conditions; 0.01 M of AN, 0.001 M of Fe^{2+}, pH 2.8 and Al_2O_3 of 74.07 g/l.

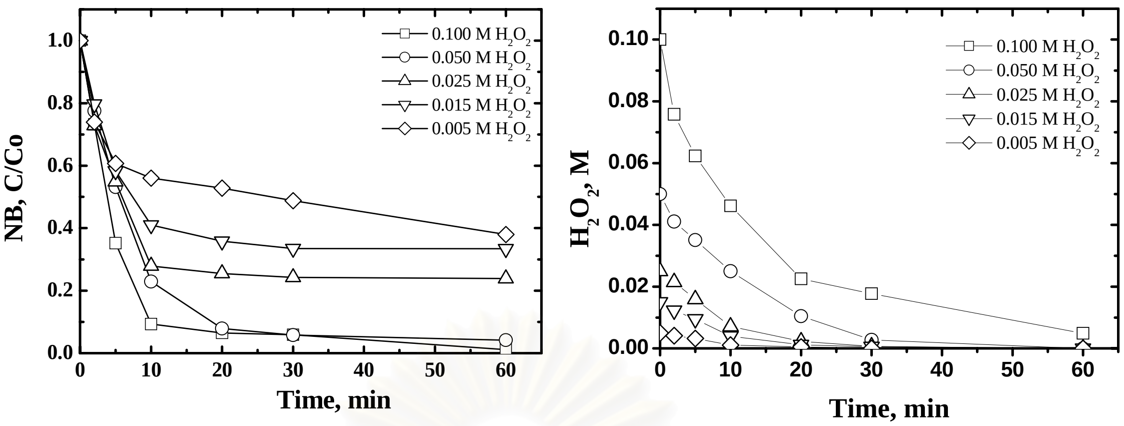

(a) Nitrobenzene remaining (b) H_2O_2 remaining

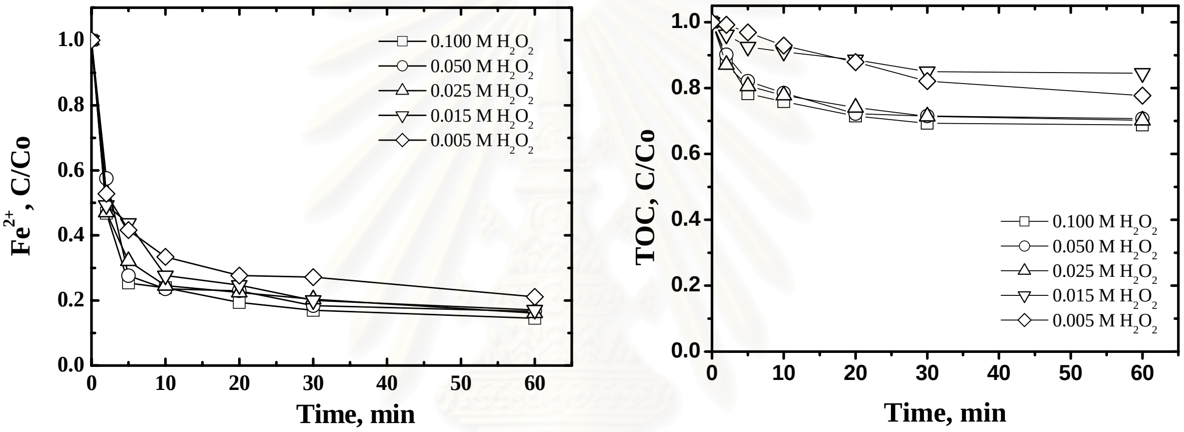

(c) Fe^{2+} remaining (d) TOC remaining

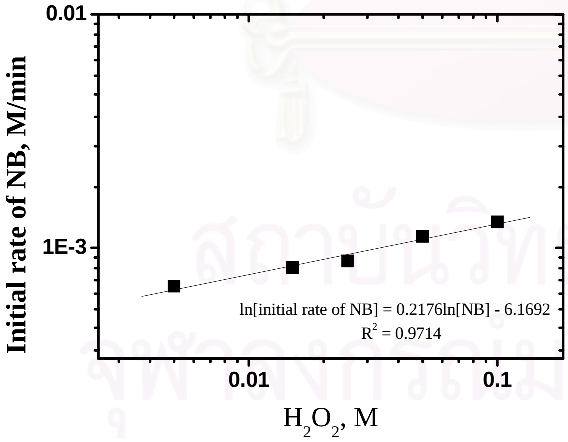

(e) Initial rate of NB vs. H_2O_2

Figure 4.15 Effect of H_2O_2 on oxidation of NB_{only} in FB-Fenton process; H_2O_2 dosage: 0.1, 0.05, 0.025, 0.015 and 0.005 M with parameter conditions; 0.01 M of NB, 0.001 M of Fe^{2+}, pH 2.8 and Al_2O_3 of 74.07 g/l.

$$-\frac{d[AN_{cb}]}{dt}=k_{H,ANcb}[H_2O_2]^{0.30} \tag{4.11}$$

$$-\frac{d[NB_{cb}]}{dt}=k_{H,NBcb}[H_2O_2]^{0.26} \tag{4.12}$$

Where "$k_{H,ANcb}$" and "$k_{H,NBcb}$" are the constants for AN and NB oxidation, respectively, with respect to H_2O_2 concentration.

4.6.3 Effect of Fe^{2+} concentration

Fe^{2+} played an important role in catalyzing H_2O_2 to produce the $OH^{\bullet}$ via Fenton reaction. To study the effect of Fe^{2+}, the decomposition of AN, NB, and combined AN/NB was investigated at various initial Fe^{2+} concentrations of 0.0025, 0.0050, 0.0075, 0.001 and 0.002 M.

The results from the experiments with AN alone were summarized in Figure 4.17. It is obvious that Fe^{2+} accelerated both degradation rate and removal efficiency of AN as shown in Figure 4.17(a). Comparing with the case of H_2O_2 in Figure 4.14(a), Fe^{2+} seems to be a more limiting factor for AN degradation rate than H_2O_2, i.e., the variation in Fe^{2+} concentration had more significant impact than that of H_2O_2. The obtained initial rates were linearized with respect with Fe^{2+}; with the slope was 1.1726. Hence, the rate equation is:

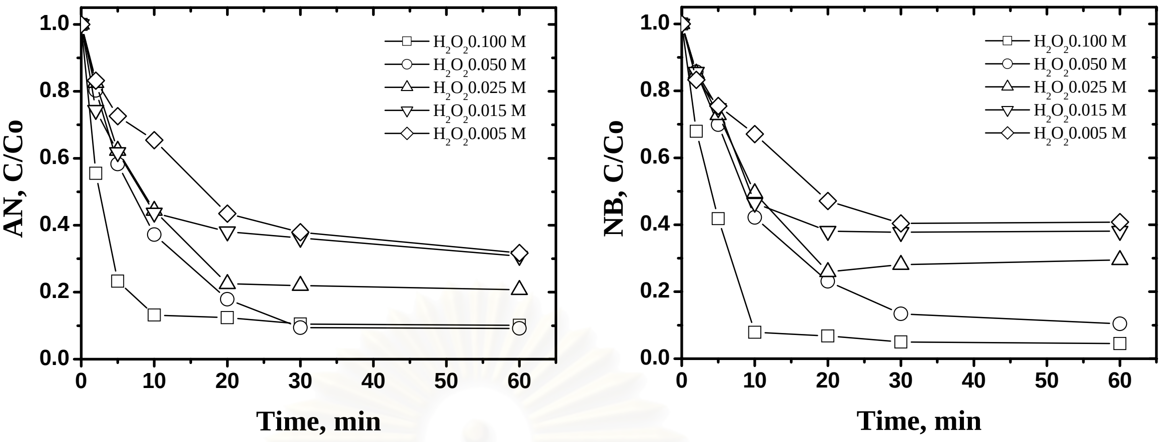

(a) Aniline remaining

(b) Nitrobenzene remaining

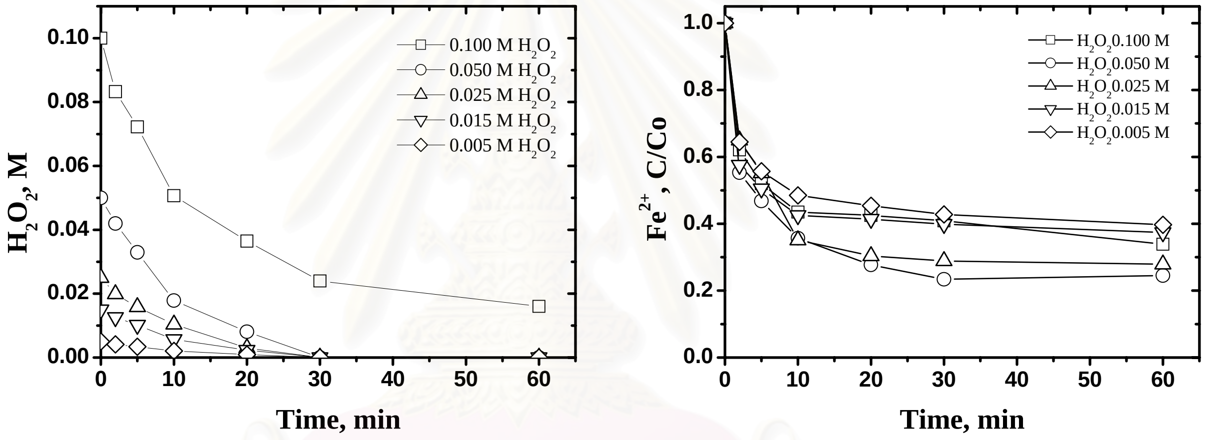

(c) H_2O_2 remaining

(d) Fe^{2+} remaining

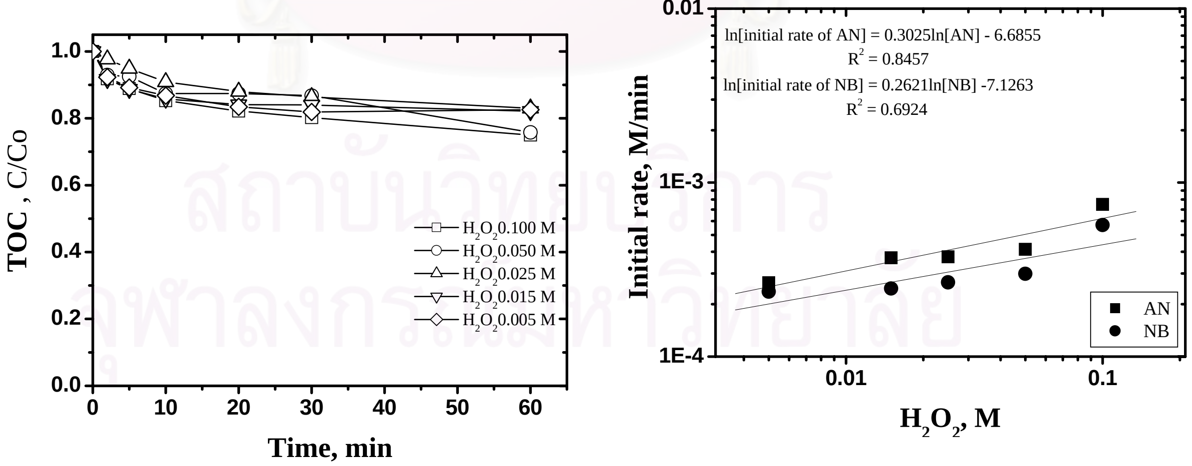

(e) TOC remaining

(f) Initial rate of AN/NB vs. H_2O_2

Figure 4.16 Effect of H_2O_2 on oxidation of AN/NB in FB-Fenton process; H_2O_2 dosage: 0.1, 0.05, 0.025, 0.015 and 0.005 M with parameter conditions; 0.005 M of AN, 0.005 M of NB, 0.001 M of Fe^{2+}, pH 2.8 and Al_2O_3 of 74.07 g/l.

$$-\frac{d[AN_{only}]}{dt} = k_{F,ANonly}[Fe^{2+}]^{1.17} \tag{4.13}$$

where, "$k_{F,ANonly}$" is the apparent rate constant for AN degradation with respect to Fe^{2+} concentration. It was also found that the consumption of H_2O_2 increased with increasing Fe^{2+}. As a result, more and more $OH^{\bullet}$ were generated and reacted with AN; thus improved the degradation performance. Nonetheless, only 20% or less of organic pollutants might be completely transformed to carbon dioxide gas.

For NB degradation, profiles of all major constituents as shown in Figure 4.18 are quite similar to those of AN experiments. Increase in Fe^{2+} dosage promoted both degradation rate and efficiency. Further analysis reveals a linear relationship between the initial rate and Fe^{2+} concentration; hence, the slope of 0.7314 became the reaction order and the rate law can be written as:

$$-\frac{d[NB_{only}]}{dt} = k_{F,NBonly}[Fe^{2+}]^{0.73} \tag{4.14}$$

Where, "$k_{F,NBonly}$" is the constant for NB oxidation with respect to Fe^{2+} concentration. Again, like previous section, TOC was removed to the greater extent in NB scenario than in AN scenario. With the highest concentration of 0.002 M of Fe^{2+}, approximately 45% of organic matters were completely oxidized to carbon dioxide gas.

For combined AN and NB experiments, an increase of Fe^{2+} had a positive impact on both AN and NB oxidation (Figure 4.19). The initial oxidation rates of AN and NB increased proportionally with Fe^{2+} concentration as shown in Figure 4.19(d).

As a result, the effect of Fe^{2+} to AN and NB degradation can be explained by the following rate laws:

$$-\frac{d[AN_{cb}]}{dt} = k_{F,ANcb}[Fe^{2+}]^{0.81} \tag{4.15}$$

$$-\frac{d[NB_{cb}]}{dt} = k_{F,NBcb}[Fe^{2+}]^{0.51} \tag{4.16}$$

where, "$k_{F,ANcb}$" and "$k_{F,NBcb}$" are the constant for AN and NB oxidation, respectively, in the combined experiments with respect to Fe^{2+}.

4.6.4 Overall Rate Equations

Up to this point, all reaction orders with respect to each individual component were identified as shown in equations (4.5), (4.9) and (4.13) for AN scenario, equations (4.6), (4.10) and (4.14) for NB scenario, and equations (4.7), (4.8), (4.11), (4.12), (4.15) and (4.16) for combined AN/NB scenario. Hence, the overall rate equations for AN and NB oxidation by FB-Fenton process become:

For AN scenario: $-\frac{d[AN_{only}]}{dt} = k_{AN}[AN]^{0.50}[H_2O_2]^{0.39}[Fe^{2+}]^{1.17}$ (4.18)

For NB scenario: $-\frac{d[NB_{only}]}{dt} = k_{NB}[NB]^{0.15}[H_2O_2]^{0.22}[Fe^{2+}]^{0.73}$ (4.19)

For AN/NB scenario:

$$-\frac{d[AN_{cb}]}{dt} = k_{AN,cb}[AN]^{0.54}[H_2O_2]^{0.30}[Fe^{2+}]^{0.81} \tag{4.20}$$

$$-\frac{d[NB_{cb}]}{dt} = k_{NB,cb}[NB]^{1.99}[H_2O_2]^{0.26}[Fe^{2+}]^{0.51} \tag{4.21}$$

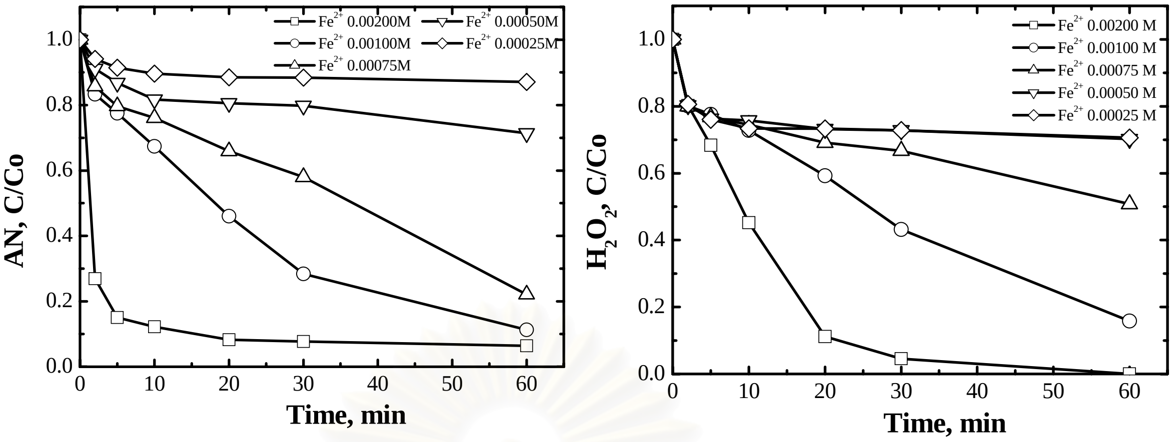

(a) Aniline remaining (b) H_2O_2 remaining

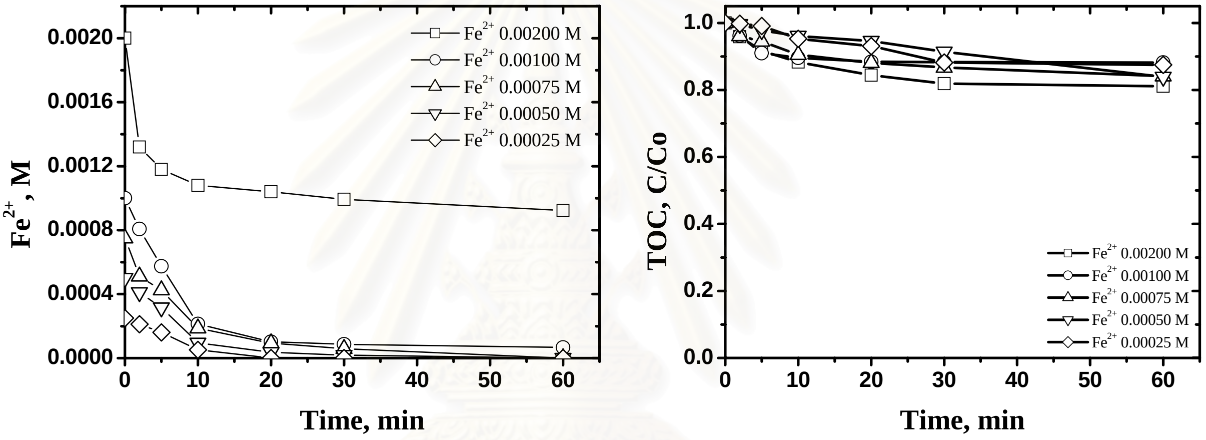

(c) Fe^{2+} remaining (d) TOC remaining

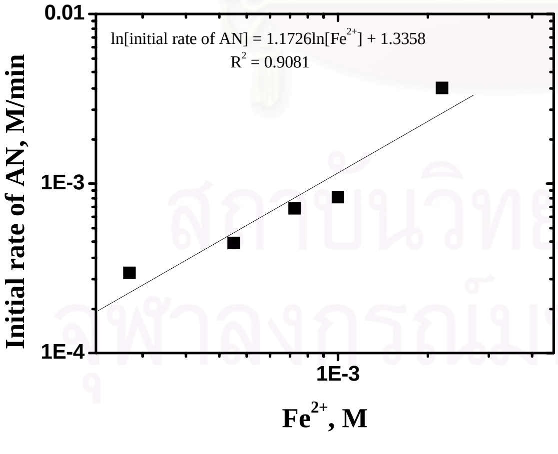

(e) Initial rate of AN vs. Fe^{2+}

Figure 4.17 Effect of Fe^{2+} on oxidation of AN in FB-Fenton process; Fe^{2+} concentration: 0.002, 0.001, 0.0075, 0.005 and 0.0025 M with parameter conditions; 0.01 M of AN, 0.05 M of H_2O_2, pH 2.8 and Al_2O_3 of 74.07 g/l.

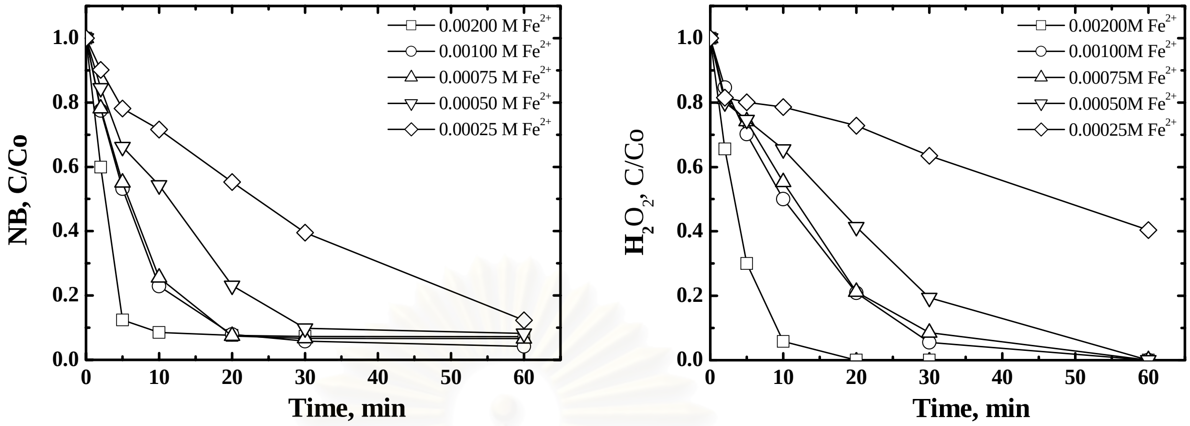

(a) Nitrobenzene remaining

(b) H_2O_2 remaining

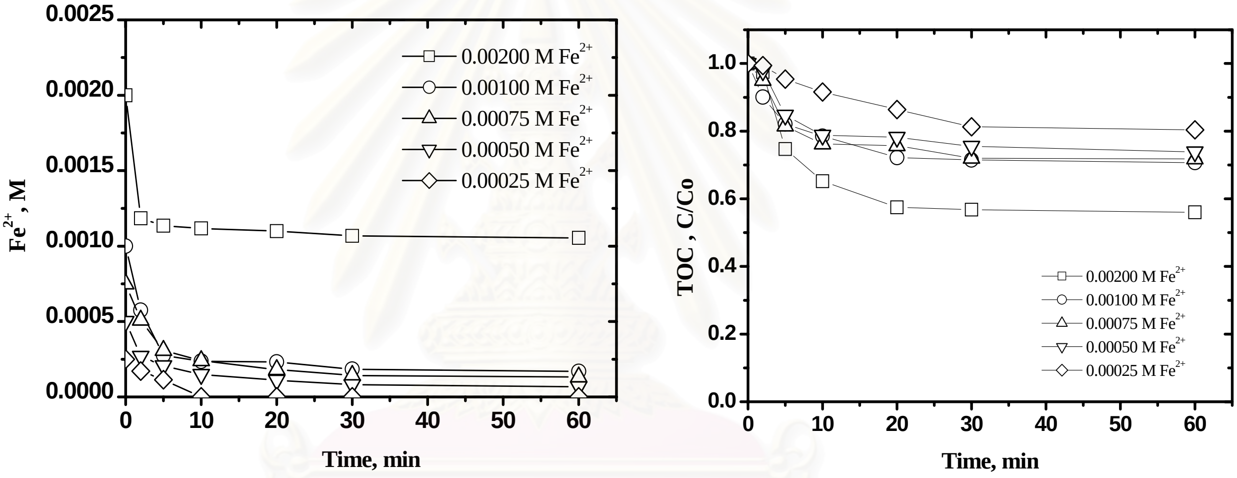

(c) Fe^{2+} remaining

(d) TOC remaining

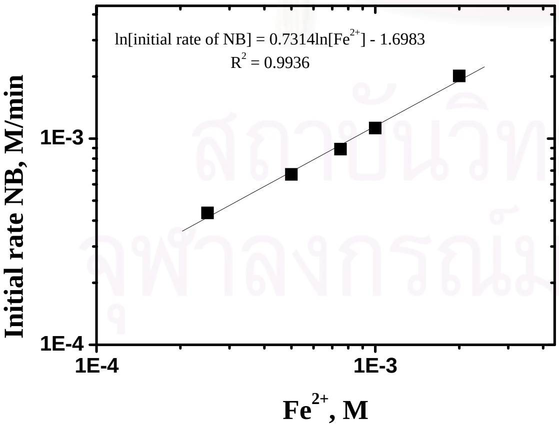

(e) Initial rate of AN vs. Fe^{2+}

Figure 4.18 Effect of Fe^{2+} on oxidation of NB in FB-Fenton process; Fe^{2+} concentration: 0.002, 0.001, 0.0075, 0.005 and 0.0025 M with parameter conditions; 0.01 M of NB, 0.05 M of H_2O_2, pH 2.8 and Al_2O_3 of 74.07 g/l.

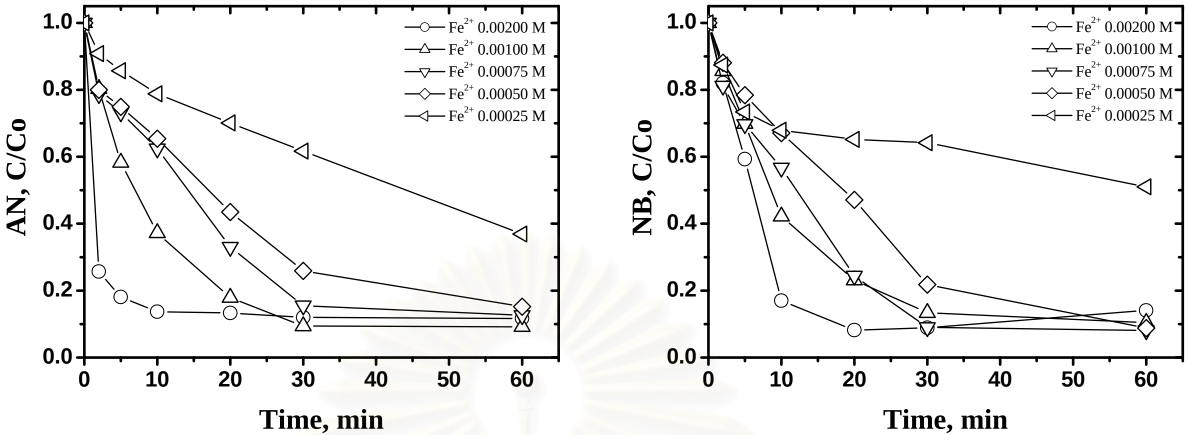

(a) Aniline remaining (b) Nitrobenzene remaining

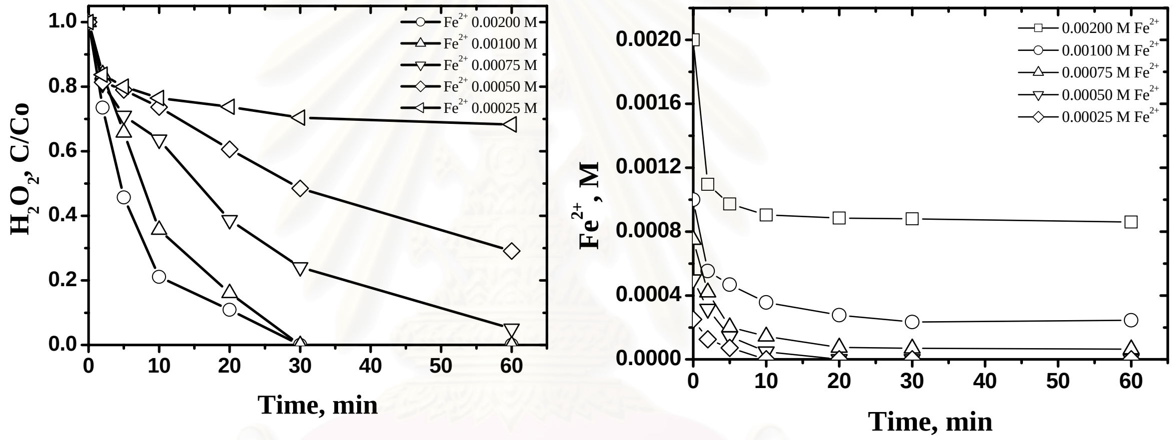

(c) H_2O_2 remaining (d) Fe^{2+} remaining

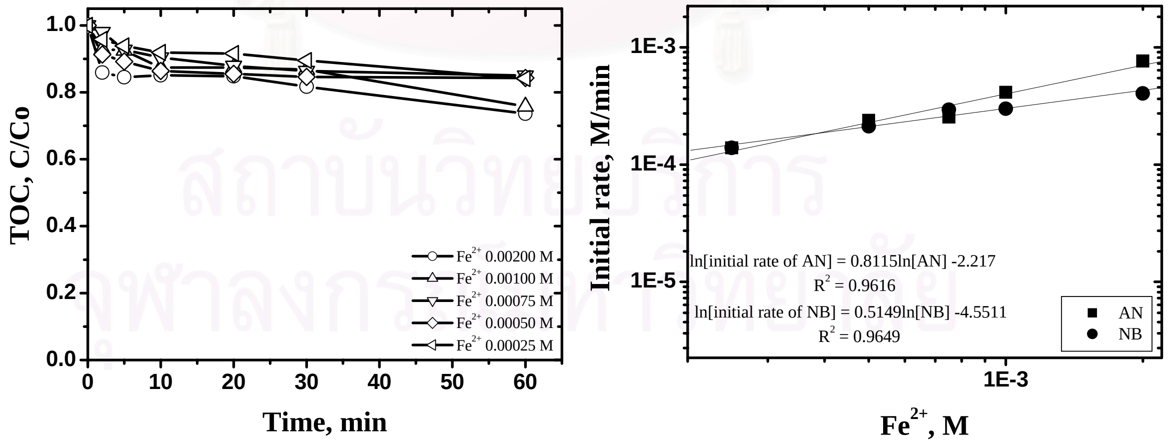

(e) TOC remaining (d) Initial rate of AN/NB vs. Fe^{2+}

Figure 4.19 Effect of Fe^{2+} on oxidation of AN/NB in FB-Fenton process; Fe^{2+} concentration: 0.002, 0.001, 0.0075, 0.005 and 0.0025 M with parameter conditions; 0.005 M of AN, 0.005 M of NB, 0.05 M of H_2O_2, pH 2.8 and Al_2O_3 of 74.07 g/l.

where “k_{ANonly}”, “k_{NBonly}”, “k_{ANcb}” and “k_{NBcb}” are the constants for aniline and nitrobenzene oxidation by FB-Fenton process under different scenarios. These “k” values can be determined by the use of a non-linear least square regression which minimizing the sum of error squares between the measured initial rates obtained from the experiments and the calculated initial rate generated by the above equations. By giving all these parameters conditions from the experiments, the final rate equations became:

$$-\frac{d[AN_{only}]}{dt} = 93.24[AN]^{0.50}[H_2O_2]^{0.39}[Fe^{2+}]^{1.17} \qquad (4.22)$$

$$-\frac{d[NB_{only}]}{dt} = 0.65[NB]^{0.15}[H_2O_2]^{0.22}[Fe^{2+}]^{0.73} \qquad (4.23)$$

$$-\frac{d[AN_{cb}]}{dt} = 5.31[AN]^{0.54}[H_2O_2]^{0.30}[Fe^{2+}]^{0.81} \qquad (4.24)$$

$$-\frac{d[NB_{cb}]}{dt} = 924.73[NB]^{1.99}[H_2O_2]^{0.26}[Fe^{2+}]^{0.51} \qquad (4.25)$$

The plot between observed and calculated values is shown in Figure 4.20. It can be seen that the slope of 0.9837 is very close to 1 with an R^2 of 0.967; hence, these empirical rate laws can be used effectively to explain the behavior of AN and NB oxidation by FB-Fenton process. Buxton et al. (1988) and Christensen (1972) proposed the rate constants for $OH^{\bullet}$ reaction with AN and NB, respectively, in equations (4.26) and (4.27):

$$OH^{\bullet} + C_6H_5NO_2 \Rightarrow HOC_6H_5NO_2 \qquad (4.26)$$

or $$\frac{d[C_6H_5NO_2]}{dt} = -k_{NB} \times [\mathrm{OH}^{\bullet}] \times [C_6H_5NO_2] \quad (k_{NB} = 3.9 \times 10^9\ (\mathrm{L\ mol^{-1}\ s^{-1}}))$$

$\mathrm{OH}^{\bullet}$ + $C_6H_5NH_3^+$ ⇨ $[C_6H_5NH_2]\bullet^+ + H_2O + HOC_6H_5NH_3^+$ (4.27)

or $$\frac{d[C_6H_5NH_3^+]}{dt} = -k_{AN} \times [\mathrm{OH}^{\bullet}] \times [C_6H_5NH_3^+] \quad (k_{AN} = 4.8 \times 10^9\ (\mathrm{Lmol^{-1}s^{-1}}))$$

It shows that AN reacts with $\mathrm{OH}^{\bullet}$ more rapidly than NB and the ratio of k_{NB}/k_{AN} was 0.813. If the concentrations of NB and AN is the same; then, the k_{NB}/k_{AN} ratio should equal to the degradation rate ratio between NB and AN. This is because the $\mathrm{OH}^{\bullet}$ concentration in equations (4.26) and (4.27) is the same since they are in the same system. In this study, there were 8 combined AN/NB experiments which began with similar concentrations of AN and NB. Therefore, the ratio of the initial rates of AN ($d[C_6H_5NH_3^+]/dt$) and NB ($d[C_6H_5NO_2]/dt$) was determined and found to be 0.805 and 0.267 for the average and standard deviation, respectively. This value is amazingly very closed to the k_{NB}/k_{AN} ratio calculated from equations (4.26) and (4.27). Hence, it can be concluded that the reaction of AN and/or NB with $\mathrm{OH}^{\bullet}$ can be effectively characterized by using reactant concentrations (equations (4.24) and (4.25)) the stoichiometric approach with $\mathrm{OH}^{\bullet}$ as shown in equations (4.26) and (4.27). This can create a huge benefit in field practice since the measurement of $\mathrm{OH}^{\bullet}$ concentration is not a simple task. With the results from this study, an engineer or scientist can explain the reaction behavior and design the FB-Fenton reactor by using the concentrations of AN and/or NB and Fenton reagents.

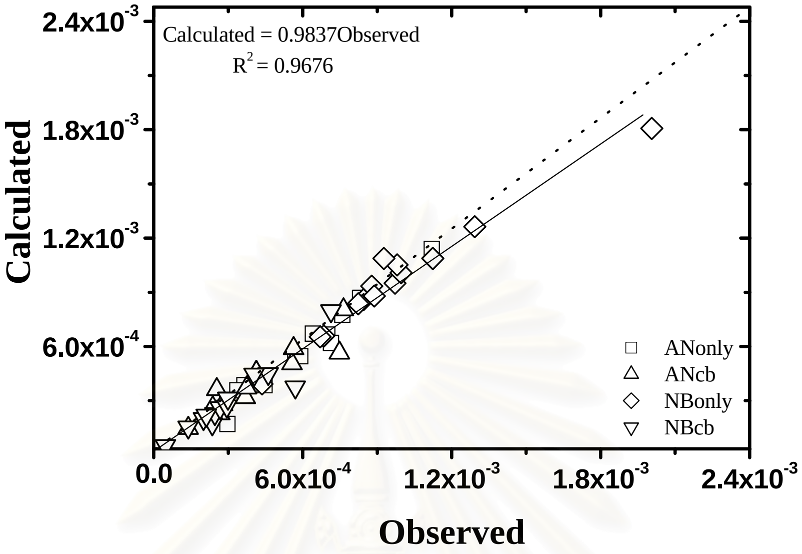

Figure 4.20 The initial rate observed vs. calculated of AN_{only}, NB_{only}, AN_{cb} and NB_{cb} with experimental conditions in this study at pH 2.8 and 74.07 g/l of Al_2O_3.

4.6.5 Competition reaction of aniline and nitrobenzene in FB-Fenton process

Further analysis on the competition between AN and NB on $OH^{\bullet}$ was also performed. Since all rate laws have already been verified in previous section, the investigation on competitive reaction was done by using rate laws rather than the observed data which can provide a better and wider systematic prospect. Table 4.1 compares the degradation rate of individual component when both chemicals were present at the same concentration of 0.005 M. It can be seen that the degradation rate of AN decreased by 22% on an average as compared with 69% in the case of NB when the other organic was present. This again confirms that AN was more vulnerable to $OH^{\bullet}$ than NB as specified in equations (4.26) and (4.27). Another interesting point that sum of the rate reduction ratio of AN and NB was 1.09 which is very closed to 1. This implies that the competitive behavior between AN and NB in FB-Fenton process was a linear relationship, i.e., approximately 72% of the $OH^{\bullet}$ being generated reacted with AN whereas the remaining of 28% was consumed by NB.

Table 4.2 The comparative degradation rate of individual component to the rate when the present of the same chemical concentration by 0.005 M

Concentration (M)			Calculated rate (M/min) x 10^{-4}					
Chemical (AN,NB)	H_2O_2	Fe^{2+}	AN_{only}	AN_{cb}	AN_{cb}/ AN_{only}	NB_{only}	NB_{cb}	NB_{cb}/ NB_{only}
0.005	0.005	0.00100	2.51	2.28	0.91	5.95	1.71	0.29
0.005	0.015	0.00100	3.84	3.18	0.83	7.55	2.28	0.30
0.005	0.025	0.00100	4.68	3.71	0.79	8.44	2.61	0.31
0.005	0.050	0.00100	6.12	4.57	0.75	9.81	3.12	0.32
0.005	0.100	0.00100	8.01	5.64	0.70	11.41	3.75	0.33
0.005	0.050	0.00050	2.72	2.39	0.88	5.90	2.19	0.37
0.005	0.050	0.00075	4.37	3.62	0.83	7.94	2.69	0.34
0.005	0.050	0.00200	13.80	8.03	0.58	16.32	4.47	0.27
			Average value = 0.78			Average value = 0.31		

4.7 Effect of Intermittent Addition of Fenton's Reagent

The effect of intermittent addition of Fenton's reagent on the oxidation of AN and NB in fluidized-bed Fenton reactor has been also determined. Since most of AN and NB degradations reached a plateau after 30 min as shown in Figure 4.21, additional Fenton's reagents were added at 30 min to observe the degradation behavior of the target compounds. The experiments were conducted at two pH values of 2.8 and 3.6 and the results were shown in Figures 4.22 and 4.23, respectively. It was surprising that the addition of Fenton' reagents either H_2O_2, Fe^{2+}, or H_2O_2 + Fe^{2+} did not provide any significant improvement in the reduction of AN, NB and TOC even with the addition of both H_2O_2 and Fe^{2+} at 50% of the initial concentrations. In other word, $OH^{\bullet}$ had not been generated in a significant amount at the second addition of Fenton's reagents. This observation cannot be explained clearly at this time; however, it should possibly be derived from the composition and chemistry of the solution. Results from repeatability usage of Al_2O_3 which will be discussed later showed similar removal efficiencies for both AN and NB as well as other behaviors up to five cycles. Hence, the carrier itself should not contribute any considerable impact on the findings of this part.

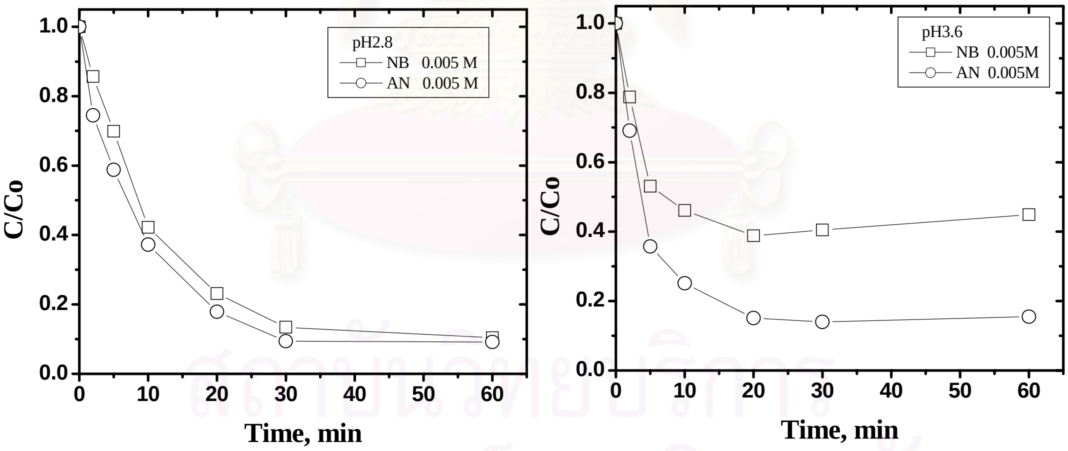

(a) AN and NB remaining at pH 2.8 (b) AN and NB remaining at pH 3.6

Figure 4.21 The oxidation of AN and NB in FB-Fenton process at initial pH 2.8 and pH 3.6;0.005 of AN, 0.005 M of NB, 0.05 M of H_2O_2 , 0.001 M of Fe^{2+}, 74.07 g/l of Al_2O_3.

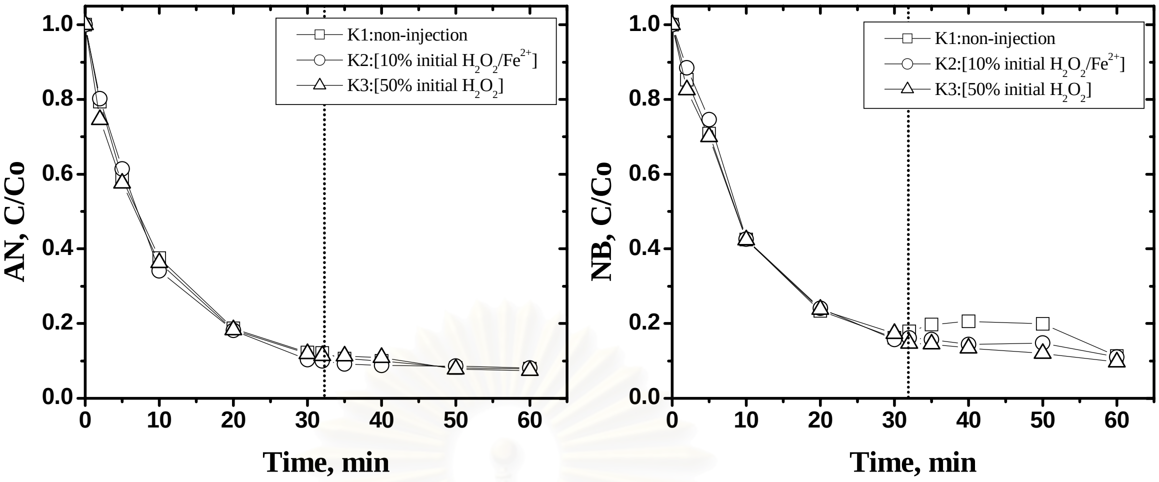

(a) Aniline remaining (b) Nitrobenzene remaining

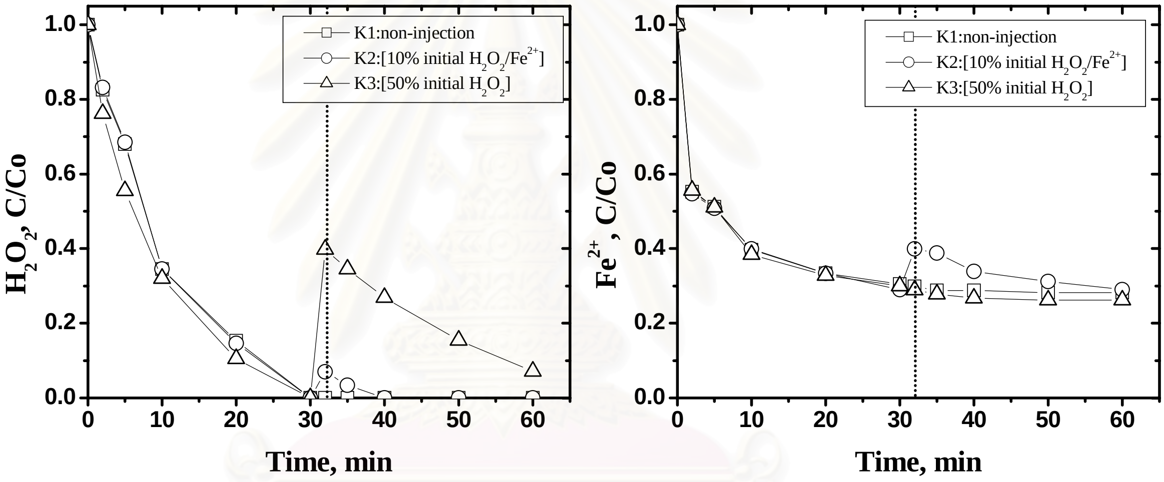

(c) H_2O_2 remaining (d) Fe^{2+} remaining

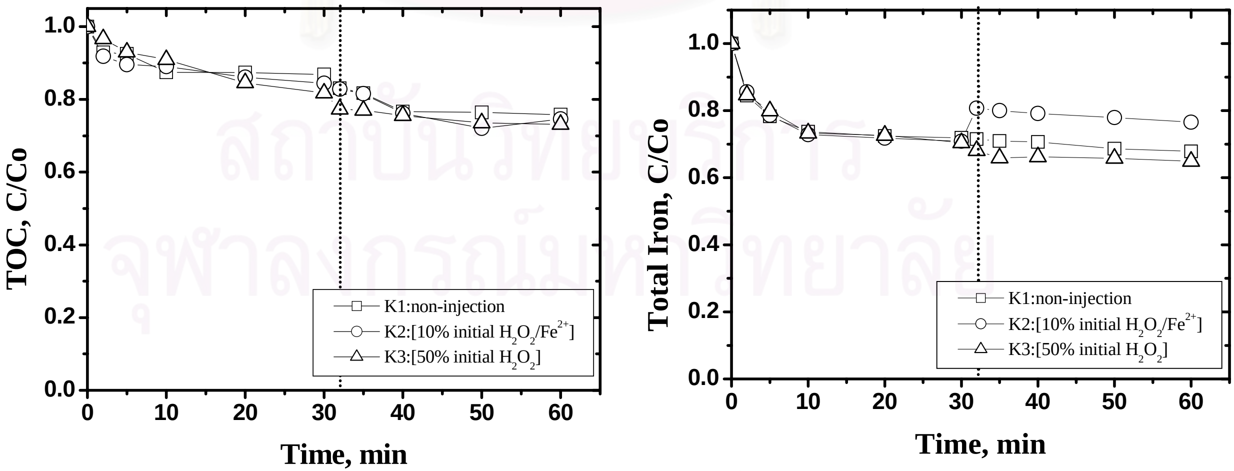

(e) TOC remaining (f) Total Iron remaining

Figure 4.22 The effect of intermittent addition of Fenton's reagent on the oxidation of AN and NB at pH 2.8; 0.005 of AN, 0.005 M of NB, 0.05 M of H_2O_2 , 0.001 M of Fe^{2+}, 74.07 g/l of Al_2O_3.

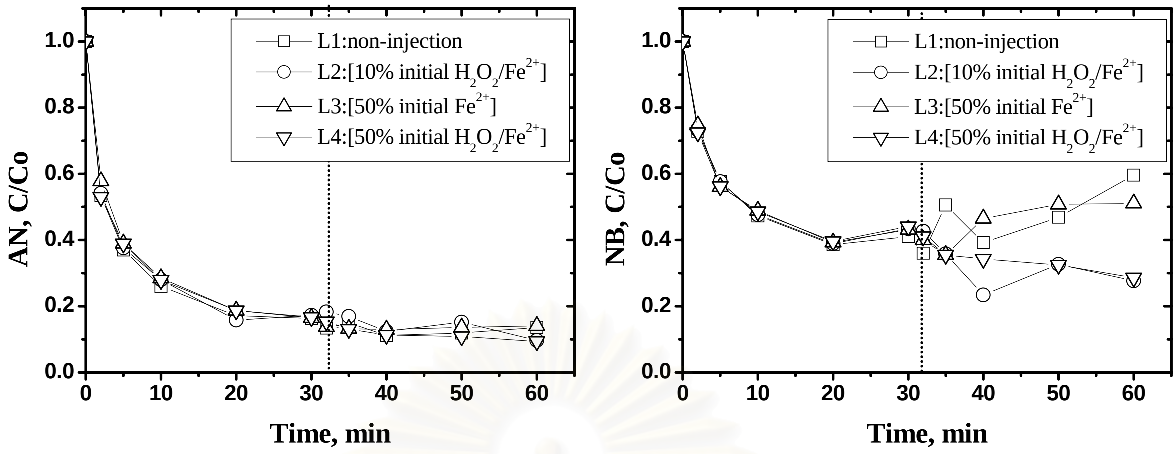

(a) Aniline remaining (b) Nitrobenzene remaining

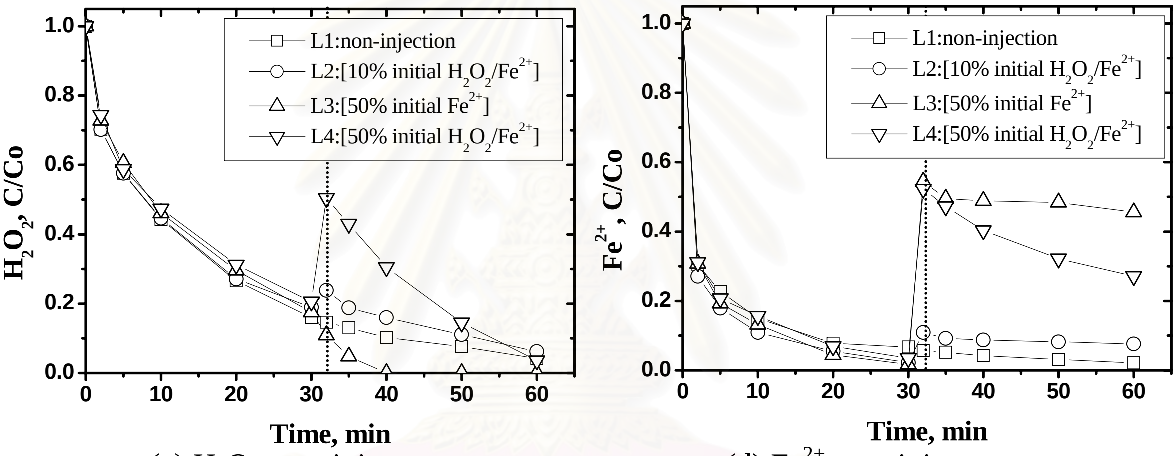

(c) H_2O_2 remaining (d) Fe^{2+} remaining

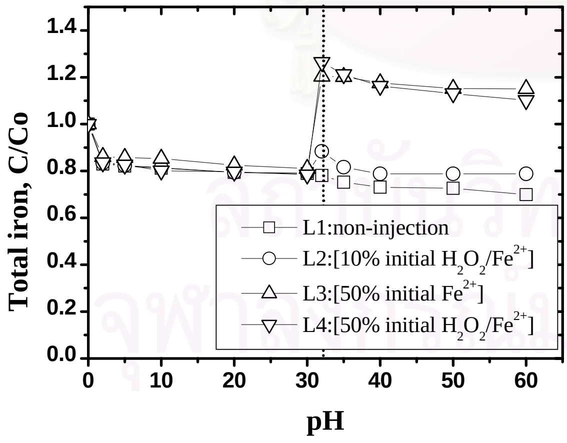

(e) Total iron remaining

Figure 4.23 The effect of intermittent addition of Fenton's reagent on the oxidation of AN and NB at pH 3.6; 0.005 of AN, 0.005 M of NB, 0.05 M of H_2O_2 , 0.001 M of Fe^{2+}, 74.07 g/l of Al_2O_3.

4.8 The Reusability of Aluminum Oxide

Fenton reaction (H_2O_2/ Fe^{2+}) can promote the non-selective oxidant as $OH^{\bullet}$ leading to the degradation of aromatic organic containing in the wastewater. In the process, Fe^{3+} is generated and can crystallize onto carrier surface. It is of interest to investigate on the reuse ability of Al_2O_3 which can lead to the reduction in sludge volume. Al_2O_3 were reused up to 5 cycles under the same conditions. Figure 4.24 summarizes all aspect of the FBR with reused Al_2O_3. It was found that the FBR behavior regarding on AN, NB, TOC, and total iron removals were quite similar for all five cycles. Lo et al., (1997) mentioned that the optimum pH and pore of specific area on the surface media played the important factor of attachment iron oxide coating. However, the impact of specific area on the surface of Al_2O_3 was not obvious in this study. This might be due to the differences in system configuration and conditions. Table 4.2 shows the composition of Al_2O_3 as a result from EDX analysis. It can be seen that portion of iron gradually increased with reused cycle. However, the appearance of Al_2O_3 were very small changed in case of size and figure due to crystallization of iron induce the carriers hardness and the absent of iron was slightly when compare with weight. These findings imply that the iron oxide coated Al_2O_3 can be reused successfully in the fluidized-bed Fenton process.

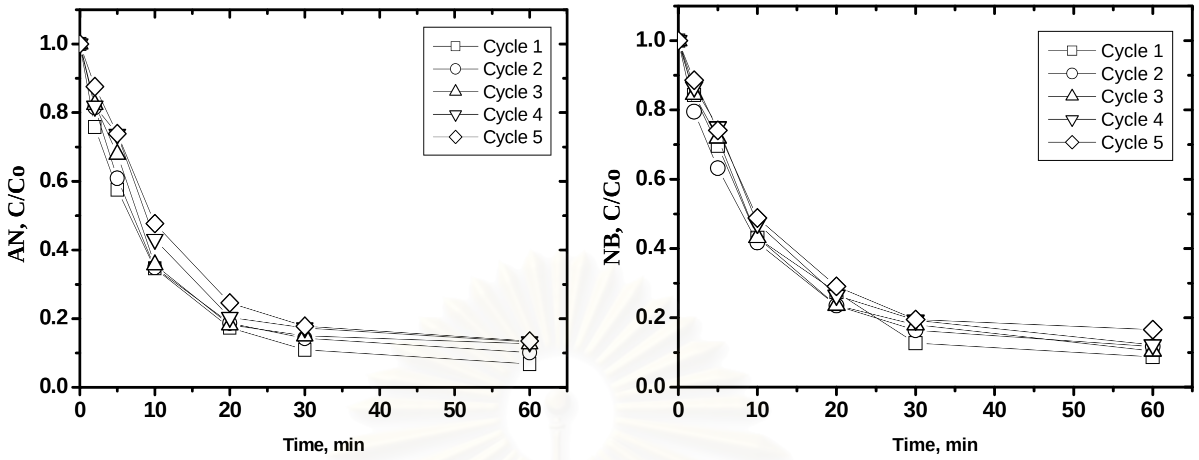

(a) Aniline remaining

(b) Nitrobenzene remaining

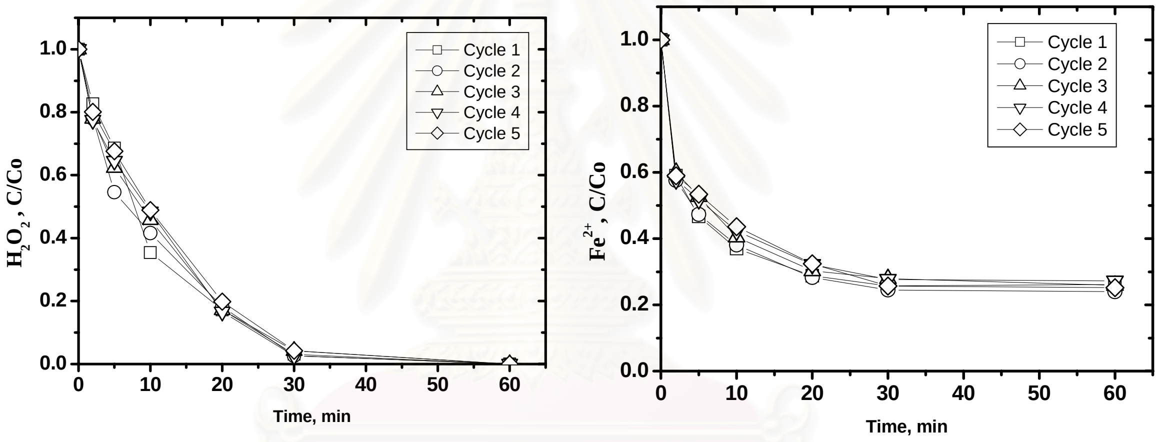

(c) H_2O_2 remaining

(d) Fe^{2+} remaining

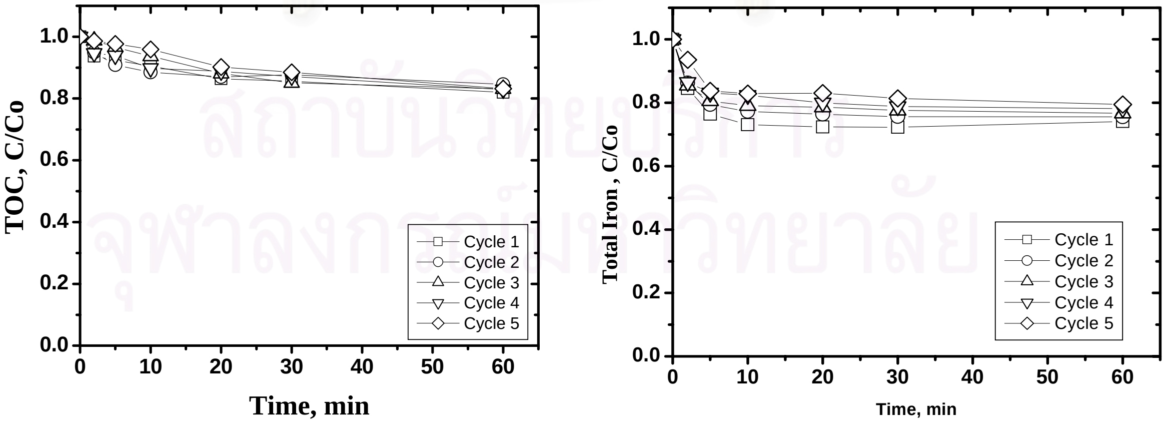

(e) TOC remaining

(f) Total Iron remaining

Figure 4.24 The reusability of aluminum oxide with 5 times recycling in FBR; 0.005 of AN, 0.005 M of NB, 0.05 M of H_2O_2 , 0.001 M of Fe^{2+}, 74.07 g/l of Al_2O_3 at initial pH 2.8.

Table 4.3 The percentage element information with the cycle order of Al_2O_3 in fluidized-bed Fenton's reactor by EDX analysis

The cycle order of Al_2O_3	Element (% weight)		
	Al	O	Fe
Blank	49.97	50.03	0
1^{st}	54.37	45.34	0.29
2^{nd}	53.30	46.38	0.31
3^{rd}	53.53	46.09	0.38
4^{th}	53.51	45.97	0.52
5^{th}	51.89	47.47	0.65

4.9 Managerial Value

The results from this study strongly showed the benefit of metal oxide carriers to Fenton process under fluidized-bed operation. Although removal efficiency was comparable to those of ordinary Fenton, FB-Fenton could removal excess iron by 20% repeatedly. The iron-crystallization performance can be promoted significantly with extra addition of metal oxide carriers which is still applicable in field practice (Chou et al. (2004) could removal soluble iron up to 90%). The amount of metal oxide carriers depend largely on their own properties, wastewater characteristics, and applied Fe^{2+} dosage. The optimum dosage of these carriers should be determined on a case-by case basis. In addition, these iron-coated metal oxides can be reused successfully as an iron source for Fenton process as reported by Chou and Huang

(1999a). Hence, puffy iron hydroxide sludge which is major drawback of ordinary Fenton process and needs further handling and disposal can be almost eliminated. Possible involvement of FB-Fenton process in wastewater treatment train is shown in Figure 4.25 in which it can be used as either a pretreatment or tertiary treatment depending on wastewater characteristics and required effluent quality.

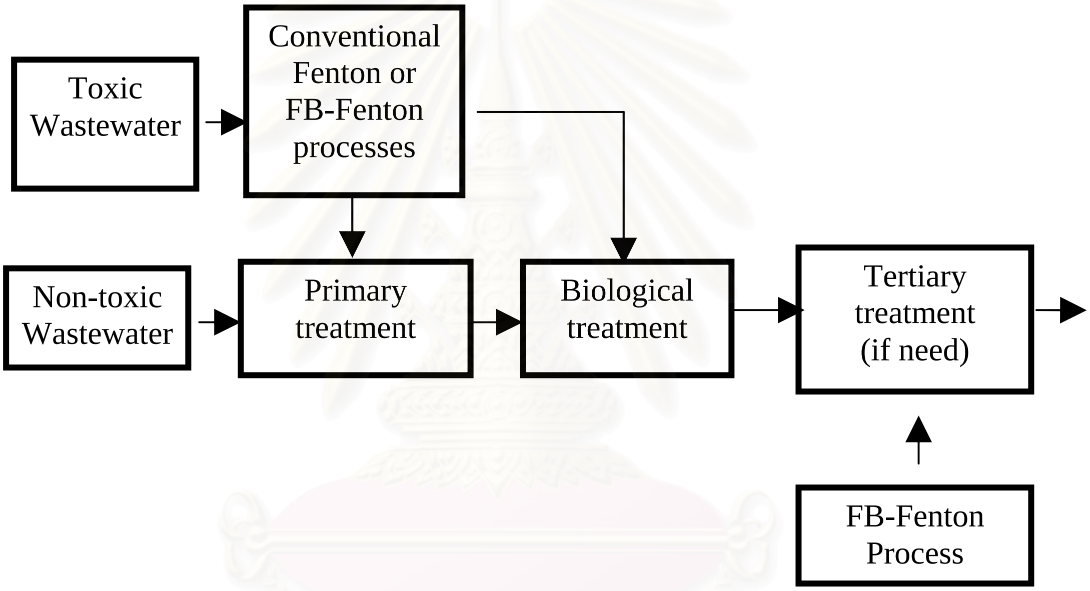

Figure 4.25 Possible application of FB-Fenton in wastewater treatment management

CHEAPTER V

CONCLUSIONS

5.1 Conclusions

The oxidation of aniline and nitrobenzene had been investigated by applying Fenton with fluidized-bed reactor which was found to be an appropriate method to efficiently remove these compounds from homogeneous solutions.

- The point of zero charge of Al_2O_3 and SiO_2 was 8.21 and 6.54 in DI water and 0.01 M of aniline plus 0.025 M of Na_2SO_4 solution, respectively.
- The high removal efficiency and initial rate of aniline, nitrobenzene and the combination of aniline and nitrobenzene oxidation were adequate at pH 3.2 , 2.8 and 2.8 in fluidized bed Fenton process, respectively. However, pH 2.8 was selected for the best overall performance.
- Aniline and nitrobenzene were effetely degraded by fluidized bed Fenton process with the use of Al_2O_3 was better than SiO_2 possibly due to higher positive-charged surface at pH 2.8.
- The degradation of AN, NB, AN/NB had high removal efficiency in fluidized-bed Fenton process as well as traditional Fenton process. The fluidized-bed Fenton process was able to remove iron whereas the ordinary Fenton process could not.

- The removal efficiency of aniline and nitrobenzene increased with the increasing of Fenton’s reagent concentration. In this study, the oxidation of aniline and nitrobenzene were not inhibited by increasing of hydrogen peroxide dosage.
- Overall kinetic equation for aniline, nitrobenzene and the combination of aniline and nitrobenzene by fluidized-bed Fenton process was:

$$-\frac{d[AN_{only}]}{dt} = 93.24[AN]^{0.50}[H_2O_2]^{0.39}[Fe^{2+}]^{1.17} \qquad (5.1)$$

$$-\frac{d[NB_{only}]}{dt} = 0.65[NB]^{0.15}[H_2O_2]^{0.22}[Fe^{2+}]^{0.73} \qquad (5.2)$$

$$-\frac{d[AN_{cb}]}{dt} = 5.31[AN]^{0.54}[H_2O_2]^{0.30}[Fe^{2+}]^{0.81} \qquad (5.3)$$

$$-\frac{d[NB_{cb}]}{dt} = 924.73[NB]^{1.99}[H_2O_2]^{0.26}[Fe^{2+}]^{0.51} \qquad (5.4)$$

In the conditions were follow as: 0.005 to 0.100 M of H_2O_2 dosage, 0.00025 to 0.00100 M of Fe^{2+}, 0.002 to 0.010 M of AN and NB, 74.07 g/l of Al_2O_3 and pH 2.8.

- Aniline was more a more vulnerable species to hydrogen radical than nitrobenzene when the present at the same concentration, 72% of the generated hydroxyl radical reacted with AN whereas the remaining of 28% with NB.

- The reuse ability of Al_2O_3 with 5 cycles has almost the same removal efficiency of aniline and nitrobenzene in fluidized-bed Fenton process. The reduction of iron oxide via crystallization onto the Al_2O_3 had been found in this study also.

5.2 Suggestions for further studies

- The oxidation intermediates of aniline and nitrobenzene degraded by fluidized-bed Fenton process should be identified during decomposition process.
- The degradation path-way of aniline and nitrobenzene oxidation should be considered.
- The toxicity of intermediates during the process should be determined.
- The real waste water should be applied to study in fluidized-bed Fenton process.

REFERENCES

Brillas, E., Mur, E., Sauleda, R., Sanchez, L., Peral, J., Domenech, X. and Casdo, J. (1998). Aniline mineralization by AOP's: anodic oxidation, photocatalysis, electro-Fenton and photoeletro-Fenton processes. Applied catalysis B:Environment, 16, 31-42.

Buxton, G.V., Breenstock, C.L., Helman, W.P. and Ross, A.B. (1988). Critical review of rate constans for reaction of hydrated electrons hydrogen atoms and hydroxyl radical ($OH^{\bullet}/O^{\bullet-}$) in aqueous solution. Journal of physical chemistry, 17, 513-886.

ChemistryDaily.com. (2005). Aniline. Chemistry Daily. Term of Use. Available from: http://www.chemistrydaily.com/chemistry/Aniline.

Chen, G., Hoag, G. E., Chedda, P., Nadim, F., Woody, B.A.and Dobbs, G. M. (2001). The mechanism and applicability of in situ oxidation of trichlorethelene with Fenton's reagent. Journal of hazardous materials, B87, 171-186.

Chou, S. and Huang, C. (1999a). Effect of Fe^{2+} on catalytic oxidation in a fluidized bed reactor. Chemospeher 39, 2, 1997-2006.

Chou, S. and Huang, C. (1999b). Application of supported iron oxyhydroxide catalyst in oxidation of benzoic acid by hydrogen peroxide. Chemoshpere, 38(12), 2719-2731.

Chou, S. and Huang, C. (1999c). Decomposition of hydrogen peroxide in a catalytic in fluidized-bed reactor. Applyied catalysis, 185, 237-245.

Chou, S. and Huang, G.H (2003). Fenton family-Advanced oxidation technologies for wastewater treatment. Asian-Pacific Regional conference on practical environmental technologies, Tainan, Taiwan, (A2-17)-(A2-24).

Chou, S., Liao, C.C., Perng, S.H. and Chang, S.H. (2004). Factors influencing the preparation of supported iron oxide in fluidized-bed crystallization. Chemosphere, 54, 859-866.

Christensen, H. (1997). Pulse radiolysis of aqueous solutions of aniline and substituted anilines. Inter tional Journal for Radiation Physics and Chemistry , 4, 311-333. Availablefrom: http://allen.rad.nd.edu/Compilations/Hydroxyl/OH_198.HTM.

Hoigné, J. (1998). Chemistry of AqueosOzone and Advanced Oxidation Processes. The Handbook of Environmental Chemistry, Springer-Verlag, Berlin 5, Part C, 83-141.

Huang, H. H., Lu, M.C. and Chen, J.N. (2001). Catalytic decomposition of hydrogen peroxide and 2-chlorophenoa with iron oxides. Water Research, 35, 9, 2291-2299.

Jodin, M-C., Gaboriaud, F. and Humbert, B. (2005). Limitations of potentiometric studies to determine the surface charge of gibbsite γ -Al(OH)$_3$ particles. Journal of colloid and interface science, 287, 581–591.

Kang W. Y. and Hwang K-Y. (2000). Effects of reaction conditions on the oxidation efficiency in the Fenton process. Water Research, 34, 10, 2786-2790.

Kang, N. and Hua, I. (2005). Enhanced chemical oxidation of aromatic hydrocarbons in soil systems. Chemosphere, 61, 909-922.

Kang, S-F., Liao, C-H. and Po, S-T. (2000). Decolorization of textile wastewater by photo-Fenton oxidation technology. Chemosphere, 41, 1287-1294.

Liao, C.H., Lu, M.C. and Su, S.H. (2001). Role of cupric ions in the H2O2/UV oxidation of humic acid. Chemosphere, 44, 913-919.

Lin, S.S. and Gurol, M.D. (1996). Heterogeneous catalytic oxidation of organic compounds by hydrogen peroxide. Water Science and Technology, 34, 9, 57-64.

Lo, S-L., Jeng, H-T. and Lai, C-H. (1997). Characteristics and adsorption properties of iron-coated sand. Water Science and Technology, 7, 63-70.

Lopez, A., Pagano, M., Volepe, A., Pinto, A.,C.,D. (2004). Fenton’s pre-treatment of mature landfill leachate. Chemosphere, 54, 1005-1010.

Lopez-Cueto, G., Ostra, M., Ubide, C., Zuriarrain, J. (2004). Fenton’s reagent for kinetic determinations. Analytica chemical acta, 515, 109-116.

Lu, M.C. (1997). Effect of inorganic ions on the oxidation of dichlorvos insecticide with Fenton’s reagent. Chemosphere, 35, 10, 2285-2293.

Lu, M.C. (1999). Oxidation of dichlorvos with hydrogen peroxide using ferrous ion as catalyst. Journal of hazardous materials, B65, 277-288.

Lu, M.C. (2000). Oxidation of chlorophenols with hydrogen peroxide in the presence of goethite. Chemosphere, 40, 125-130.

Lu, M.C., Chang, Y.-F., Chen, I.M. and Huang, Y.Y. (2005). Effect of chloride ions on the oxidation of aniline by Fenton’s reagent. Journal of Environmental Management, 75:177-182.

Lu, M.C., Chen, J.N. and Huang, H. H. (2002). Role of goethite dissolution in the oxidation of 2-chlorophenol with hydrogen peroxide. Chemosphere, 40, 125-130.

Lunar L., Sicilia D., Rubio S., Perez-Bendito D. and Nickel U. (2000). Degradation of photographic developers by Fenton's reagent: condition optimization and kinetics for metol oxidation. Water Research, 34, 6, 1791-1802.

Mustafa, S., Dilara, B., Neelofer, Z., Naeem, A. and Tasleem, S. (1998). Temperature Effect on the Surface Charge Properties of γ-Al_2O_3. Journal of colloid and interface science, 204, 284–293.

National toxicology program (NTP). (2002). Report on Carcinogens Background for Nitrobenzene. Available from: http://ntp-serve.niehs.nih.gov/newhomeroc/roc11/NitrobenzenePub.pdf.

National toxicology program (NTP). (2005). Substance Profiles. Report on Carcinogens for Nitrobenzene, Eleventh Edition. Available from: http://ntp.niehs.nih.gov/ntp/roc/eleventh/profiles/s121zntb.pdf.

Neyens, E. and Baeyens, J. (2003). A review of classic Fenton's peroxidation as an advanced oxidation technique. Journal of hazardous materials, B98, 33-50.

Noh, J.S. and Schwarz, J.A. (1988). Estimation of the point of zero charge of simple oxides by mass titration. Journal of colloid and interface science, 130, 157-164.

Panizza M. and Cerisola G. (2001). Removal of organic pollutants from industrial wastewater by electrogenerated Fenton's reagent. Water Research, 35, 16, 3987-3992.

Peres A. J., Heredia. D. J., Dominguez R. J. (2003). Integrated Fenton's reagent – coagulation/flocculation process for the treatment of cork processing wastewaters. Journal of hazardous materials, B107, 115-121.

Piccinini, P., Minero C., Vincenti, M. and Pelizzetti, E. (1997). Photocatalytic mineralization of nitrogen-containing benzene derivatives. Catalysis Today, 39, 187-195.

Pignatello, J.J. (1992). Dark and photo-assisted Fe^{3+}-catalyzed degradation of chlorophenoxy herbicides by hydrogen peroxide. Environmental Science and Technology, 26, 944-951.

Preocanin, T. and Kallay, N. (1998). Application of Mass titration to determination of surface charge of metal oxides. Croatica Chemica Acta, 71, 4, 1117-1125.

Reymond, J.P. and Kolenda, F. (1999). Estimation of the point of zero charge of simple and mixed oxides by mass titration. Powder Technology, 103, 30-36.

Rodgers, D. J. and Bunce, N.J. (2001). Review Paper, Treatment methodos for the remediation of nitroaromatic explosives. Water Research, 35, 9, 2101-2111.

Roriguez M., Timokhin I. V., Chamarro E. and Esplugas S. (2003). Rate equation for the degradation on nitrobenzene by 'Fenton-like' reagent. Advances in environmentl research, 7, 583-595.

Sakulkitimasak, P. (2004). Oxidation of nitrobenzene by fluidized-bed Fenton process. Master's thesis, Department of engineering environmental engineering faculty of engineering, King Mongkut's Uninversity of Technology Thonburi.

Sánchez, L., Pera,l J.and Domènech, X. (1998). Aniline degradation by comebined photocatalysis and ozonation. Applied catalysis B: environmental, 19,59-65.

Sarasa, J., Corté, S., Ormad, P., Gracia, R.and Ovelleiro, J.L. (2002). Study of the aromatic by-products from ozonation of anililnes in aqueous solution. Water Research, 36,3035-3044.

Sauleda, R. and Brillas, E. (2001). Mineralization of aniline and 4-chlorophenol in acidic solution by ozonation catalyzed with Fe^{2+} and UVA light. Applied catalysis B: Environmental, 29,135-145.

Tai, C.Y. (1999). Crystal growth kinetics of two-step growth process in liquid fluidized-bed crystallizers. Journal of Crystal Growth, 206,109-108.

Teel, A.L., Warberg, C.R., Atkinson, D.A. and Watts, R.J. (2001). Comparison of mineral and soluble iron Fenton's catalysts for the treatment of trichloroethylene. Water Research, 35, 4, 977-984.

U.S. EPA. (1994). Aniline fact sheet: Support document (CAST NO. 62-53-3). OPPT chemical fact sheets, pollution prevention and toxic, 7407.

U.S. EPA. (1995). Nitrobenzene fact sheet: Support document (CAST NO. 98-95-3). OPPT chemical fact sheets, pollution prevention and toxic, 7407.

Utse, B., Garcia, J., Casado, J., Domenech, X. and Peral, J. (2000). Replacement of H_2O_2 by O_2 in Fenton and photo-Fenton reactions. Chemosphere, 41, 1187-1192.

Zepp, R. G. (1992). Hydroxyl radical formation in aqueous reactions (pH3-8) of Iron (II) with hydrogen peroxide: The photo-Fenton Reaction. Environmental Science and Technology, 26, 2, 313-319.

APPENDIXES

APPENDIX A

Standard iodometric, (Kingzett, C.T., 1880)

Principle

Hydrogen peroxide oxidizes iodide to iodine in the presence of acid and molybdate catalyst. The iodine formed is titrated with thiosulfate solution, incorporating a starch indicator as demonstrated in the following equation:

$$H_2O_2 + 2\,KI + N_2SO_4 \Rightarrow I_2 + K_2SO_4 + 2\,H_2O \qquad (B.1)$$

$$I_2 + 2\,Na_2S_2O_3 \Rightarrow Na_2S_4O_6 + 2NaI \qquad (B.2)$$

Interferences

Other oxidizing agents will also produce iodine, whereas reducing agents (and unsaturated organics) will react with the liberated iodine. The contribution from other oxidizing agents can be determined by omitting the acid and molybdate catalyst.

Reagents

1. potassium iodide solution (1 % w/v): dissolve 10 gram KI into 1 l of RO water.
2. Ammonium molybdate solution: dissolve 9 grams ammonium molybdate in 10 ml 6N NH_4OH, add 24 grams NH_4OH_3 and dilute to 100 ml with RO water.
3. Sulfuric acid solution (1:4 N_2SO_4): carefully add one part N_2SO_4 98% to four parts RO water.
4. Starch indicator
5. Sodium thiosulfate solution (0.0125 N)

Apparatus

1. Analytical balance (+/- mg/l)
2. Small weighing bottle (<5 ml)
3. 250 ml Erlenmeyer flask
4. 50 ml burette (Class A)
5. Medicine dropper

Procedure

1. Transfer sample to Erlenmeyer flask.
2. Add to Erlenmeyer flask 50 ml of RO water. Next, 10 ml of sulfuric acid solution and 15 ml of potassium iodide were added. Then two drops ammonium molybdate solution was added.
3. Titrate with 0.0125 N sodium thiosulfate to faint yellow or straw color. Swirl or stir gently during titration to minimize iodine loss.
4. Add about 2 ml starch indicator, and continue titration until the blue color just disappears.
5. Repeat steps 2-4 on a blank sample of water.
6. Note ml of 0.0125 N $Na_2S_2O_3$ for samples and blanks analysis.

Calculation

$$H_2O_2, mg/l = \frac{(A-B) x N x 17 x 1{,}000}{ml.sample}$$

Where:

A = ml of $Na_2S_2O_3$ for sample

B = ml of $Na_2S_2O_3$ for blank

N = Normality of $Na_2S_2O_3$

APPENDIX B

Analysis of Ferrous Ions

Background

The 1,10-phenantrhroline complex with iron (II) was first discovered by Blau. Aspectrophotometric determination of iron dependent on the formation of the iron(II)-1,10-phenantrhroline complex was developed by Fortune Mellon. The iron(II)-1, 10-phenanthroline complex reddish orange in color.

Apparatus

1. Colorimetric Equipment; Spectrophotometer (Shimadsu UV-1201). The absorbance used for ferrous (Fe^{2+}) analysis was 510 nm.
2. Acid-washed Glassware. All glass wares were washed with conc. HCl and rinsed with DI water to remove deposit of iron oxide.
3. Membrane Filter: a 0.45 μm membrane filter was used to filter the sample to remove precipitation particle on solution.
4. Reagents:

All of reagents were prepared by distilled water. Reagents were stored in glass bottles. The HCL and ammonium acetate solutions were stable indefinitely if they were tightly closed the bottles. The standard ferrous ion (Fe^{2+}) solutions were not stable, it was prepared daily.

HCl: 20 ml of concentrated hydrochloric acid was diluted to 1000 ml with DI water.

Ammonium Acetate Buffer Solution: 500 g of $NH_4C_2H_3O_2$ was dissolved in 300 ml of DI water. Then, 1400 mo of concentrated acetic acid was filled up to the mark of 2000 ml.

Phenanthroline Solution: 5 g of 1,10-phenanthroline monohydrate, $C_{12}H_8N_2H_2O$, was dissolved and 1 ml of concentrated hydrochloric acid was added. Then, DI water was used to make the mark of 1000 ml.

Stock Ferrous Ion Solution: 20 mo of concentrated H_2SO_4 was slowly added to 25 ml DI water. Then 5 ml of stock ferrus ion solution was diluted to 50 ml with DI water. The standard solution was 50 mg/l as Fe^{2+}.

Procedure

1. Sample preparation for calibration curves: The satandard ferrous (Fe^{2+}) solution was prepared in the range 0 to 10 mg/l as Fe^{2+}. 25 mo of HCl from stock solution was prepared in six 50 ml volumetric flasks. Then, 10 ml of phenanthroline solution and 5 mo of ammonium acetate solution were added with vigorous stirring. 1, 2, 3, 4, 5 and 10 mo of 50 mg/l as Fe^{2+} standard solution were pipetted, respectively. After that, the samples were diluted to 50 ml with DI water, mixed thoroughly.

2. Ferrous Ion analysis: To determine ferrous ion, 25 mo of HCl from stock solution was prepared in 5o ml volumetric flask. Then, 10 ml of phenanthroline solution and 5 ml of ammonium acetate solution were added with vigorous stirring. 2 ml of sample was filled and diluted to 50 ml with DI water. After that, it had to stand for 30 min. Do not expose to sunlight. (Color development was rapidly in the presence of excess phenanthroline.)

Calculation

$y = 5.0694x – 0.1313$

Where: $y = Fe^{2+}$, mg/l , x = absorbance at 510 nm.

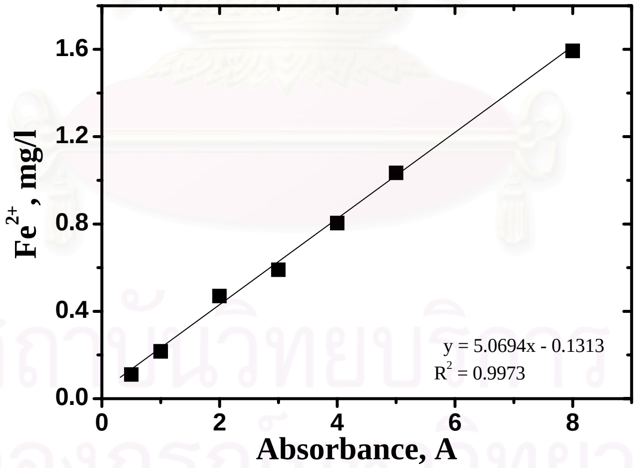

Figure A.1 Ferrous vs. Absorbance

APPENDIX C

Table C-1 pH_{pzc} of Al_2O_3

Mass, g/l	pH	
	DI water	Aniline & ionic strength[a]
0.000	5.050	6.830
0.200	6.50	7.020
0.400	6.550	7.310
0.600	6.860	7.480
1.200	7.150	7.910
2.400	7.430	8.010
5.000	7.970	8.150
10.000	8.210	8.440
20.000	8.410	8.660
30.000	8.540	8.710
40.000	8.640	8.710
50.000	8.660	8.740

Note: 24 hours of reaction, 0.010 M NB and 0.0250 M Na_2SO_4

Table C-2 pH_{pzc} of SiO_2

Mass, g/l	pH	
	DI water	Aniline & ionic strength[a]
0.000	7.370	7.370
0.200	7.240	7.240
0.400	7.200	7.200
0.600	7.070	7.010
1.200	6.890	6.870
2.400	6.790	6.790
5.000	6.640	6.640
10.000	6.540	6.510
20.000	6.400	6.370
30.000	6.400	6.390
40.000	6.410	6.380
50.000	6.420	6.300

Note: 24 hours of reaction, 0.010 M NB and 0.0250 M Na_2SO_4

Table C-3 Aniline remaining of control experiment

Time, min	AN, C/Co					
	only	+ H_2O_2	+ Al_2O_3	+ H_2O_2 + Al_2O_3	+ SiO_2	+ H_2O_2 + SiO_2
0	1.000	1.000	1.000	1.000	1.000	1.000
2	0.996	0.996	0.970	0.949	0.999	0.980
5	0.995	0.994	0.951	0.935	0.999	0.978
10	0.992	0.980	0.949	0.920	0.998	0.962
20	0.986	0.975	0.930	0.909	0.983	0.953
30	0.975	0.960	0.929	0.876	0.967	0.943
60	0.970	0.958	0.895	0.873	0.964	0.927

Note: 0.010 of AN, pH 2.8, Al_2O_3 74.070 g/l.

Table C-4 Combined H_2O_2 with AN remaining of control experiment

Time, min	H_2O_2, C/Co		
	+ H_2O_2	+ H_2O_2 + Al_2O_3	+ H_2O_2 + SiO_2
0	0.000	1.000	1.000
2	2.000	0.917	0.937
5	5.000	0.916	0.909
10	10.000	0.915	0.838
20	20.000	0.902	0.822
30	30.000	0.884	0.813
60	60.000	0.866	0.789

Note: H_2O_2 0.050 M.

Table C-5 H_2O_2 remaining combine with NB of control experiment

Time, min	NB, C/Co					
	only	+ H_2O_2	+ Al_2O_3	+ H_2O_2 + Al_2O_3	+ SiO_2	+ H_2O_2 + SiO_2
0	1.000	1.000	1.000	1.000	1.000	1.000
2	0.979	0.949	0.981	0.955	0.986	0.986
5	0.942	0.919	0.945	0.916	0.958	0.958
10	0.906	0.880	0.918	0.883	0.932	0.932
20	0.882	0.861	0.892	0.874	0.903	0.903
30	0.871	0.839	0.886	0.870	0.895	0.895
60	0.860	0.836	0.857	0.855	0.857	0.857

Note: 0.010 of AN, pH 2.8, Al_2O_3 74.070 g/l.

Table C-6 Combined H_2O_2 remaining with NB in control experiment

Time, min	H_2O_2, C/Co		
	+ H_2O_2	+ H_2O_2 + Al_2O_3	+ H_2O_2 + SiO_2
0	1.000	1.000	1.000
2	0.919	0.848	0.853
5	0.903	0.836	0.834
10	0.889	0.784	0.796
20	0.882	0.780	0.792
30	0.878	0.776	0.785
60	0.873	0.729	0.761

Note: H_2O_2 0.050 M.

Table C-7 The media comparison onto the degradation of AN within Al_2O_3 system

Time, min	C/Co			
	AN	H_2O_2	Fe^{2+}	TOC
0	1.000	1.000	1.000	1.000
2	0.833	0.801	0.807	0.962
5	0.775	0.776	0.574	0.910
10	0.674	0.728	0.214	0.896
20	0.460	0.592	0.102	0.884
30	0.284	0.432	0.087	0.883
60	0.113	0.158	0.066	0.882

Note: 0.010 M of AN, 0.050 M of H_2O_2, 0.001 M of Fe^{2+}, 74.070 g/l of Al_2O_3 and initial pH 2.8.

Table C-8 The media comparison onto the degradation of AN within SiO_2 system

Time, min	C/Co			
	AN	H_2O_2	Fe^{2+}	TOC
0	1.000	1.000	1.000	1.000
2	0.882	0.884	0.636	0.934
5	0.767	0.820	0.582	0.925
10	0.729	0.725	0.549	0.916
20	0.682	0.711	0.522	0.898
30	0.622	0.697	0.468	0.892
60	0.554	0.649	0.343	0.889

Note: 0.010 M of AN, 0.050 M of H_2O_2, 0.001 M of Fe^{2+}, 74.070 g/l of $SiO_2$and initial pH 2.8.

Table C-9 The media comparison onto the degradation of NB within Al_2O_3 system

Time, min	C/Co			
	NB	H_2O_2	Fe^{2+}	TOC
0	1.000	1.000	1.000	1.000
2	0.775	0.847	0.575	0.901
5	0.532	0.702	0.276	0.821
10	0.229	0.500	0.237	0.785
20	0.079	0.209	0.232	0.722
30	0.058	0.055	0.184	0.715
60	0.042	0.000	0.169	0.707

Note: 0.010 M of NB, 0.050 M of H_2O_2, 0.001 M of Fe^{2+}, 74.070 g/l of Al_2O_3 and initial pH 2.8.

Table C-10 The media comparison onto the degradation of NB within SiO_2 system

Time, min	C/Co			
	NB	H_2O_2	Fe^{2+}	TOC
0	1.000	1.000	1.000	1.000
2	0.738	0.782	0.636	0.942
5	0.534	0.660	0.582	0.929
10	0.274	0.457	0.549	0.924
20	0.118	0.122	0.522	0.889
30	0.098	0.100	0.468	0.824
60	0.079	0.041	0.343	0.721

Note: 0.010 M of NB, 0.050 M of H_2O_2, 0.001 M of Fe^{2+}, 74.070 g/l of SiO_2 and initial pH 2.8.

Table C-11 The media comparison onto the degradation of AN/NB within Al_2O_3

Time, min	C/Co				
	AN	NB	H_2O_2	Fe^{2+}	TOC
0	1.000	1.000	1.000	1.000	1.000
2	0.690	0.805	0.755	0.684	0.994
5	0.303	0.552	0.527	0.521	0.981
10	0.225	0.156	0.310	0.434	0.926
20	0.142	0.013	0.106	0.408	0.890
30	0.071	0.000	0.034	0.383	0.847
60	0.006	0.000	0.029	0.378	0.825

Note: 0.005 M of AN, 0.005 M of NB , 0.050 M of H_2O_2, 0.001 M of Fe^{2+}, 74.070 g/l of Al_2O_3 and initial pH 2.8.

Table C-12 The effect of pH on the degradation of AN in FBR; H_2O_2 remaining

Time, min	H_2O_2 , C/Co				
	pH 2.4	pH 2.8	pH 3.2	pH 3.6	pH 4.0
0	1.000	1.000	1.000	1.000	1.000
2	0.834	0.801	0.537	0.657	0.811
5	0.789	0.776	0.391	0.419	0.575
10	0.778	0.728	0.288	0.371	0.475
20	0.757	0.592	0.159	0.293	0.416
30	0.744	0.432	0.098	0.175	0.359
60	0.653	0.158	0.000	0.083	0.234

Note: 0.010 M of AN, 0.050 M of H_2O_2 , 0.001 M of Fe^{2+}, 74.070 g/l of Al_2O_3.

Table C-13 the effect of pH on the degradation of AN in FBR; Fe^{2+} remaining

Time, min	Fe^{2+} , C/Co				
	pH 2.4	pH 2.8	pH 3.2	pH 3.6	pH 4.0
0	1.000	1.000	1.000	1.000	1.000
2	0.369	0.807	0.446	0.667	0.616
5	0.354	0.574	0.285	0.521	0.332
10	0.339	0.214	0.182	0.413	0.308
20	0.324	0.102	0.104	0.381	0.296
30	0.308	0.087	0.052	0.343	0.231
60	0.213	0.066	0.037	0.287	0.219

Note: 0.010 M of AN, 0.050 M of H_2O_2 , 0.001 M of Fe^{2+}, 74.070 g/l of Al_2O_3.

Table C-14 The effect of pH on the degradation of AN in FBR; Total iron remaining

Time, min	Total iron , C/Co				
	pH 2.4	pH 2.8	pH 3.2	pH 3.6	pH 4.0
0	1.000	1.000	1.000	1.000	1.000
2	0.736	0.7845	0.879	0.764	0.808
5	0.672	0.6715	0.836	0.735	0.753
10	0.647	0.640	0.810	0.734	0.723
20	0.638	0.5936	0.769	0.723	0.689
30	0.614	0.5758	0.764	0.713	0.680
60	0.596	0.5608	0.741	0.735	0.675

Note: 0.010 M of AN, 0.050 M of H_2O_2 , 0.001 M of Fe^{2+}, 74.070 g/l of Al_2O_3.

Table C-15 The effect of pH on the degradation of NB in FBR; NB remaining

Time, min	NB, C/Co				
	pH 2.4	pH 2.8	pH 3.2	pH 3.6	pH 4.0
0	1.000	1.000	1.000	1.000	1.000
2	0.926	0.775	0.687	0.933	0.758
5	0.902	0.532	0.55	0.816	0.702
10	0.785	0.229	0.364	0.742	0.647
20	0.355	0.079	0.148	0.594	0.643
30	0.140	0.058	0.110	0.499	0.640
60	0.105	0.042	0.108	0.429	0.556

Note: 0.010 M of NB, 0.050 M of H_2O_2 , 0.001 M of Fe^{2+}, 74.070 g/l of Al_2O_3.

Table C-16 The effect of pH on the degradation of NB in FBR; H_2O_2 remaining

Time, min	H_2O_2 , C/Co				
	pH 2.4	pH 2.8	pH 3.2	pH 3.6	pH 4.0
0	1.000	1.000	1.000	1.000	1.000
2	0.798	0.847	0.751	0.681	0.855
5	0.759	0.702	0.650	0.567	0.769
10	0.727	0.500	0.520	0.546	0.749
20	0.551	0.209	0.235	0.517	0.738
30	0.275	0.055	0.079	0.465	0.705
60	0.000	0.000	0.000	0.352	0.679

Note: 0.010 M of NB, 0.050 M of H_2O_2 , 0.001 M of Fe^{2+}, 74.070 g/l of Al_2O_3.

Table 17 The effect of pH on the degradation of NB in FBR; Fe^{2+} remaining

Time, min	Fe^{2+} , C/Co				
	pH 2.4	pH 2.8	pH 3.2	pH 3.6	pH 4.0
0	1.000	1.000	1.000	1.000	1.000
2	0.203	0.575	0.288	0.864	0.829
5	0.289	0.276	0.276	0.776	0.787
10	0.528	0.236	0.294	0.762	0.698
20	0.589	0.230	0.403	0.680	0.509
30	0.559	0.184	0.414	0.606	0.497
60	0.583	0.167	0.546	0.585	0.533

Note: 0.010 M of NB, 0.050 M of H_2O_2 , 0.001 M of Fe^{2+}, 74.070 g/l of Al_2O_3.

Table C-18 The effect of pH on the degradation of NB in FBR; Total iron remaining

Time, min	Total iron , C/Co				
	pH 2.4	pH 2.8	pH 3.2	pH 3.6	pH 4.0
0	1.000	1.000	1.000	1.000	1.000
2	0.203	0.575	0.288	0.864	0.829
5	0.289	0.276	0.276	0.776	0.787
10	0.528	0.236	0.294	0.762	0.698
20	0.589	0.230	0.403	0.680	0.509
30	0.559	0.184	0.414	0.606	0.497
60	0.583	0.167	0.546	0.585	0.533

Note: 0.010 M of NB, 0.050 M of H_2O_2 , 0.001 M of Fe^{2+}, 74.070 g/l of Al_2O_3.

Table C-19 The effect of pH on the degradation of AN/NB in FBR; AN remaining

Time, min	AN , C/Co			
	pH 2.4	pH 2.8	pH 3.2	pH 3.6
0	1.000	1.000	1.000	1.000
2	0.894	0.745	0.585	0.691
5	0.727	0.588	0.300	0.357
10	0.608	0.372	0.216	0.251
20	0.431	0.179	0.150	0.151
30	0.257	0.094	0.122	0.140
60	0.188	0.092	0.133	0.155

Note: 0.005 M of AN, 0.005 M of NB, 0.050 M of H_2O_2 , 0.001 M of Fe^{2+}, 74.070 g/l of Al_2O_3.

Table C-20 The effect of pH on the degradation of AN/NB in FBR; NB remaining

Time, min	NB, C/Co			
	pH 2.4	pH 2.8	pH 3.2	pH 3.6
0	1.000	1.000	1.000	1.000
2	0.952	0.857	0.766	0.788
5	0.891	0.699	0.324	0.531
10	0.785	0.422	0.243	0.461
20	0.552	0.231	0.201	0.388
30	0.441	0.134	0.226	0.405
60	0.613	0.104	0.268	0.449

Note: 0.005 M of AN, 0.005 M of NB, 0.050 M of H_2O_2 , 0.001 M of Fe^{2+}, 74.070 g/l of Al_2O_3.

Table C-21 The effect of pH on the degradation of AN/NB in FBR; H_2O_2 remaining

Time, min	H_2O_2 , C/Co			
	pH 2.4	pH 2.8	pH 3.2	pH 3.6
0	1.000	1.000	1.000	1.000
2	0.672	0.839	0.749	0.727
5	0.601	0.658	0.494	0.577
10	0.478	0.357	0.311	0.441
20	0.224	0.161	0.131	0.301
30	0.119	0.000	0.071	0.185
60	0.000	0.000	0.000	0.085

Note: 0.005 M of AN, 0.005 M of NB, 0.050 M of H_2O_2 , 0.001 M of Fe^{2+}, 74.070 g/l of Al_2O_3.

Table C-22 The effect of pH on the degradation of AN/NB in FBR; Fe^{2+} remaining

Time, min	Fe^{2+} , C/Co			
	pH 2.4	pH 2.8	pH 3.2	pH 3.6
0	1.000	1.000	1.000	1.000
2	0.443	0.553	0.614	0.271
5	0.334	0.468	0.529	0.202
10	0.309	0.357	0.449	0.15
20	0.299	0.277	0.324	0.069
30	0.274	0.234	0.307	0.047
60	0.264	0.245	0.302	0.029

Note: 0.005 M of AN, 0.005 M of NB, 0.050 M of H_2O_2 , 0.001 M of Fe^{2+}, 74.070 g/l of Al_2O_3.

Table C-23 The comparison between Fenton and FB-Fenton process onto the degradation of AN in FBR

Time, min	Fenton (C/Co)				FB-Fenton (C/Co)			
	AN	H_2O_2	Fe^{2+}	Total iron	AN	H_2O_2	Fe^{2+}	Total iron
0	1.000	1.000	1.000	1.000	1.000	1.000	1.000	1.000
2	0.323	0.493	0.421	0.987	0.361	0.537	0.446	0.935
5	0.281	0.447	0.332	0.9519	0.270	0.391	0.285	0.869
10	0.248	0.415	0.235	0.9352	0.194	0.288	0.182	0.841
20	0.220	0.353	0.182	0.9215	0.132	0.159	0.104	0.776
30	0.195	0.316	0.155	0.9362	0.108	0.098	0.052	0.751
60	0.167	0.224	0.115	0.9174	0.105	0.000	0.037	0.716

Note: 0.010 M of AN, 0.050 M of H_2O_2, 0.001 M of Fe^{2+}, 74.070 g/l of Al_2O_3 and initial pH 3.2.

Table C-24 The comparison between Fenton and FB-Fenton process onto the degradation of NB in FBR

Time, min	Fenton (C/Co)				FB-Fenton (C/Co)			
	NB	H_2O_2	Fe^{2+}	Total iron	NB	H_2O_2	Fe^{2+}	Total iron
0	1.000	1.000	1.000	1.000	1.000	1.000	1.000	1.000
2	0.682	0.832	0.370	0.975	0.775	0.847	0.575	0.858
5	0.446	0.762	0.340	0.983	0.532	0.702	0.276	0.757
10	0.318	0.631	0.285	0.972	0.229	0.500	0.237	0.709
20	0.141	0.357	0.275	0.954	0.079	0.209	0.232	0.701
30	0.100	0.158	0.215	0.966	0.058	0.055	0.184	0.680
60	0.090	0.000	0.185	0.959	0.042	0.000	0.169	0.677

Note: 0.010 M of NB, 0.050 M of H_2O_2, 0.001 M of Fe^{2+}, 74.070 g/l of Al_2O_3 and initial pH 2.8.

Table C-25 The comparison between Fenton and FB-Fenton process onto the degradation of AN/NB in FBR;

Time, min	Fenton (C/Co)			FB-Fenton (C/Co)		
	AN	H_2O_2	Fe^{2+}	AN	H_2O_2	Fe^{2+}
0	1.000	1.000	1.000	1.000	1.000	1.000
2	0.803	0.839	0.553	0.811	0.761	0.724
5	0.583	0.658	0.468	0.666	0.701	0.670
10	0.372	0.357	0.357	0.381	0.575	0.645
20	0.179	0.161	0.277	0.172	0.277	0.641
30	0.094	0.000	0.234	0.130	0.185	0.621
60	0.092	0.000	0.245	0.082	0.058	0.606

Note: 0.005 M of AN, 0.005 M of NB, 0.050 M of H_2O_2 , 0.001 M of Fe^{2+}, 74.070 g/l of Al_2O_3.

Table C-26 The comparison between Fenton and FB-Fenton process onto the degradation of NB in FBR

Time, min	Fenton (C/Co)			FB-Fenton (C/Co)		
	NB	Total iron	TOC	NB	Total iron	TOC
0	1.000	1.000	1.000	1.000	1.000	1.000
2	0.857	0.849	0.929	0.952	0.847	0.981
5	0.699	0.782	0.925	0.795	0.702	0.963
10	0.422	0.732	0.874	0.444	0.500	0.905
20	0.231	0.723	0.874	0.161	0.209	0.860
30	0.134	0.712	0.868	0.144	0.055	0.838
60	0.104	0.687	0.758	0.108	0.000	0.803

Note: 0.005 M of AN, 0.005 M of NB, 0.050 M of H_2O_2 , 0.001 M of Fe^{2+}, 74.070 g/l of Al_2O_3.

Table C-27 AN remaining for kinetic removal rate was affected by [AN]

Time, min	AN (C/Co)				
	0.010 M	0.008 M	0.006 M	0.004 M	0.002 M
0	1.000	1.000	1.000	1.000	1.000
2	0.833	0.810	0.793	0.707	0.635
5	0.775	0.635	0.467	0.287	0.286
10	0.674	0.306	0.225	0.250	0.269
20	0.460	0.155	0.114	0.192	0.265
30	0.284	0.141	0.104	0.180	0.256
60	0.113	0.143	0.096	0.170	0.219

Note: 0.05 M of H_2O_2 , 0.001 M of Fe^{2+}, 74.070 g/l of Al_2O_3, pH 2.8.

Table C-28 H_2O_2 remaining for kinetic removal rate was affected by [AN]

Time, min	H_2O_2 (C/Co)				
	0.010 M	0.008 M	0.006 M	0.004 M	0.002 M
0	1.000	1.000	1.000	1.000	1.000
2	0.801	0.759	0.81	0.738	0.745
5	0.776	0.644	0.735	0.521	0.579
10	0.728	0.554	0.577	0.382	0.463
20	0.592	0.348	0.344	0.233	0.254
30	0.432	0.276	0.222	0.138	0.217
60	0.158	0.102	0.086	0.000	0.129

Note: 0.050 M of H_2O_2 , 0.001 M of Fe^{2+}, 74.070 g/l of Al_2O_3, pH 2.8

Table C-29 Fe^{2+} remaining for kinetic removal rate was affected by [AN]

Time, min	Fe^{2+} (C/Co)				
	0.010 M	0.008 M	0.006 M	0.004 M	0.002 M
0	1.000	1.000	1.000	1.000	1.000
2	0.807	0.587	0.566	0.739	0.695
5	0.574	0.386	0.44	0.596	0.509
10	0.214	0.256	0.341	0.488	0.277
20	0.102	0.169	0.252	0.296	0.08
30	0.087	0.163	0.226	0.212	0.074
60	0.066	0.169	0.063	0.000	1.000E-3

Note: 0.05 M of H_2O_2 , 0.001 M of Fe^{2+}, 74.07 g/l of Al_2O_3, pH 2.8.

Table C-30 TOC remaining for kinetic removal rate was affected by [AN]

Time, min	TOC (C/Co)				
	0.010 M	0.008 M	0.006 M	0.004 M	0.002 M
0	1.000	1.000	1.000	1.000	1.000
2	0.962	0.853	0.923	0.911	0.977
5	0.910	0.847	0.916	0.898	0.946
10	0.896	0.842	0.889	0.886	0.915
20	0.884	0.837	0.871	0.877	0.876
30	0.883	0.830	0.855	0.860	0.858
60	0.882	0.815	0.826	0.782	0.840

Note: 0.050 M of H_2O_2 , 0.001 M of Fe^{2+}, 74.070 g/l of Al_2O_3, pH 2.8.

Table C-31 NB remaining for kinetic removal rate was affected by [NB]

Time, min	NB (C/Co)				
	0.010 M	0.008 M	0.006 M	0.004 M	0.002 M
0	1.000	1.000	1.000	1.000	1.000
2	0.775	0.769	0.579	0.514	0.155
5	0.532	0.389	0.156	0.199	0.069
10	0.229	0.113	0.104	0.064	0.011
20	0.079	0.070	0.071	0.038	0.000
30	0.058	0.062	0.062	0.028	0.000
60	0.042	0.061	0.058	0.019	0.000

Note: 0.050 M of H_2O_2 , 0.001 M of Fe^{2+}, 74.070 g/l of Al_2O_3, pH 2.8.

Table C-32 H_2O_2 remaining for kinetic removal rate was affected by [NB]

Time, min	H_2O_2 (C/Co)				
	0.010 M	0.008 M	0.006 M	0.004 M	0.002 M
0	1.000	1.000	1.000	1.000	1.000
2	0.847	0.787	0.786	0.773	0.734
5	0.702	0.578	0.553	0.508	0.512
10	0.5	0.319	0.29	0.38	0.408
20	0.209	0.058	0.079	0.227	0.283
30	0.055	0.000	0.000	0.074	0.202
60	0.000	0.000	0.000	0.000	0.085

Note: 0.050 M of H_2O_2 , 0.001 M of Fe^{2+}, 74.070 g/l of Al_2O_3, pH 2.8

Table C-33 Fe^{2+} remaining for kinetic removal rate was affected by [NB]

Time, min	Fe^{2+} (C/Co)				
	0.010 M	0.008 M	0.006 M	0.004 M	0.002 M
0	1.000	1.000	1.000	1.000	1.000
2	0.575	0.506	0.591	0.620	0.642
5	0.276	0.451	0.553	0.560	0.548
10	0.236	0.430	0.506	0.500	0.490
20	0.230	0.397	0.452	0.468	0.453
30	0.184	0.359	0.442	0.457	0.442
60	0.167	0.348	0.426	0.441	0.395

Note: 0.050 M of H_2O_2 , 0.001 M of Fe^{2+}, 74.070 g/l of Al_2O_3, pH 2.8.

Table C-34 TOC remaining for kinetic removal rate was affected by [NB]

Time, min	TOC (C/Co)				
	0.010 M	0.008 M	0.006 M	0.004 M	0.002 M
0	1.000	1.000	1.000	1.000	1.000
2	0.901	0.861	0.840	0.863	0.872
5	0.821	0.791	0.789	0.758	0.820
10	0.785	0.781	0.761	0.718	0.772
20	0.722	0.738	0.744	0.713	0.733
30	0.715	0.718	0.721	0.698	0.714
60	0.707	0.694	0.682	0.690	0.725

Note: 0.050 M of H_2O_2 , 0.001 M of Fe^{2+}, 74.070 g/l of Al_2O_3, pH 2.8.

Table C-35 AN remaining for kinetic removal rate was affected by [AN:NB]

Time, min	AN (C/Co)				
	2 : 8 mM	4:6 mM	5:5 mM	6:4 mM	8:2 mM
0	1.000	1.000	1.000	1.000	1.000
2	0.277	0.427	0.857	0.846	0.963
5	0.086	0.323	0.699	0.438	0.884
10	0.029	0.146	0.422	0.146	0.702
20	0.013	0.034	0.231	0.034	0.161
30	0.000	0.043	0.134	0.043	0.190
60	0.000	0.074	0.104	0.074	0.070

Note: 0.050 M of H_2O_2 , 0.001 M of Fe^{2+}, 74.070 g/l of Al_2O_3, pH 2.8.

Table C-36 NB remaining for kinetic removal rate was affected by [AN:NB]

Time, min	NB (C/Co)				
	2 : 8 mM	4:6 mM	5:5 mM	6:4 mM	8:2 mM
0	1.000	1.000	1.000	1.000	1.000
2	0.277	0.427	0.857	0.846	0.963
5	0.086	0.323	0.699	0.438	0.884
10	0.029	0.146	0.422	0.146	0.702
20	0.013	0.034	0.231	0.034	0.161
30	0.000	0.043	0.134	0.043	0.190
60	0.000	0.074	0.104	0.074	0.070

Note: 0.050 M of H_2O_2 , 0.001 M of Fe^{2+}, 74.070 g/l of Al_2O_3, pH 2.8.

Table C-37 H_2O_2 remaining for kinetic removal rate was affected by [AN:NB]

Time, min	H_2O_2 (C/Co)				
	2 : 8 mM	4:6 mM	5:5 mM	6:4 mM	8:2 mM
0	1.000	1.000	1.000	1.000	1.000
2	0.755	0.828	0.839	0.788	0.799
5	0.527	0.764	0.658	0.730	0.750
10	0.310	0.543	0.357	0.598	0.705
20	0.106	0.220	0.161	0.359	0.415
30	0.034	0.107	0.000	0.226	0.389
60	0.029	0.092	0.000	0.046	0.102

Note: 0.050 M of H_2O_2 , 0.001 M of Fe^{2+}, 74.070 g/l of Al_2O_3, pH 2.8

Table C-38 Fe^{2+} remaining for kinetic removal rate was affected by [AN:NB]

Time, min	Fe^{2+} (C/Co)				
	2 : 8 mM	4:6 mM	5:5 mM	6:4 mM	8:2 mM
0	1.000	1.000	1.000	1.000	1.000
2	0.684	0.444	0.553	0.505	0.859
5	0.521	0.346	0.468	0.454	0.762
10	0.434	0.289	0.357	0.387	0.551
20	0.408	0.258	0.277	0.289	0.144
30	0.383	0.238	0.234	0.279	0.109
60	0.378	0.248	0.245	0.227	0.073

Note: 0.050 M of H_2O_2 , 0.001 M of Fe^{2+}, 74.070 g/l of Al_2O_3, pH 2.8.

Table C-39 TOC **remaining for kinetic removal rate was affected by [AN:NB]**

Time, min	TOC (C/Co)				
	2 : 8 mM	4:6 mM	5:5 mM	6:4 mM	8:2 mM
0	1.000	1.000	1.000	1.000	1.000
2	0.994	0.982	0.929	0.879	0.963
5	0.981	0.815	0.925	0.854	0.955
10	0.926	0.762	0.874	0.851	0.942
20	0.89	0.734	0.874	0.847	0.900
30	0.847	0.739	0.868	0.844	0.891
60	0.825	0.714	0.758	0.875	0.857

Note: 0.050 M of H_2O_2 , 0.001 M of Fe^{2+}, 74.070 g/l of Al_2O_3, pH 2.8.

Table C-40 AN remaining for kinetic removal rate was affected by [H_2O_2]

Time, min	AN (C/Co)				
	0.100 M	0.050 M	0.025 M	0.015 M	0.005 M
0	1.000	1.000	1.000	1.000	1.000
2	0.777	0.833	0.86	0.882	0.933
5	0.636	0.775	0.797	0.783	0.832
10	0.276	0.674	0.712	0.697	0.795
20	0.100	0.460	0.502	0.562	0.748
30	0.078	0.284	0.317	0.479	0.716
60	0.048	0.113	0.137	0.272	0.666

Note: 0.010 M of AN , 0.001 M of Fe^{2+}, 74.070 g/l of Al_2O_3, pH 2.8.

Table C-41 H_2O_2 remaining for kinetic removal rate was affected by [H_2O_2]

Time, min	H_2O_2 (C/Co)				
	0.100 M	0.050 M	0.025 M	0.015 M	0.005 M
0	1.000	1.000	1.000	1.000	1.000
2	0.789	0.801	0.809	0.832	0.842
5	0.764	0.776	0.747	0.69	0.478
10	0.737	0.728	0.682	0.582	0.239
20	0.597	0.592	0.520	0.492	0.104
30	0.461	0.432	0.408	0.395	0.000
60	0.220	0.158	0.123	0.042	0.000

Note: 0.010 M of AN , 0.001 M of Fe^{2+}, 74.070 g/l of Al_2O_3, pH 2.8.

Table C-42 Fe^{2+} remaining for kinetic removal rate was affected by [H_2O_2]

Time, min	Fe^{2+} (C/Co)				
	0.100 M	0.050 M	0.025 M	0.015 M	0.005 M
0	1.000	1.000	1.000	1.000	1.000
2	0.578	0.807	0.756	0.702	0.593
5	0.377	0.574	0.620	0.518	0.468
10	0.217	0.214	0.364	0.363	0.332
20	0.093	0.102	0.158	0.160	0.163
30	0.073	0.087	0.109	0.140	0.153
60	0.062	0.066	0.087	0.125	0.131

Note: 0.010 M of AN , 0.001 M of Fe^{2+}, 74.070 g/l of Al_2O_3, pH 2.8.

Table C-43 TOC remaining for kinetic removal rate was affected by [H_2O_2]

Time, min	TOC (C/Co)				
	0.100 M	0.050 M	0.025 M	0.015 M	0.005 M
0	1.000	1.000	1.000	1.000	1.000
2	0.908	0.962	0.951	0.939	0.977
5	0.868	0.910	0.939	0.902	0.974
10	0.841	0.896	0.938	0.897	0.970
20	0.812	0.884	0.921	0.893	0.96
30	0.809	0.883	0.913	0.892	0.903
60	0.802	0.882	0.916	0.887	0.884

Note: 0.010 M of AN , 0.001 M of Fe^{2+}, 74.070 g/l of Al_2O_3, pH 2.8.

Table C-44 NB remaining for kinetic removal rate was affected by [H_2O_2]

Time, min	NB (C/Co)				
	0.100 M	0.050 M	0.025 M	0.015 M	0.005 M
0	1.000	1.000	1.000	1.000	1.000
2	0.732	0.775	0.729	0.797	0.739
5	0.352	0.532	0.549	0.583	0.607
10	0.093	0.229	0.279	0.410	0.560
20	0.065	0.079	0.255	0.358	0.528
30	0.059	0.058	0.243	0.335	0.488
60	0.012	0.042	0.239	0.334	0.38

Note: 0.010 M of NB , 0.001 M of Fe^{2+}, 74.070 g/l of Al_2O_3, pH 2.8.

Table C-45 H_2O_2 remaining for kinetic removal rate was affected by [H_2O_2]

Time, min	H_2O_2 (C/Co)				
	0.100 M	0.050 M	0.025 M	0.015 M	0.005 M
0	1.000	1.000	1.000	1.000	1.000
2	0.758	0.822	0.859	0.818	0.822
5	0.623	0.702	0.636	0.634	0.645
10	0.462	0.500	0.285	0.263	0.218
20	0.225	0.209	0.092	0.080	0.094
30	0.177	0.055	0.027	0.038	0.000
60	0.049	0.000	0.000	0.000	0.000

Note: 0.010 M of NB , 0.001 M of Fe^{2+}, 74.070 g/l of Al_2O_3, pH 2.8.

Table C-46 Fe^{2+} remaining for kinetic removal rate was affected by $[H_2O_2]$

Time, min	Fe^{2+} (C/Co)				
	0.100 M	0.050 M	0.025 M	0.015 M	0.005 M
0	1.000	1.000	1.000	1.000	1.000
2	0.468	0.575	0.471	0.493	0.528
5	0.254	0.276	0.321	0.437	0.416
10	0.239	0.236	0.246	0.277	0.334
20	0.194	0.230	0.225	0.247	0.277
30	0.170	0.184	0.204	0.201	0.272
60	0.145	0.167	0.161	0.171	0.211

Note: 0.010 M of NB , 0.001 M of Fe^{2+}, 74.070 g/l of Al_2O_3, pH 2.8.

Table C-47 TOC remaining for kinetic removal rate was affected by $[H_2O_2]$

Time, min	TOC (C/Co)				
	0.100 M	0.050 M	0.025 M	0.015 M	0.005 M
0	1.000	1.000	1.000	1.000	1.000
2	0.888	0.901	0.871	0.962	0.992
5	0.783	0.821	0.806	0.925	0.969
10	0.759	0.785	0.778	0.91	0.929
20	0.715	0.722	0.741	0.886	0.879
30	0.693	0.715	0.714	0.850	0.821
60	0.688	0.707	0.702	0.845	0.777

Note: 0.010 M of NB, 0.001 M of Fe^{2+}, 74.070 g/l of Al_2O_3, pH 2.8.

Table C-48 AN:NB remaining for kinetic removal rate was affected by $[H_2O_2]$

Time, min	AN (C/Co)				
	0.100 M	0.050 M	0.025 M	0.015 M	0.005 M
0	1.000	1.000	1.000	1.000	1.000
2	0.555	0.803	0.826	0.744	0.832
5	0.233	0.583	0.623	0.618	0.726
10	0.132	0.372	0.444	0.437	0.654
20	0.124	0.179	0.225	0.381	0.435
30	0.105	0.094	0.220	0.362	0.379
60	0.101	0.092	0.207	0.308	0.317

Note: 0.005 M of AN, 0.005 M of NB , 0.001 M of Fe^{2+}, 74.070 g/l of Al_2O_3, pH 2.8.

Table C-49 AN:NB remaining for kinetic removal rate was affected by [H_2O_2]

Time, min	NB (C/Co)				
	0.100 M	0.050 M	0.025 M	0.015 M	0.005 M
0	1.000	1.000	1.000	1.000	1.000
2	0.679	0.857	0.852	0.856	0.833
5	0.418	0.699	0.728	0.748	0.755
10	0.079	0.422	0.495	0.465	0.671
20	0.068	0.231	0.259	0.381	0.471
30	0.050	0.134	0.281	0.378	0.404
60	0.045	0.104	0.295	0.381	0.408

Note: 0.005 M of AN, 0.005 M of NB , 0.001 M of Fe^{2+}, 74.070 g/l of Al_2O_3, pH 2.8.

Table C-50 H_2O_2 remaining for kinetic removal rate was affected by [H_2O_2]

Time, min	H_2O_2 (C/Co)				
	0.100 M	0.050 M	0.025 M	0.015 M	0.005 M
0	1.000	1.000	1.000	1.000	1.000
2	0.833	0.839	0.795	0.839	0.822
5	0.722	0.658	0.632	0.676	0.676
10	0.506	0.357	0.416	0.378	0.406
20	0.365	0.161	0.119	0.153	0.187
30	0.240	0.000	0.000	0.000	0.000
60	0.160	0.000	0.000	0.000	0.000

Note: 0.005 M of AN, 0.005 M of NB , 0.001 M of Fe^{2+}, 74.070 g/l of Al_2O_3, pH 2.8.

Table C-51 Fe^{2+} remaining for kinetic removal rate was affected by [H_2O_2]

Time, min	Fe^{2+} (C/Co)				
	0.100 M	0.050 M	0.025 M	0.015 M	0.005 M
0	1.000	1.000	1.000	1.000	1.000
2	0.621	0.553	0.650	0.576	0.645
5	0.520	0.468	0.552	0.505	0.557
10	0.435	0.357	0.351	0.425	0.485
20	0.425	0.277	0.304	0.414	0.454
30	0.409	0.234	0.289	0.399	0.428
60	0.339	0.245	0.279	0.374	0.397

Note: 0.005 M of AN, 0.005 M of NB , 0.001 M of Fe^{2+}, 74.070 g/l of Al_2O_3, pH 2.8.

Table C-52 TOC remaining for kinetic removal rate was affected by [H_2O_2]

Time, min	TOC (C/Co)				
	0.100 M	0.050 M	0.025 M	0.015 M	0.005 M
0	1.000	1.000	1.000	1.000	1.000
2	0.918	0.929	0.977	0.917	0.923
5	0.889	0.925	0.949	0.887	0.892
10	0.853	0.874	0.909	0.858	0.868
20	0.822	0.874	0.880	0.841	0.834
30	0.802	0.868	0.864	0.840	0.819
60	0.750	0.758	0.830	0.821	0.826

Note: 0.005 M of AN, 0.005 M of NB , 0.001 M of Fe^{2+}, 74.070 g/l of Al_2O_3, pH 2.8.

Table C-53 AN remaining for kinetic removal rate was affected by [Fe^{2+}]

Time, min	AN (C/Co)				
	0.000200 M	0.00100 M	0.00075 M	0.00050 M	0.00025 M
0	1.000	1.000	1.000	1.000	1.000
2	0.269	0.833	0.857	0.911	0.941
5	0.151	0.775	0.797	0.868	0.914
10	0.122	0.674	0.761	0.817	0.896
20	0.083	0.460	0.659	0.806	0.885
30	0.077	0.284	0.580	0.798	0.884
60	0.064	0.113	0.221	0.714	0.871

Note: 0.010 M of AN , 0.050 M of H_2O_2, 74.070 g/l of Al_2O_3, pH 2.8.

Table C-54 H_2O_2 remaining for kinetic removal rate was affected by [Fe^{2+}]

Time, min	H_2O_2 (C/Co)				
	0.000200 M	0.00100 M	0.00075 M	0.00050 M	0.00025 M
0	1.000	1.000	1.000	1.000	1.000
2	0.802	0.801	0.800	0.803	0.806
5	0.684	0.776	0.768	0.763	0.760
10	0.452	0.728	0.745	0.758	0.734
20	0.112	0.592	0.691	0.732	0.733
30	0.046	0.432	0.667	0.728	0.728
60	0.000	0.158	0.508	0.702	0.706

Note: 0.010 M of AN , 0.050 M of H_2O_2, 74.070 g/l of Al_2O_3, pH 2.8.

Table C-55 Fe^{2+} remaining for kinetic removal rate was affected by $[Fe^{2+}]$

Time, min	Fe^{2+} (C/Co)				
	0.000200 M	0.00100 M	0.00075 M	0.00050 M	0.00025 M
0	1.000	1.000	1.000	1.000	1.000
2	0.661	0.807	0.692	0.642	0.560
5	0.589	0.574	0.542	0.420	0.384
10	0.541	0.214	0.241	0.199	0.238
20	0.521	0.102	0.121	0.075	0.003
30	0.496	0.087	0.076	0.038	0.003
60	0.461	0.066	1.000E-3	1.000E-3	0.003

Note: 0.010 M of AN , 0.050 M of H_2O_2, 74.070 g/l of Al_2O_3, pH 2.8.

Table C-56 TOC remaining for kinetic removal rate was affected by $[Fe^{2+}]$

Time, min	TOC (C/Co)				
	0.000200 M	0.00100 M	0.00075 M	0.00050 M	0.00025 M
0	1.000	1.000	1.000	1.000	1.000
2	0.959	0.962	0.961	0.996	0.998
5	0.917	0.910	0.945	0.978	0.991
10	0.883	0.896	0.905	0.961	0.953
20	0.844	0.884	0.881	0.946	0.931
30	0.819	0.883	0.867	0.914	0.882
60	0.811	0.882	0.841	0.839	0.875

Note: 0.010 M of AN , 0.050 M of H_2O_2, 74.070 g/l of Al_2O_3, pH 2.8.

Table C-57 NB remaining for kinetic removal rate was affected by $[Fe^{2+}]$

Time, min	NB (C/Co)				
	0.000200 M	0.00100 M	0.00075 M	0.00050 M	0.00025 M
0	1.000	1.000	1.000	1.000	1.000
2	0.599	0.775	0.781	0.845	0.901
5	0.124	0.532	0.551	0.662	0.781
10	0.085	0.229	0.256	0.543	0.716
20	0.076	0.079	0.074	0.231	0.553
30	0.073	0.058	0.067	0.098	0.395
60	0.072	0.042	0.066	0.082	0.123

Note: 0.010 M of NB , 0.050 M of H_2O_2, 74.070 g/l of Al_2O_3, pH 2.8.

Table C-58 H_2O_2 remaining for kinetic removal rate was affected by [Fe^{2+}]

Time, min	H_2O_2 (C/Co)				
	0.000200 M	0.00100 M	0.00075 M	0.00050 M	0.00025 M
0	1.000	1.000	1.000	1.000	1.000
2	0.656	0.847	0.811	0.801	0.815
5	0.300	0.702	0.742	0.747	0.801
10	0.058	0.500	0.553	0.655	0.786
20	0.000	0.209	0.212	0.414	0.728
30	0.000	0.055	0.085	0.194	0.635
60	0.000	0.000	0.000	0.000	0.404

Note: 0.010 M of NB , 0.050 M of H_2O_2, 74.070 g/l of Al_2O_3, pH 2.8.

Table C-59 Fe^{2+} remaining for kinetic removal rate was affected by [Fe^{2+}]

Time, min	Fe^{2+} (C/Co)				
	0.000200 M	0.00100 M	0.00075 M	0.00050 M	0.00025 M
0	1.000	1.000	1.000	1.000	1.000
2	0.841	0.575	0.68	0.539	0.106
5	0.807	0.276	0.412	0.414	0.064
10	0.762	0.237	0.321	0.299	0.002
20	0.735	0.232	0.242	0.222	0.002
30	0.733	0.184	0.190	0.164	0.002
60	0.721	0.169	0.177	0.135	0.002

Note: 0.010 M of NB , 0.050 M of H_2O_2, 74.070 g/l of Al_2O_3, pH 2.8.

Table C-60 TOC remaining for kinetic removal rate was affected by [Fe^{2+}]

Time, min	TOC (C/Co)				
	0.000200 M	0.00100 M	0.00075 M	0.00050 M	0.00025 M
0	1.000	1.000	1.000	1.000	1.000
2	0.975	0.901	0.95	0.978	0.994
5	0.747	0.821	0.815	0.847	0.954
10	0.652	0.785	0.762	0.788	0.916
20	0.575	0.722	0.757	0.782	0.864
30	0.568	0.715	0.720	0.755	0.813
60	0.560	0.707	0.718	0.739	0.804

Note: 0.010 M of NB , 0.050 M of H_2O_2, 74.070 g/l of Al_2O_3, pH 2.8.

Table C-61 AN:NB remaining for kinetic removal rate was affected by [Fe^{2+}]

Time, min	AN (C/Co)				
	0.000200 M	0.00100 M	0.00075 M	0.00050 M	0.00025 M
0	1.000	1.000	1.000	1.000	1.000
2	0.257	0.803	0.787	0.800	0.908
5	0.181	0.583	0.732	0.749	0.857
10	0.137	0.372	0.624	0.654	0.788
20	0.133	0.179	0.330	0.435	0.701
30	0.120	0.094	0.155	0.259	0.617
60	0.117	0.092	0.126	0.152	0.369

Note: 0.005 M of AN, 0.0050 M of NB , 0.050 M of H_2O_2, 74.070 g/l of Al_2O_3, pH 2.8.

Table C-62 AN:NB remaining for kinetic removal rate was affected by [Fe^{2+}]

Time, min	NB (C/Co)				
	0.000200 M	0.00100 M	0.00075 M	0.00050 M	0.00025 M
0	1.000	1.000	1.000	1.000	1.000
2	0.775	0.82	0.857	0.812	0.881
5	0.532	0.593	0.699	0.697	0.784
10	0.229	0.170	0.422	0.567	0.671
20	0.079	0.082	0.231	0.244	0.471
30	0.058	0.089	0.134	0.090	0.218
60	0.042	0.141	0.104	0.081	0.088

Note: 0.005 M of AN, 0.005 M of NB , 0.050 M of H_2O_2, 74.070 g/l of Al_2O_3, pH 2.8.

Table C-63 H_2O_2 remaining for kinetic removal rate was affected by [Fe^{2+}]

Time, min	H_2O_2 (C/Co)				
	0.100 M	0.050 M	0.025 M	0.015 M	0.005 M
0	1.000	1.000	1.000	1.000	1.000
2	0.735	0.839	0.809	0.814	0.837
5	0.457	0.658	0.710	0.790	0.800
10	0.211	0.357	0.636	0.737	0.765
20	0.109	0.161	0.387	0.606	0.738
30	0.000	0.000	0.241	0.485	0.704
60	0.000	0.000	0.051	0.291	0.683

Note: 0.005 M of AN, 0.005 M of NB , 0.050 M of H_2O_2, 74.070 g/l of Al_2O_3, pH 2.8.

Table C-64 Fe^{2+} remaining for kinetic removal rate was affected by [Fe^{2+}]

Time, min	Fe^{2+} (C/Co)				
	0.100 M	0.050 M	0.025 M	0.015 M	0.005 M
0	1.000	1.000	1.000	1.000	1.000
2	0.841	0.553	0.787	0.630	0.502
5	0.807	0.468	0.440	0.346	0.288
10	0.762	0.357	0.263	0.100	0.004
20	0.735	0.277	0.100	1.000E-3	0.004
30	0.733	0.234	0.093	1.000E-3	0.004
60	0.721	0.245	0.086	1.000E-3	0.004

Note: 0.005 M of AN, 0.005 M of NB , 0.050 M of H_2O_2, 74.070 g/l of Al_2O_3, pH 2.8.

.

Table C-65 TOC remaining for kinetic removal rate was affected by [Fe^{2+}]

Time, min	TOC (C/Co)				
	0.100 M	0.050 M	0.025 M	0.015 M	0.005 M
0	1.000	1.000	1.000	1.000	1.000
2	0.859	0.929	0.980	0.913	0.958
5	0.845	0.925	0.927	0.892	0.939
10	0.851	0.874	0.904	0.864	0.919
20	0.848	0.874	0.879	0.855	0.916
30	0.817	0.868	0.864	0.846	0.895
60	0.736	0.758	0.850	0.843	0.841

Note: 0.005 M of AN, 0.005 M of NB , 0.050 M of H_2O_2, 74.070 g/l of Al_2O_3, pH 2.8.

Table C-66 The initial rate of AN as the individual target compound in FBR

AN (only)					
[H_2O_2] M	[Fe^{2+}] M	[AN] M	Initial rate observed (M/min)	Initial rate calculation (M/min)	ESS
5.000E-02	1.000E-03	2.000E-03	2.770E-04	2.797E-04	4.360E-10
5.000E-02	1.000E-03	4.000E-03	4.058E-04	4.060E-04	5.223E-10
5.000E-02	1.000E-03	5.000E-03	4.134E-04	4.577E-04	9.271E-10
5.000E-02	1.000E-03	6.000E-03	5.568E-04	5.048E-04	2.695E-10
5.000E-02	1.000E-03	8.000E-03	5.634E-04	5.893E-04	1.226E-09
5.000E-03	1.000E-03	1.000E-02	2.660E-04	2.281E-04	3.920E-10
1.500E-02	1.000E-03	1.000E-02	3.686E-04	3.180E-04	1.971E-09
2.500E-02	1.000E-03	1.000E-02	3.740E-04	3.711E-04	1.174E-09
5.000E-02	1.000E-03	1.000E-02	4.130E-04	4.577E-04	1.226E-09
1.000E-01	1.000E-03	1.000E-02	7.480E-04	5.645E-04	3.634E-10
5.000E-02	2.500E-04	1.000E-02	1.390E-04	1.486E-04	1.590E-08
5.000E-02	5.000E-04	1.000E-02	2.380E-04	2.608E-04	3.708E-09
5.000E-02	7.500E-04	1.000E-02	2.540E-04	3.624E-04	8.858E-09
5.000E-02	1.000E-03	1.000E-02	4.130E-04	4.577E-04	1.414E-09
k= 93.24 $M^{-2}min^{-1}$				sum	3.838E-08

Note: 74.070 g/l of Al_2O_3, pH 2.8.

Table C-67 The initial rate of NB as the individual target compound in FBR

NB (only)					
[H_2O_2] M	[Fe^{2+}] M	[NB] M	Initial rate observed (M/min)	Initial rate calculation (M/min)	ESS
5.000E-02	1.000E-03	2.000E-03	8.450E-04	8.591E-04	1.999E-10
5.000E-02	1.000E-03	4.000E-03	9.720E-04	9.506E-04	4.594E-10
5.000E-02	1.000E-03	5.000E-03	9.960E-04	1.008E-03	1.562E-10
5.000E-02	1.000E-03	6.000E-03	9.800E-04	1.052E-03	5.145E-09
5.000E-02	1.000E-03	8.000E-03	1.124E-03	1.087E-03	1.411E-09
5.000E-03	1.000E-03	1.000E-02	6.850E-04	6.583E-04	7.114E-10
1.500E-02	1.000E-03	1.000E-02	8.230E-04	8.361E-04	1.719E-10
2.500E-02	1.000E-03	1.000E-02	8.780E-04	9.344E-04	3.182E-09
5.000E-02	1.000E-03	1.000E-02	1.124E-03	1.087E-03	1.411E-09
1.000E-01	1.000E-03	1.000E-02	1.293E-03	1.263E-03	8.752E-10
5.000E-02	2.500E-04	1.000E-02	4.360E-04	3.927E-04	1.874E-09
5.000E-02	5.000E-04	1.000E-02	6.700E-04	6.532E-04	2.817E-10
5.000E-02	7.500E-04	1.000E-02	8.880E-04	8.797E-04	6.922E-11
5.000E-02	1.000E-03	1.000E-02	9.270E-04	1.087E-03	2.545E-08
5.000E-02	2.000E-03	1.000E-02	2.006E-03	1.807E-03	3.948E-08
k= 0.650 $M^{-2}min^{-1}$				sum	1.914E-07

Note: 74.07 g/l of Al_2O_3, pH 2.8.

Table C-68 The initial rate of AN in the combination of AN/NB in FBR

AN (combination)					
[H_2O_2] M	[Fe^{2+}] M	[NB] M	Initial rate observed (M/min)	Initial rate calculation (M/min)	ESS
5.000E-02	1.000E-03	2.000E-03	2.797E-04	3.856E-04	7.292E-12
5.000E-02	1.000E-03	4.000E-03	4.060E-04	5.471E-04	2.973E-14
5.000E-02	1.000E-03	5.000E-03	4.577E-04	6.124E-04	1.965E-09
5.000E-02	1.000E-03	6.000E-03	5.048E-04	6.714E-04	2.702E-09
5.000E-02	1.000E-03	8.000E-03	5.893E-04	7.764E-04	6.683E-10
5.000E-03	1.000E-03	5.000E-03	2.281E-04	2.514E-04	1.438E-09
1.500E-02	1.000E-03	5.000E-03	3.180E-04	3.845E-04	2.563E-09
2.500E-02	1.000E-03	5.000E-03	3.711E-04	4.684E-04	8.247E-12
5.000E-02	1.000E-03	5.000E-03	4.577E-04	6.124E-04	1.999E-09
1.000E-01	1.000E-03	5.000E-03	5.645E-04	8.006E-04	3.368E-08
5.000E-02	2.500E-04	5.000E-03	1.486E-04	1.205E-04	9.213E-11
5.000E-02	5.000E-04	5.000E-03	2.608E-04	2.717E-04	5.196E-10
5.000E-02	7.500E-04	5.000E-03	3.624E-04	4.370E-04	1.175E-08
5.000E-02	1.000E-03	5.000E-03	4.577E-04	6.124E-04	1.999E-09
5.000E-02	2.000E-03	5.000E-03	8.033E-04	1.380E-03	1.559E-09
k = 5.310 $M^{-2}min^{-1}$				sum	5.289E-08

Note: 74.070 g/l of Al_2O_3, pH 2.8.

Table C-69 The initial rate of NB in the combination of AN/NB in FBR

NB (combination)					
[H2O2] M	[Fe2+] M	[NB] M	Initial rate observed (M/min)	Initial rate calculation (M/min)	ESS
5.000E-02	1.000E-03	2.000E-03	4.680E-05	5.033E-05	1.244E-11
5.000E-02	1.000E-03	4.000E-03	2.000E-04	2.003E-04	9.529E-14
5.000E-02	1.000E-03	5.000E-03	2.990E-04	3.125E-04	1.817E-10
5.000E-02	1.000E-03	6.000E-03	4.610E-04	4.494E-04	1.350E-10
5.000E-02	1.000E-03	8.000E-03	7.140E-04	7.972E-04	6.930E-09
5.000E-03	1.000E-03	5.000E-03	2.356E-04	1.709E-04	4.186E-09
1.500E-02	1.000E-03	5.000E-03	2.460E-04	2.279E-04	3.270E-10
2.500E-02	1.000E-03	5.000E-03	2.673E-04	2.606E-04	4.531E-11
5.000E-02	1.000E-03	5.000E-03	2.986E-04	3.125E-04	1.929E-10
1.000E-01	1.000E-03	5.000E-03	5.698E-04	3.747E-04	3.805E-08
5.000E-02	2.500E-04	5.000E-03	1.390E-04	1.530E-04	1.973E-10
5.000E-02	5.000E-04	5.000E-03	2.117E-04	2.187E-04	4.881E-11
5.000E-02	7.500E-04	5.000E-03	2.944E-04	2.695E-04	6.221E-10
5.000E-02	1.000E-03	5.000E-03	2.986E-04	3.125E-04	1.927E-10
5.000E-02	2.000E-03	5.000E-03	4.044E-04	4.465E-04	1.772E-09
k = 924.729 $M^{-2}min^{-1}$				sum	5.289E-08

Note: 74.070 g/l of Al_2O_3, pH 2.8.

Table C-70 The effect of intermittent addition of Fenton's reagent on the oxidation of AN/NB in FBR at pH 2.8; [K1 non-injection]

Time, min	C/Co					
	AN	NB	H_2O_2	Fe^{2+}	Total iron	TOC
0	1.000	1.000	1.000	1.000	1.0000	1.0000
2	0.794	0.853	0.826	0.552	0.8451	0.9292
5	0.589	0.708	0.680	0.512	0.7828	0.9252
10	0.375	0.425	0.345	0.397	0.7372	0.8741
20	0.187	0.234	0.153	0.334	0.7243	0.8735
30	0.122	0.162	0.000	0.305	0.7191	0.8683
32	0.121	0.179	0.000	0.299	0.7153	0.8306
35	0.106	0.197	0.000	0.288	0.7096	0.8173
40	0.100	0.206	0.000	0.288	0.7067	0.7662
50	0.081	0.199	0.000	0.282	0.6864	0.7639
60	0.079	0.113	0.000	0.282	0.6785	0.7581

Note: 0.005 M of AN, 0.005 M of NB , 0.050M of H_2O_2, 0.001 M of Fe^{2+}, 74.070 g/l of Al_2O_3 and initial pH 2.8.

Table C-71 The effect of intermittent addition of Fenton’s reagent on the oxidation of AN/NB in FBR at pH 2.8; K2 [10% initial H_2O_2/Fe^{2+} , after 30 min.]

Time, min	C/Co					
	AN	NB	H_2O_2	Fe^{2+}	Total iron	TOC
0	1.000	1.000	1.000	1.000	1.000	1.000
2	0.802	0.885	0.832	0.547	0.856	0.919
5	0.614	0.746	0.685	0.508	0.786	0.896
10	0.341	0.426	0.345	0.399	0.729	0.890
20	0.182	0.241	0.146	0.334	0.718	0.861
30	0.103	0.157	0.000	0.290	0.709	0.844
32	0.100	0.162	0.070	0.399	0.808	0.829
35	0.092	0.157	0.034	0.388	0.800	0.815
40	0.088	0.144	0.000	0.339	0.792	0.762
50	0.086	0.148	0.000	0.312	0.779	0.720
60	0.081	0.110	0.000	0.290	0.766	0.746

Note: 0.005 M of AN, 0.005 M of NB , 0.050 M of H_2O_2, 0.001 M of Fe^{2+}, 74.070 g/l of Al_2O_3 and initial pH 2.8.

Table C-72 The effect of intermittent addition of Fenton’s reagent on the oxidation of AN/NB in FBR at pH 2.8; K3 [50% initial H_2O_2 , after 30 min.]

Time, min	C/Co					
	AN	NB	H_2O_2	Fe^{2+}	Total iron	TOC
0	1.000	1.000	1.000	1.000	1.000	1.000
2	0.746	0.826	0.762	0.556	0.847	0.966
5	0.576	0.700	0.555	0.511	0.799	0.930
10	0.363	0.424	0.320	0.384	0.733	0.909
20	0.183	0.238	0.105	0.328	0.727	0.845
30	0.119	0.173	0.000	0.300	0.704	0.817
32	0.114	0.147	0.398	0.289	0.681	0.773
35	0.113	0.145	0.345	0.278	0.659	0.770
40	0.109	0.134	0.269	0.267	0.662	0.755
50	0.078	0.120	0.154	0.262	0.658	0.735
60	0.074	0.097	0.071	0.262	0.649	0.731

Note: 0.005 M of AN, 0.005 M of NB , 0.050 M of H_2O_2, 0.001 M of Fe^{2+}, 74.070 g/l of Al_2O_3 and initial pH 2.8.

Table C-73 The effect of intermittent addition of Fenton's reagent on the oxidation of AN/NB in FBR at pH 3.6;L1 [non-injection]

Time, min	C/Co				
	AN	NB	H_2O_2	Fe^{2+}	Total iron
0	1.000	1.000	1.000	1.000	1.000
2	0.535	0.729	0.703	0.304	0.830
5	0.370	0.576	0.576	0.227	0.821
10	0.260	0.473	0.443	0.150	0.812
20	0.172	0.386	0.266	0.078	0.794
30	0.163	0.411	0.160	0.067	0.789
32	0.134	0.360	0.146	0.057	0.781
35	0.150	0.506	0.130	0.052	0.752
40	0.112	0.392	0.102	0.042	0.731
50	0.119	0.469	0.076	0.031	0.726
60	0.136	0.596	0.042	0.021	0.699

Note: 0.005 M of AN, 0.005 M of NB , 0.050 M of H_2O_2, 0.001 M of Fe^{2+}, 74.070 g/l of Al_2O_3 and initial pH 3.6.

Table C-74The effect of intermittent addition of Fenton's reagent on the oxidation of AN/NB in FBR at pH 3.6;L2 [10% initial H_2O_2/Fe^{2+}, after 30 min.]

Time, min	C/Co				
	AN	NB	H_2O_2	Fe^{2+}	Total iron
0	1.000	1.000	1.000	1.000	1.000
2	0.541	0.733	0.702	0.271	0.834
5	0.376	0.576	0.576	0.179	0.824
10	0.280	0.476	0.446	0.109	0.814
20	0.158	0.389	0.271	0.055	0.794
30	0.173	0.434	0.189	0.022	0.791
32	0.183	0.427	0.238	0.109	0.884
35	0.169	0.358	0.188	0.092	0.816
40	0.124	0.234	0.160	0.087	0.788
50	0.152	0.327	0.111	0.082	0.788
60	0.097	0.277	0.062	0.076	0.788

Note: 0.005 M of AN, 0.005 M of NB , 0.050 M of H_2O_2, 0.001 M of Fe^{2+}, 74.070 g/l of Al_2O_3 and initial pH 3.6.

Table C-75 The effect of intermittent addition of Fenton's reagent on the oxidation of AN/NB in FBR at pH 3.6;L3 [50% initial Fe^{2+}, after 30 min.]

Time, min	C/Co				
	AN	NB	H_2O_2	Fe^{2+}	Total iron
0	1.000	1.000	1.000	1.000	1.000
2	0.578	0.747	0.728	0.308	0.861
5	0.390	0.561	0.606	0.193	0.857
10	0.285	0.489	0.461	0.132	0.854
20	0.187	0.393	0.296	0.044	0.825
30	0.165	0.432	0.175	0.017	0.810
32	0.138	0.400	0.109	0.544	1.204
35	0.132	0.355	0.048	0.495	1.202
40	0.130	0.465	0.000	0.489	1.176
50	0.136	0.508	0.000	0.484	1.152
60	0.141	0.511	0.000	0.456	1.151

Note: 0.005 M of AN, 0.005 M of NB , 0.050 M of H_2O_2, 0.001 M of Fe^{2+}, 74.070 g/l of Al_2O_3 and initial pH 3.6.

Table C-76 The effect of intermittent addition of Fenton's reagent on the oxidation of AN/NB in FBR at pH 3.6;L4 [50% initial $H_2O_2/Fe2^+$, after 30 min.]

Time, min	C/Co				
	AN	NB	H_2O_2	Fe^{2+}	Total iron
0	1.000	1.000	1.000	1.000	1.000
2	0.530	0.725	0.744	0.311	0.834
5	0.389	0.562	0.588	0.207	0.827
10	0.279	0.486	0.474	0.156	0.801
20	0.187	0.396	0.312	0.069	0.797
30	0.167	0.441	0.206	0.035	0.784
32	0.154	0.411	0.504	0.523	1.264
35	0.131	0.355	0.430	0.472	1.212
40	0.113	0.343	0.305	0.403	1.163
50	0.109	0.325	0.145	0.322	1.131
60	0.094	0.286	0.036	0.271	1.101

Note: 0.005 M of AN, 0.005 M of NB , 0.050 M of H_2O_2, 0.0010 M of Fe^{2+}, 74.070 g/l of Al_2O_3 and initial pH 3.6.

Table C-77 The reusability of aluminum oxide with 5 times recycling in FBR

Time, min	1st cycle, C/Co					
	AN	NB	H_2O_2	Fe^{2+}	Total iron	TOC
0	1.000	1.000	1.000	1.000	1.000	1.000
2	0.758	0.843	0.827	0.590	0.845	0.937
5	0.576	0.697	0.686	0.467	0.764	0.924
10	0.346	0.431	0.354	0.370	0.731	0.905
20	0.174	0.274	0.172	0.288	0.724	0.864
30	0.109	0.127	0.031	0.257	0.723	0.856
60	0.068	0.087	0.000	0.262	0.741	0.820

Note: 0.005 M of AN, 0.005 M of NB, 0.050 M of H_2O_2, 0.001 M of Fe^{2+}, 74.070 g/l of Al_2O_3, pH 2.8.

Table C-78 The reusability of aluminum oxide with 5 times recycling in FBR

Time, min	2nd cycle, C/Co					
	AN	NB	H_2O_2	Fe^{2+}	Total iron	TOC
0	1.000	1.000	1.000	1.000	1.000	1.000
2	0.815	0.795	0.780	0.576	0.863	0.949
5	0.609	0.632	0.546	0.473	0.794	0.909
10	0.349	0.417	0.416	0.381	0.773	0.885
20	0.187	0.235	0.182	0.283	0.764	0.870
30	0.143	0.164	0.026	0.245	0.756	0.877
60	0.101	0.117	0.000	0.240	0.755	0.846

Note: 0.005 M of AN, 0.005 M of NB, 0.050 M of H_2O_2, 0.001 M of Fe^{2+}, 74.070 g/l of Al_2O_3, pH 2.8.

Table C-79 The reusability of aluminum oxide with 5 times recycling in FBR

Time, min	3rd cycle, C/Co					
	AN	NB	H_2O_2	Fe^{2+}	Total iron	TOC
0	1.000	1.000	1.000	1.000	1.000	1.000
2	0.824	0.845	0.780	0.600	0.855	0.988
5	0.679	0.719	0.624	0.527	0.806	0.966
10	0.357	0.432	0.458	0.405	0.791	0.937
20	0.182	0.236	0.172	0.303	0.786	0.881
30	0.150	0.180	0.042	0.279	0.776	0.851
60	0.127	0.104	0.000	0.259	0.767	0.831

Note: 0.005 M of AN, 0.005 M of NB, 0.050 M of H_2O_2, 0.001 M of Fe^{2+}, 74.070 g/l of Al_2O_3, pH 2.8.

Table C-80 The reusability of aluminum oxide with 5 times recycling in FBR

Time, min	4th cycle, C/Co					
	AN	NB	H_2O_2	Fe^{2+}	Total iron	TOC
0	1.000	1.000	1.000	1.000	1.000	1.000
2	0.819	0.866	0.775	0.578	0.865	0.947
5	0.737	0.751	0.645	0.518	0.831	0.939
10	0.431	0.472	0.484	0.423	0.824	0.898
20	0.204	0.265	0.166	0.322	0.799	0.888
30	0.173	0.193	0.026	0.277	0.788	0.871
60	0.132	0.122	0.000	0.272	0.782	0.829

Note: 0.005 M of AN, 0.005 M of NB, 0.050 M of H_2O_2, 0.001 M of Fe^{2+}, 74.070 g/l of Al_2O_3, pH 2.8.

Table C-81 The reusability of aluminum oxide with 5 times recycling in FBR

Time, min	5th cycle, C/Co					
	AN	NB	H_2O_2	Fe^{2+}	Total iron	TOC
0	1.000	1.000	1.000	1.000	1.000	1.000
2	0.876	0.886	0.801	0.590	0.936	0.986
5	0.739	0.741	0.676	0.534	0.837	0.977
10	0.477	0.488	0.489	0.436	0.829	0.959
20	0.246	0.291	0.198	0.324	0.830	0.902
30	0.178	0.195	0.042	0.257	0.814	0.885
60	0.135	0.166	0.000	0.252	0.795	0.832

Note: 0.005 M of AN, 0.005 M of NB, 0.050 M of H_2O_2, 0.001 M of Fe^{2+}, 74.070 g/l of Al_2O_3, pH 2.8.

APPENDIX D

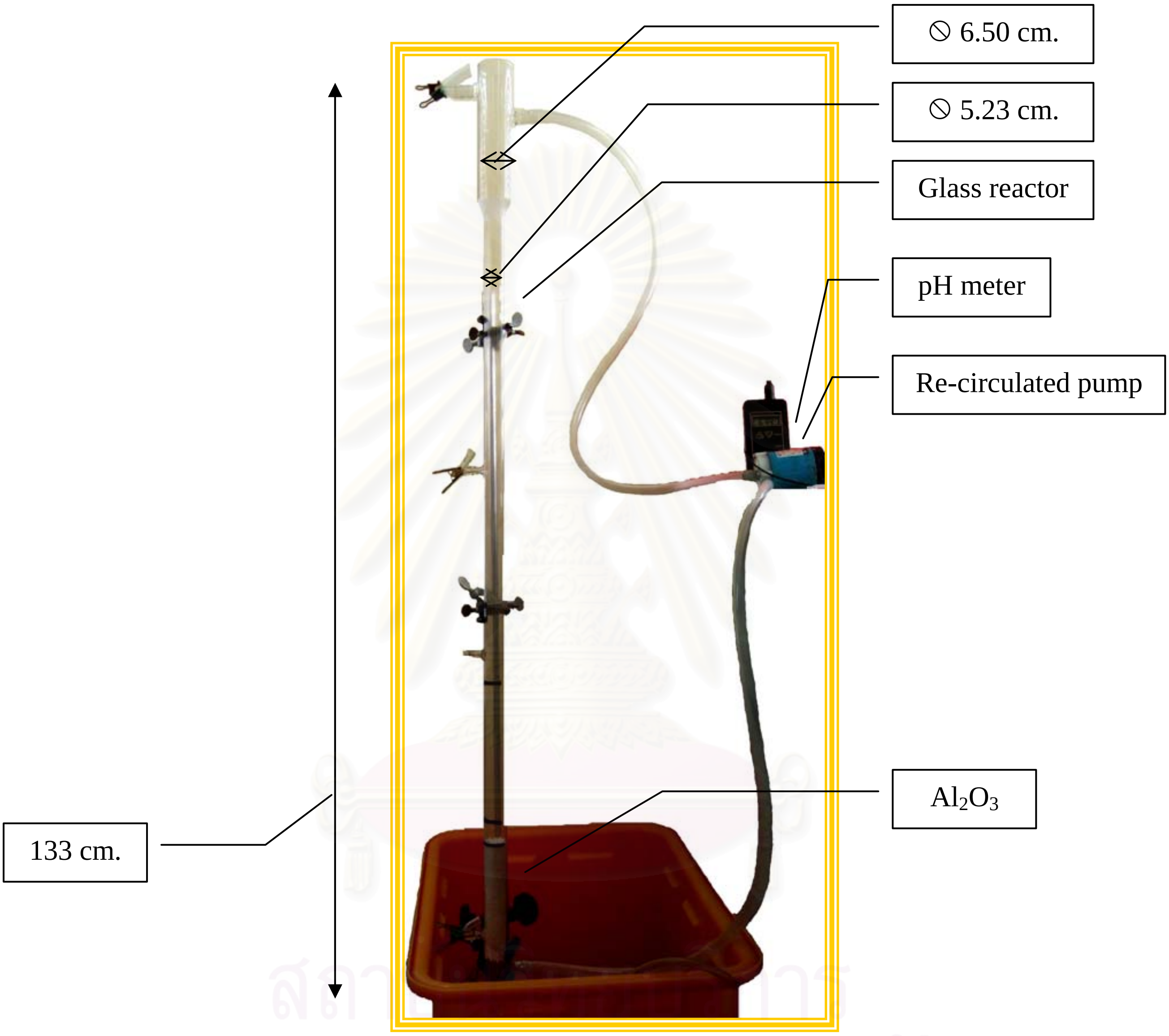

Figure D-1 Fluidized-bed Reactor

Figure D-2 Al_2O_3

Figure D-3 SiO_2

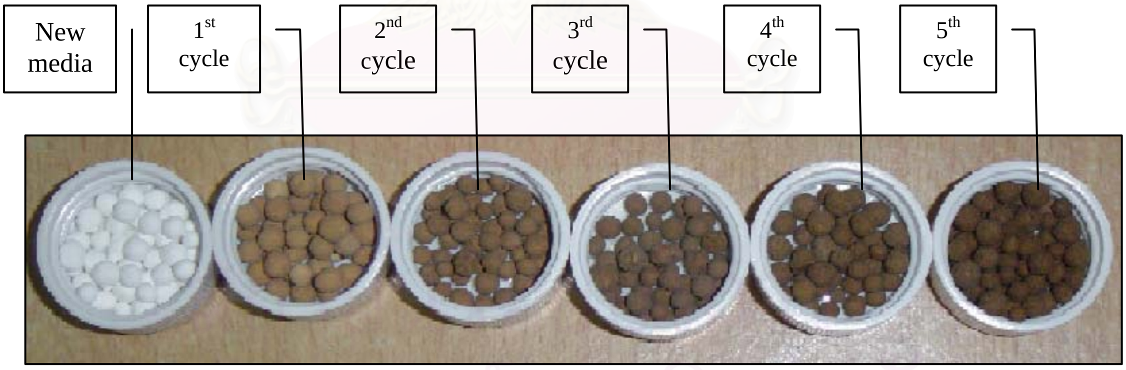

Figure D-4 The reusability of Al_2O_3 with 5 cycles; AN/NB of 5/5 mM, H_2O_2 0.05 M, Fe^{2+} 0.001 M, pH 2.8 and Al_2O_3 74.07 g/l.

Element	Weight%	Atomic%
O K	50.03	62.81
Al K	49.97	37.19
Totals	100.00	

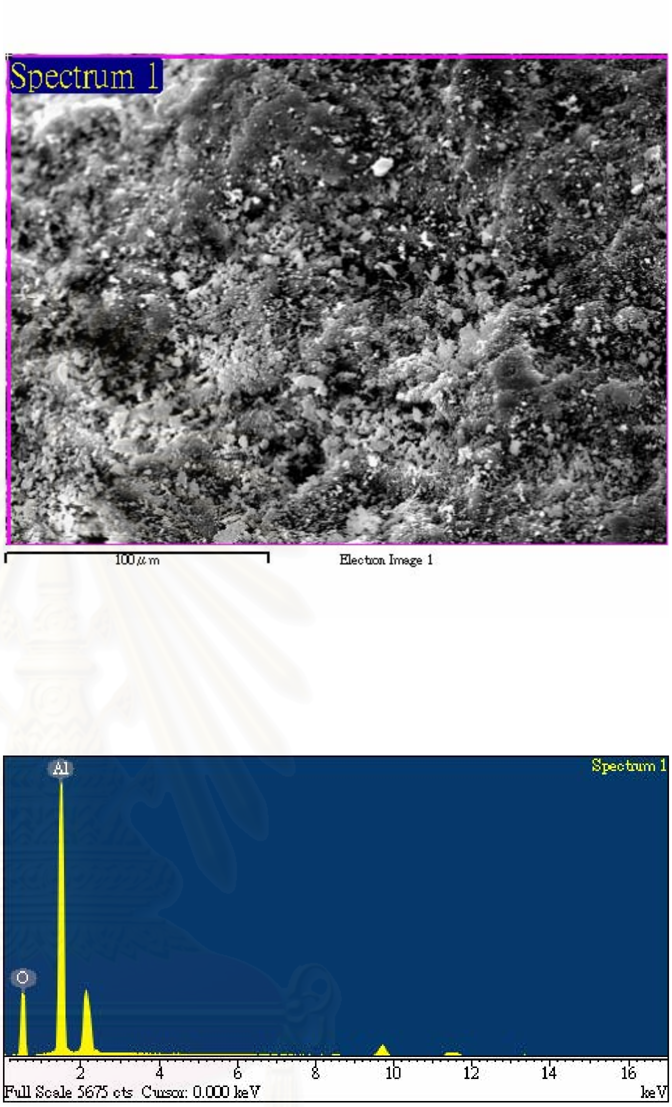

Figure D-5 EDX/SEM information, to investigate the element within new Al_2O_3.

Element	Weight%	Atomic%
O K	47.49	60.56
Al K	51.86	39.21
Fe K	0.65	0.24
Totals	100.00	

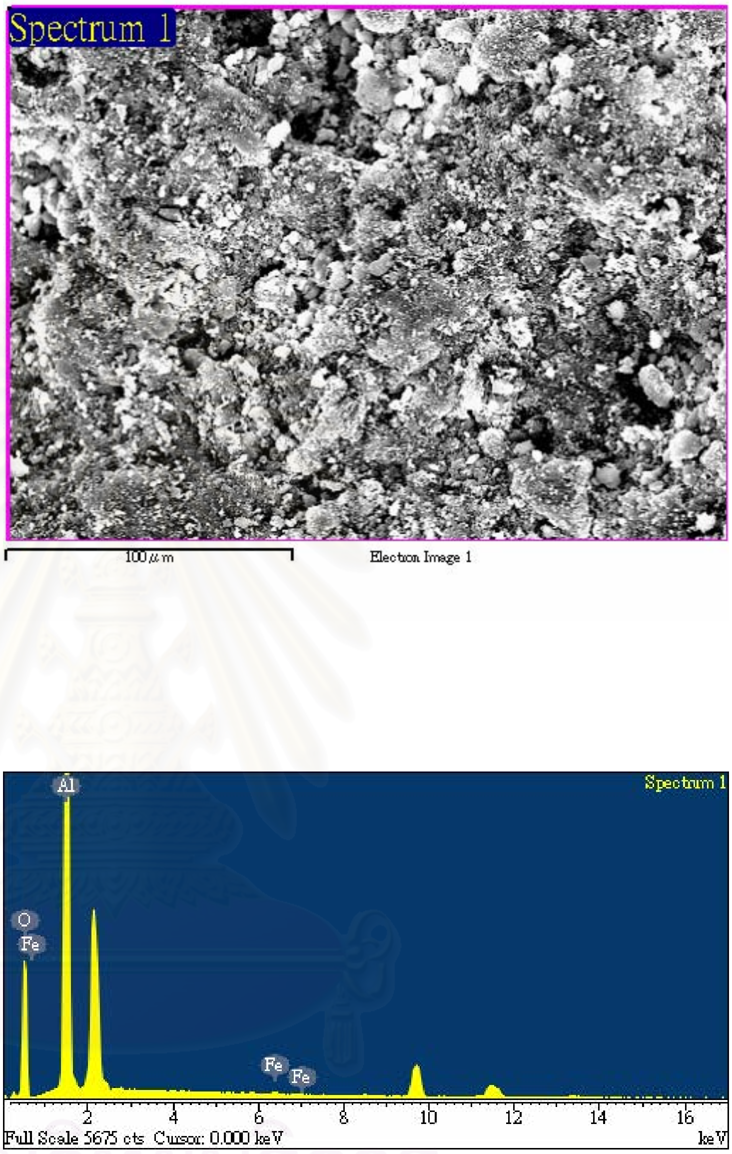

Figure D-6 EDX/SEM information, to investigate the element of Al_2O_3 within the latest cycle of the oxidation of AN/NB(5 mM:5 mM), 0.05 M of H_2O_2, 0.002 M of Fe^{2+}, pH 2.8 and 74.07 g/l of Al_2O_3.

BIOGHAPHY

Ms. Ladaporn Khunikakorn was born on July 14th , 1981 in Roi-Et, Thailand. She graduated Bacherlor's degree in General Science from the Faculty of Science, Chulalongkorn University 2004. She pursued her Master Degree in the International Postgraduate Program in Environmental Management (Hazardous Waste Management), Inter-Department of Environmental Management Chulalongkorn University, Bangkok, Thailand on May, 2004. She had attended to oral presentation and submitted a publication with her advisor, Associate Professor Jin Anotai and co-advisor Professor Ming-Chun Lu, in the subject of "the competitive oxidation of aniline and nitrobenzene in fluidized-bed Fenton process", the international conference hazardous waste management for a sustainable future 10-12 January, 2006, Bangkok, Thailand.